A Statistical Approach to Link Flux and Fouling to Sludge Characteristics for an Anaerobic Membrane Bioreactor Treating Dairy Cheese Wastewater.

Author: Rogelio Peschard Navarrete

Committee members:

TU Delft Prof. Dr. Ir. Jules van Lier
TU Delft Assoc. Prof. Dr. Ir. Henri Spanjers
TU Delft Prof. Dr. Ir. Bas Heijman

Company supervisor:

Dr. Ana Lucia Morgado Ferreira

TU Delft Delft University of Technology VEOLIA BIOTHANE

A Statistical Approach to Link Flux and Fouling to Sludge Characteristics for an Anaerobic Membrane Bioreactor Treating Dairy Cheese Wastewater

A thesis submitted to Delft University of Technology in partial fulfillment of the requirements for the degree of

Master of Science in Civil Engineering

Environmental Engineering

Rogelio Peschard Navarrete

15/11/2020

Committee Members:

TU Delft Prof. Dr. Ir. Jules van Lier

TU Delft Assoc. Prof. Dr. Ir. Henri Spanjers

TU Delft Prof. Dr. Ir. Bas Heijman

Acknowledgements

The completion of my master's thesis would have not been possible without the help of my supervisors, professors, colleagues, friends, and my family. It truly took a village to help me get to this point.

I would like to thank the team at Biothane. First to Santiago Pacheco-Ruiz and Ana Morgado Ferreira for entrusting me with this project. To Rewin Pale, because without his help the reactor would have fallen apart. To Patrick van der Linden, for teaching me how to properly do the analytical methods and for his support in the lab. Also, to the rest of the team at Biothane, since it was a complicated year for everyone, but they were always willing to help me with my project.

The final version of my thesis would have not been possible without the critical feedback from my committee members. Each of their comments were very valuable and they helped me with improving the thesis. Their questions and comments not only helped with my thesis, but also helped me to think more like a scientific researcher (or at least try to).

I also want to thank Lea Chua Tan and Salma Ebrahimzadeh. Their discussions helped me immensely, specially with the final piece of the puzzle for my thesis. They helped me to develop a more skeptical and critical mind to perform a more in-depth analysis of my data.

Finally, my family and friends in a way were the biggest contributors of this thesis by showing me endless support. If I specified how each one of them contributed to this project, the thesis would end up with at least 20 more pages. To avoid doing that, I just want to say that without their help and support literally this project would be nothing. This is as much as an accomplishment for them, as it is for me. For that they will always have my support and my gratitude.

Abstract

Fouling is the main limitation to the application of membrane bioreactors (MBRs). Understanding the complexity of fouling has led to better decision making for design and operation of MBRs. However, studies have shown contradictory results of the impact of sludge characteristics on membrane filtration performance and fouling propensity. The purpose of this study was to characterize the sludge under different operating conditions of an anaerobic membrane bioreactor (AnMBR) treating dairy wastewater, to assess the impact on the filtration. The real flux method was used to determine the flux, while the characteristics of the sludge varied in time. The real flux method is when the feed, retentate and transmembrane pressures are controlled to induce similar hydrostatic conditions applied in full-scale anMBR in crossflow configuration. Total solids (TS), volatile solids (VS), total suspended solids (TSS), volatile suspended solids (VSS), viscosity, and different fractions of the chemical oxygen demand (COD) were performed for sludge characterization. The specific resistance to filtration (SRF), capillary suction time (CST), and supernatant filterability were used as parameters for filterability of the sludge and supernatant. Principal component analysis (PCA) was used to determine the correlation between the sludge characterization and the filterability methods. Five principal components (PC) attributing to 91% of the variance were extracted, based on an eigenvalue greater than 1. The principal components showed the correlation between the different variables studied. PC1 consisted of fraction of solids (total dissolved solids, VSS/TSS, and fixed suspended solids), the CST, and the normalized versions of the CST (CST/TSS, CST/Viscosity, CST/TSS/Viscosity). Five of the variables in PC1 are derived from the TSS concentration most likely indicating why they were grouped under this principal component. PC2 consisted of the particle size distribution of particles ranging from 0 to 10 micrometer. PC3 consisted mainly of a different fraction of solids (VSS, VS, TS, and TSS) and SRF. SRF is a function of TSS, this can explain why these variables were grouped together in PC3. PC4 consisted of the soluble and colloid particles. PC5 consisted of the hydrostatic conditions of the membrane. A multiple linear regression of the PC revealed statistically significance (ANOVA, p-value <0.05) to estimate the flux. A stepwise multiple linear regression was done to determine what variables can be used to estimate the flux based on the data obtained. The selection of the best model from the multilinear regression was based on the highest R squared value, statistical significance from ANOVA, and the variance inflation factor to take into consideration collinearity. Based on the criteria from the PCA and the multiple linear regression, the independent variables for predicting the flux were the CST/TSS, crossflow velocity, the SRF, and the VS/TS.

Table of Contents

List of Figures

Table of Tables

Abbreviations

AnMBR Anaerobic Membrane Bioreactor

CCOD Colloidal Chemical Oxygen Demand

CIP Cleaning in Place

COD Chemical Oxygen Demand

CST Capillary Suction Time

CWP Clean Water Permeability

DFCm Delft Filtration Characterization Method

EPS Extracellular Polymeric Substances

HRT Hydraulic Retention Time

MBR Membrane Bioreactor

PC Principal Component

PCA Principal Component Analysis

PCOD Particulate Chemical Oxygen Demand

PSD Particle Size Distribution

SCOD Soluble Chemical Oxygen Demand

SMP Soluble Microbial Products

SRF Specific Resistance to Filtration

SRT Solids Retention Time

TMP Transmembrane Pressure

TS Total Solids

TSS Total Suspended Solids

UF Ultra Filtration

VS Volatile Solids

VSS Volatile Suspended Solids

Chapter 1 Introduction

1.1 Background

Treating wastewater can pose many complex challenges, due to the wide variety of pollutants that can be found in it. Among industrial wastewaters, dairy wastewater present unique challenges. Dairy wastewater typically contains high contents of organic pollutants, fats, and salts that can cause complications for their treatment (Carvalho et al. 2013, Prazeres et al. 2012). Several studies have shown, that biological treatment technologies can be suitable for treating dairy wastewater (Andrade et al. 2013, Demirel et al. 2005, Dereli et al. 2019, Goli et al. 2019, Kalyuzhnyi 1997, Prazeres et al. 2012). One of the many technologies that show promising results is anaerobic membrane bioreactors (anMBRs). One of the reasons anMBRs can be beneficial is that, besides effectively treating the dairy wastewater, the water quality of the permeate is rather high.

However, the biggest drawback of this technology is membrane fouling. Fouling is the accumulation of feed water and sludge constituents in the membrane pores, or on the membrane surface (Geilvoet 2010). As a result, fouling leads to a decrease in permeate flux or an increase in the transmembrane pressure (TMP) (Zhang et al. 2012). This phenomenon of fouling has been widely studied for all kinds of membrane technologies.

Henze (2008) defines the impacts of fouling as follows; fouling removed by physical cleaning, such as backwashing and relaxation is generally termed hydraulically “reversible” or “temporary” fouling. The fouling that is removed by applying chemicals is often termed “irreversible” or “permanent” fouling, although the term chemically “reversible” is also used. In the case of membrane bioreactors, there can be three factors that can impact fouling. These factors are the membrane and module characteristics, the biomass characteristics, and the operation characteristics. Under these three factors, there are several variables to consider as well. Therefore, fouling has been a taxing concept to understand and interpret, which still poses challenges today.

Several studies have investigated the biomass characteristics to assess their impact on fouling. One of the main issues, is that the inter relation of these variables and factors makes the understanding of fouling even more complex. Additionally, studies have shown contradictory results meaning that one single parameter cannot be used to determine the impacts of fouling. The following chapter goes in depth about the challenges posed by fouling and the efforts done to understands it.

.

Chapter 2 Literature Review

2.1 Dairy Wastewater

In the food industry, the dairy industry is considered one of the most polluting industries in regards to its large water consumption (Vourch et al. 2008). Additionally, variations in fat content, suspended solids, and nutrients can make the treatment of this wastewater a challenging task (Prazeres et al. 2012). The characteristics of the dairy wastewater are dependent on the process of the product that is made (e.g. milk, cheese, ice cream, etc.). The dairy wastewater may also be diluted with washing waters that may contain alkaline and/or acidic chemicals (Carvalho et al. 2013, Prazeres et al. 2012).

The wastewater produced from the cheese industry is highly contaminated and difficult to treat (Goli et al. 2019). There are three main types of effluents from the cheese industry: Cheese whey (resulting from cheese production), second cheese whey (resulting from cottage cheese production), and the washing water aforementioned (Carvalho et al. 2013). The type of cheese production also influences the characteristics of the produced cheese whey (Carvalho et al. 2013).

Due to the different production processes of cheese, the physiochemical characteristics of cheese effluents can vary widely. Table 2.1 summarizes the range of values of some of the physiochemical characteristics found in cheese effluents (Prazeres et al. 2012).

Table 2.1 Ranges of physiochemical characteristics of streams produced during cheese manufacturing. Values adapted from (Prazeres et al. 2012).

Parameter	Value range
Total Suspended solids (kg/m^3)	0.1-22
pH	3.3-9.0
Phosphorus (kg/m^3)	0.006-0.5
Total Kjeldahl Nitrogen (kg/m^3)	0.01-1.7
Organic Load (kg/m^3)	0.6-102
Chemical Oxygen Demand (kg/m^3)	0.1-100
Lactose (kg/m^3)	0.18-60
Protein (kg/m^3)	1.4-33.5
Fats (kg/m^3)	0.08-10.58

2.2 Fouling

As it has been stated previously, fouling is probably the most important parameter to consider for the design of membrane bioreactors, since it affects the pretreatment needs, cleaning requirements, operating conditions, cost, and performance (Tchobanoglous et al. 2003). Fouling has been the main research focus in the previous years. The extensive research has provided us with a better understanding on fouling, however it remains a complicated concept to fully grasp, due to the several variables at play. Zhang et al. (2012) divides the types of foulants into two categories, the macro-scale and the micro-scale foulants. The macro-scale

foulants include large particles of biological or inorganic origins. In contrast, micro-scale foulants are categorized based on the mechanisms that cause the fouling, which are particulate or colloidal foulants, chemical reactions, organic foulants, inorganic foulants, and biological foulants. Table 2.2 summarizes some of the typical wastewater constituents that correspond to the different types of foulants.

Table 2.2 Types of foulants and examples of their respective wastewater constituents adapted from (Tchobanoglous et al. 2003, Zhang et al. 2012)

Type of micro-scale foulant	Wastewater Constituent
Particulate/colloidal fouling	Organic and inorganic colloids Emulsified oils Clays and Silts Silica Iron and manganese oxides Oxidized metals Metal salt coagulant products Powdered activated carbon
Inorganic foulants (scaling)	Barium Sulfate Calcium carbonate Calcium fluoride Calcium phosphate Strontium sulfate Silica
Organic Foulants	Natural organic matter (NOM) including humic and fulvic acids, proteins and polysaccharides Emulsified oils Polymers used in treatment processes
Biological Foulants	Dead microorganisms Living microorganism Polymers produced by microorganisms
Chemical Reactions	Acids Bases pH extremes Free chlorine Free oxygen

These foulants have a diverse interaction with the biomass characteristics, the membrane and module characteristics and the operating conditions of the membrane (Figure 2.1) (Zhang et al. 2012). Understanding each variable and the mechanisms of their interaction, is paramount to comprehend fouling. These factors and their respective variables will be discussed in the following sections.

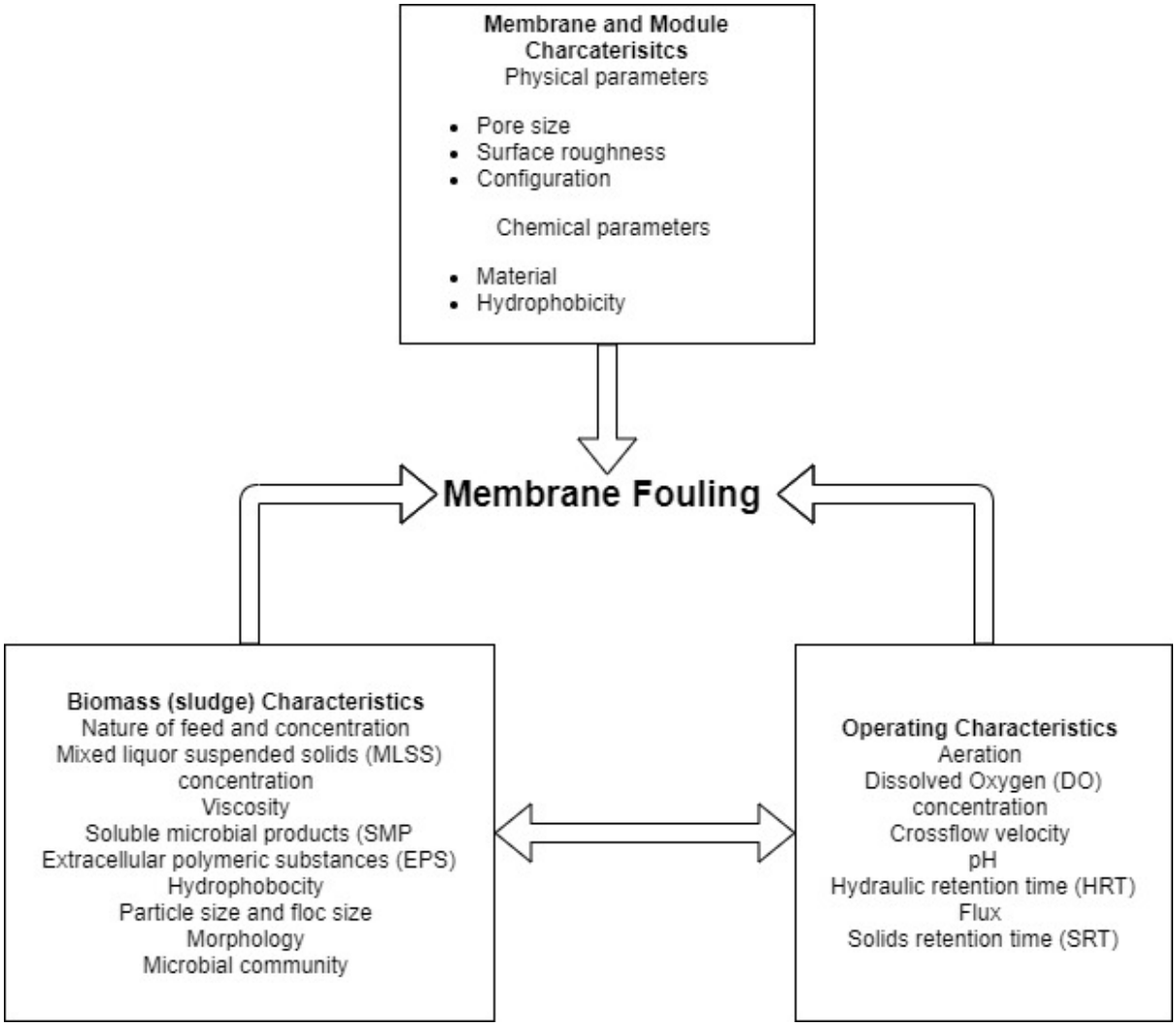

Figure 2.1 Factors affecting membrane fouling adapted from (Zhang et al. 2012)

2.2.1Membrane & Module Characteristics

Membrane and module characteristics play an important role in the fouling of the system. The different types of membrane are identified by the driving force of the separation mechanism and their cutoff in pore size (Tchobanoglous et al. 2003). The main separation mechanism for ultrafiltration membranes is sieving and the pore size can range between 2 up to 50 nm. Ultrafiltration membranes can come in three types of configurations; spiral wound, hollow fiber, and plate and frame (Tchobanoglous et al. 2003). Additionally, the material of the membranes is also important and needs to be taken into consideration. Studies have reported the impact of membrane material on fouling. The study by Metsämuuronen et al. (2002) concluded that interactions between membranes made from hydrophobic material and

hydrophobic compounds, had a higher fouling propensity. Extensive work has supported that smooth hydrophilic membranes attribute to less fouling (Fane and Fell 1987, Marshall et al. 1993, Matthiasson 1983, Nilsson 1990).

The nominal pore size is an important variable to take into consideration, since it has been reported that the pore size has in impact on the hydraulic resistance and the adsorption of compounds into the membrane (Ognier et al. 2002b). In some cases formation of a cake layer can also serve as a prefilter that can protect the membrane from pore blocking (Le-Clech, 2006) .Studies determined that the adsorption of colloids and pore blocking, depends on the pore size distribution and on the surface chemistry of the membrane (Jiang et al. 2005, Ma et al. 2005, Ognier et al. 2002a). Additionally, pore blocking and/or restriction is expected if there are particles smaller than the nominal pore size (Le-Clech et al. 2006).

The configuration of the membrane has an impact on the different fouling mechanisms. For this study, a side stream tubular membrane in crossflow configuration was selected since other types of configurations have been researched more. The most commonly studied configuration reported, is submerged membrane bioreactors (Le-Clech et al. 2006).

2.2.2 Operating Characteristics

The Operational conditions of the membrane also has a significant impact on the way fouling behaves. Membranes are usually operated at a constant pressure or at a constant flux. Under constant pressure operation, there is usually a rapid flux decline until the flux stabilizes. Under constant flux operation, the TMP increases over time causing the permeability to decrease. Zhang et al. (2006) proposed a three-stage fouling mechanism for MBRs operated at constant flux conditions. The three-stage fouling model mechanism, divides the behavior of fouling into conditioning fouling, steady fouling, and TMP jump (Zhang et al. 2006). The mechanism and factors involved in these fouling stages are summarized in Figure 2.2.

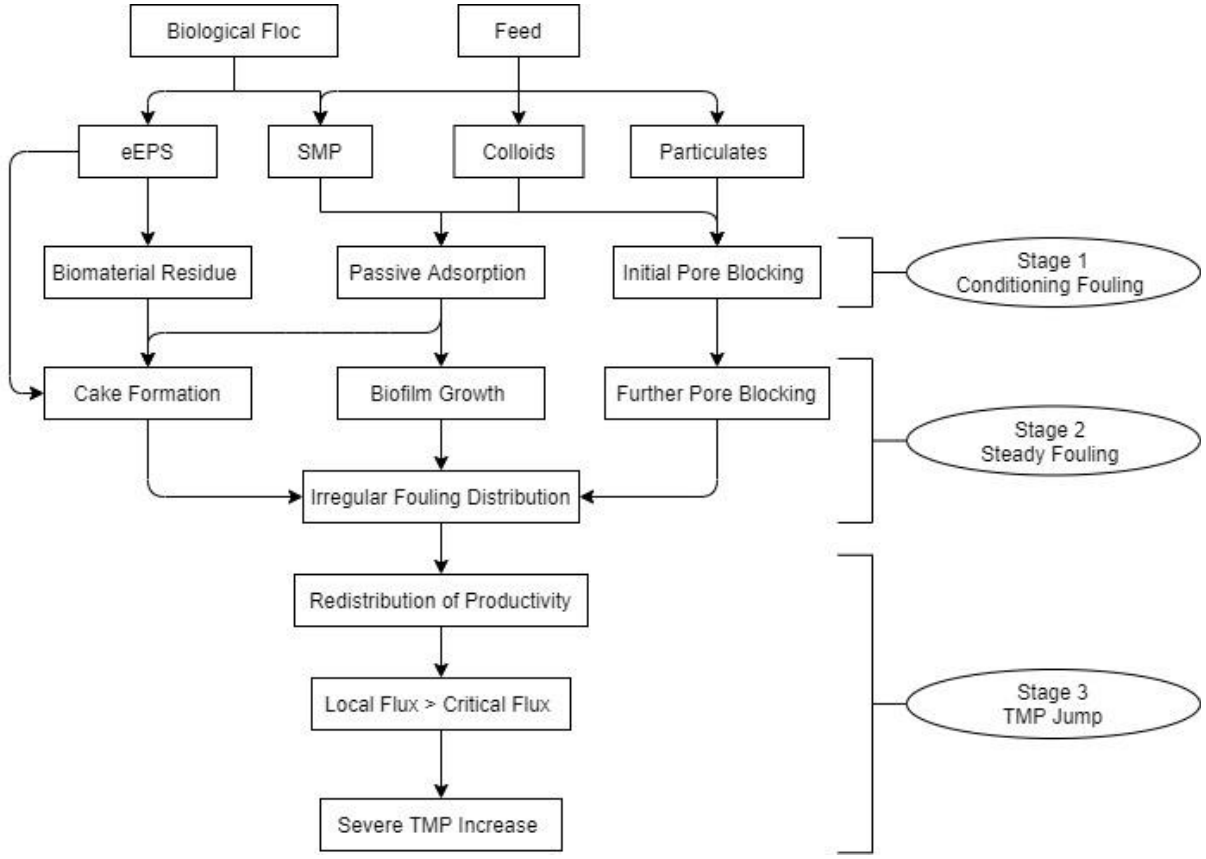

Figure 2.2 Three stage fouling for membranes operated in constant flux, adapted from (Zhang et al. 2006)

Additionally, the solids retention time (SRT), The hydraulic retention time (HRT), and the crossflow velocity have also been reported to have an impact on the fouling of the membrane. It is believed that the SRT is one of the most important operational parameters that has an impact on fouling, since it has a direct impact on the physiochemical characteristics of the sludge and on the microbial community. (Le-Clech et al. 2006).

Choi et al. (2006) reported that the impact of crossflow velocity on fouling can differ based on different pore size. It is expected that higher crossflow velocities will yield higher flux due to the increase in shear forces which enhances the shear-induced hydrodynamic diffusion (Lee and Clark 1998). However, as the crossflow velocity increases, it may allow smaller particles to deposit on the membrane surface which could lead to an increase in specific resistance (Le-Clech et al. 2006). Another study by Choi et al. (2005) reported that the increasing crossflow velocity did not decrease the fouling intensity when the position layer starts to govern the permeate flux behavior, which led to more irreversible fouling, while in the absence of crossflow velocity the flux decline was mainly caused by reversible fouling.

2.2.3 Biomass Characteristics

Apart from the operational conditions, which play an important role in the behavior of fouling, it is also important to understand the complexity of the mixed liquor. Undeniably, the wastewater itself has an impact on the filtration (Fuchs et al. 2006, Judd and Jefferson 2003, Schrader et al. 2005). However, the interaction between the sludge and the membrane causes the majority of the fouling problems (Choi et al. 2005). The interactions of sludge and wastewater with the membrane can be different on a case to case basis (e.g. extremely saline

wastewater). Detailed studies also reported the impact of specific substrates in the wastewater on the sludge characteristics, which can result in negative impacts on the fouling propensity (Dereli et al. 2014a, Dereli et al. 2015, Dereli et al. 2014b, Dereli et al. 2019). The detailed observations of the changes in the biomass due to the different substrates, has provided more insight about the impact of the biomass on the fouling of the membrane.

The total suspended solids have been studied extensively, most of the studies have concluded that higher concentrations of solids can lead to more fouling (Madaeni et al. 1999, Sato and Ishii 1991). However, there have been contradictory findings, where a higher concentration of TSS had a positive impact on the hydraulic performance (Lee et al. 2001, Shin 2002), while other studies have reported negligible influence of TSS concentration on membrane fouling (Cicek et al. 1998, Hong et al. 2002, Zhang et al. 2012). Rosenberger et al. (2006) provided a more detailed frame of reference, where concentrations below 6 g/L decreased fouling rate, concentrations higher than 15 g/L negatively impacted the membrane through fouling, and concentrations between 8 and 12 g/L seemed to have no significant impact on the fouling. Proper estimation of fouling propensity by just looking at the concentration of TSS has not been successful (Zhang et al. 2012). Additionally, the solids content has been reported to be correlated to several parameters.

Viscosity has been reported to be related by the concentration of TSS (Lee and Yeom 2007), EPS, and SMP concentrations (Jeong et al. 2007, Meng et al. 2006a). Viscosity tends to increases slowly as the concentration of the TSS increases, until it reaches its critical value, where the viscosity starts to increase exponentially (Itonaga et al. 2004). Viscosity itself is not a foulant but it can be a variable used to have some insight on the fouling ,due to its relation to TSS concentrations, EPS, and SMP (Lee and Yeom 2007).

Another variable that has been reported to be associated with membrane fouling is relative hydrophobicity. Relative hydrophobicity is measured by the affinity of bacteria in the sludge suspension to hydrocarbons (Zhang et al. 2012). Generally, it is believed that hydrophobic membranes are more prone to fouling due to interactions with hydrophobic compounds (Knoell et al. 1999, Leslie et al. 1993, Pasmore et al. 2001). However, it is also reported that highly hydrophobic flocs may also cause fouling on hydrophilic membranes (Le-Clech et al. 2006)

As mentioned, the concentration of solids is important to take into consideration, but the size distributions of the particles and flocs is another important variable to consider. The particle size of flocs can vary widely, mean particle size has been reported to be from 5 up to 240 µm (Lee et al. 2003).Particle and floc size can have an impact on the porosity of the cake layer and therefore the hydraulic resistance. Large floc size can result in formation of more porous cake layers and can enhance filtration (Zhang et al. 2012). There has been contradictory results reported, where bigger floc size resulted in more severe fouling (Meng et al. 2006a), and where the large floc sizes had no impact on the membrane fouling (Jeong et al. 2007).

The morphology of the flocs has also been reported to have an impact on the flux. Irregular shaped flocs and filamentous bacteria can more easily adhere to the membrane surface causing a decline in flux. Additionally, Meng et al. (2006a) reported that filamentous

bacteria also can entrap foulants causing further decline in the flux. On the other hand, Li et al. (2008) reported that filamentous bacteria has an important impact on the floc size and floc morphology, but their effect on the membrane fouling rate may be negligible, and the variations of bound EPS might be a more important factor contributing to the fouling.

As mentioned, the morphology of the biomass has an impact on the filtration, which means it is directly related to the microbial community present in the sludge. The microbial community is affected by the operation of the system, e.g. in aerobic MBRs *proteobacteria* tend to be the dominant group (Zhang et al. 2012). In the case of anerobic technologies the microbial communities have been extensively studied, due to their symbiotic relationships for methane production. For anaerobic technologies, the dominant microbial communities are the organisms responsible for hydrolysis, acetogenesis, acidogenesis, and methanogenesis. As mentioned, filamentous bacteria have been reported to cause the most problems regarding fouling (Li et al. 2008). However, other studies also have reported that no particular organism was more predominant to attach to the membrane surface (Ma et al. 2006), while another study proved that there was no correlation between filamentous bacteria to the filtration resistance (Bugge et al. 2013). Additionally, operation of the system is important, especially the SRT, for selection pressure of microorganisms which can results on different impacts on the fouling (Le-Clech et al. 2006).

Extracellular polymeric substances (EPS) and soluble microbial products (SMP) have been the focus of some studies to determine their impact on membrane fouling. The review study by Le-Clech et al. (2006) summarized the impacts on fouling, where it is suspected that the EPS and SMP concentration can be one of the major foulants, however, it is hard to compare the results among different studies, since the results rely heavily on the extraction methods for the SMP and the EPS. EPS and SMP are important variables to keep in mind since they have shown correlation with other variables, such as viscosity. For this study they were not measured, since the results rely on the extraction method used.

Studies have also looked at using particle count to measure the integrity of the membrane. Lousada-Ferreira et al. (2011) studied whether, particle counting techniques can be used to determine the deflocculation of the suspended biomass, which could indicate a decrease in filterability. Their study concluded that the deflocculation of the sludge might be masked by the large amount of particles in the sample, however it cannot be discarded that submicron particles could be a potential source of filtration deterioration (Lousada-Ferreira et al. 2011). Another study performed particle count on different MBRs and concluded that the results varied widely, most likely because of the difference in the hydrodynamic conditions or the difference in TSS concentrations(Lousada-Ferreira et al.). It seems like the particle count could be used as an indicator for sludge characterization, but this method requires further research, to determine if it can be used for filtration or fouling characterization for MBRs.

As stated previously, the wastewater and sludge characterization have an impact on fouling. Dereli et al. (2014a) studied the supernatant filterability to use it as an indicator for fouling propensity. The study found a negative correlation with the filterability of the membrane, most likely caused by the solutes and fine particles found in the supernatant, and

it concluded that the SRT had an impact on the accumulation of solutes and fine particles (Dereli et al. 2014a).

2.3 Filtration & Fouling Measurements

Several methods have been developed to quantify the filterability of the sludge. Capillary suction time and specific resistance to filtration, are methods used for dewaterability of the sludge, but it has been reported that these methods have been used for filterability of sludge in membrane filtration (Dereli et al. 2014a, Le-Clech et al. 2006, Pollice et al. 2008, Vesilind 1988). The critical flux method is the most common methods reported in literature and it's used to assess the fouling in a membrane bioreactor (Espinasse et al. 2002, Le Clech et al. 2003). The Delft filtration characterization method (DFCm) was a method developed to provide specific information about the potential of a sludge sample to cause fouling (Geilvoet 2010). These methods have provided important insight, used for the development of MBRs, but there is still research that needs to be done to improve these methods and to consolidate them to the mechanisms pertaining to fouling.

2.4 Filtration Models

Efforts have been made to present the impacts of the fouling on the filtration by presenting different types of models. Sato and Ishii (1991) presented an empirical model were the filtration resistance was a function of the pressure drop, the TSS, COD and viscosity with an accuracy of ±24%. The study concluded that the soluble COD attributed for the most effect on the flux, while the viscosity attributed to the least (Sato and Ishii 1991). Other models have also been used to try to simplify fouling. Naessens et al. (2012) did a review on studies focusing on biokinetics and filtration models. For the filtration models, the study focused on the benefits and the disadvantages of the resistance models in series, artificial neural network models, and models from advanced regression techniques. Overall, the study concluded that special attention is needed in regards to overparameterization, providing sufficient model calibration with data collection, and validating the models further before they can be practically applied (Naessens et al. 2012). Chew et al. (2020) claimed that additional modeling work needs to be done for incorporation of crossflow, factor in pore size distribution and account for a variety of foulants with different characteristics.

2.5 Knowledge Gaps & Problem Statement

From research on both aerobic and anaerobic MBRs, it was determined that one single variable cannot be used to understand the propensity of the fouling on the membrane, due to the complex relationships between the variables (Chew et al. 2020, Le-Clech et al. 2006). A fouling measurement still needs to be developed, which is capable of being more explicit (Lousada-Ferreira et al. 2014). Therefore, one of the main issues is to determine what variables can be used to give a good representation of the flux and fouling. To find what variables give a good representation of flux and fouling, it is important to understand the methods used to measure the characteristics of the biomass, the relationships between the biomass and flux, the relationship between the biomass and fouling, and the relationship between all the biomass characteristics.

Evidently, not all variables that have a relationship to flux and fouling can be measured in one single study. Therefore, selecting the right variables also needs to be taken into consideration. As mentioned before, there are three factors that can affect fouling; membrane and module characteristics, biomass characteristics, and operating conditions (Zhang et al. 2012). The focus of the current study is mainly on the variables pertaining the biomass characteristics. For this project, the variables selected were investigated in terms of practicability. In other words, the experimental methods used in the current research, that are widely available methods, and methods that have been standardized. Based on these criteria, the variables selected to characterize the sludge were: Capillary suction time (CST), total solids (TS), volatile solids (VS), total suspended solids (TSS), volatile suspended solids (VSS), specific resistance to filtration (SRF), particle size distribution (PSD) of the sludge and supernatant, particle count of the sludge, total chemical oxygen demand (COD), particulate COD (PCOD), colloidal COD (CCOD), soluble COD (SCOD), supernatant filterability (SF) and protein concentration of the supernatant.

2.6 Objective & Research Question

As discussed in the previous sections, overcoming the impacts of fouling is still one of the biggest challenges for anMBRs. Previous research has helped identifying the different types of foulants and the mechanism affecting the membrane. Due to the complex interactions of the different foulants and the factors causing fouling, it is hard to explicitly measure the impacts of fouling. Therefore, the research objective is to determine possible indicators that can predict the flux, while considering the impacts of fouling caused by biomass on the membrane. To attempt to achieve this objective, the following research questions were proposed:

1. Which of the measured biomass and filterability variables can be used as an indicator for predicting flux and fouling of an AnMBR in crossflow configuration?
2. Are these variables correlated to the real flux method and fouling?
3. What are possible mechanistic explanations to justify these variables as indicators for the prediction of the flux and fouling?

If the CCOD, CST and the normalized CST (CST/TSS, CST/Viscosity, or CST/TSS/Viscosity), the TSS, SRF, particle count, SF, and PSD show good correlation with the results from the real flux measurement, then these variables could be used as indicators for predicting the flux while taking into account the impacts of the biomass on membrane fouling. To define the correlations and to determine if these variables can be good indicators, a statistical approach was held to analyze the measured data and try to identify what could be the best indicators to characterize the filtration and fouling.

Chapter 3 Materials & Methodology

3.1 Inoculum & Wastewater Characterization

The inoculum anaerobic flocculant sludge was taken from a food and beverage treatment plant from Poland. 10 L of the sludge were used to seed the reactor with a TSS concentration of 10.5 g/L. The dairy wastewater was provided by a dairy industry in Greece. The wastewater was composed of whey and wash water at a ratio of 1:4.5. Table 3.1 shows the complete composition of the wash water and the whey. Additional nutrient solution was added to the feed at a concentration of 14.38 ml/L composed of 2.5ml/L Vithane solution (Univar, The Netherlands) and 10.2 ml/L 40% $FeCl_3 \cdot 7H_2O$. The prepared feed was stored at 4°C to prevent degradation. The target organic loading rate for this research was 6.0 gCOD/L·d.

Table 3.1 Physiochemical characterization of wash water and whey.

Parameter	Unit	Wash water	Whey
pH	-	4.5	5.0
Conductivity	mS/cm	5.3	6.6
Total COD	mg/L	3751	59600
Colloidal COD	mg/L	3511	56100
Soluble COD	mg/L	3347	56000
Acetic Acid (C2)	mg/L	88	1055
Propionic Acid (C3)	mg/L	7	28
Isobutyric Acid (iC4)	mg/L	0	0
Butyric Acid (C4)	mg/L	0	7
Isovaleric Acid (iC5)	mg/L	0	0
Valeric Acid (C5)	mg/L	0	0
Hexanoic Acid (C6)	mg/L	0	0
Total Solids (TS)	g/kg	6.0	49.6
Organic Total Solids (OTS)	g/kg	2.7	45.0
Suspended Solids (SS)	g/kg	0.2	0.6
Volatile Suspended Solids (VSS)	g/kg	0.2	0.5
Total Phosphorus	mg/L	89.9	423.0
Ortho-phosphate	mg/L	75.8	272.0
Total Alkalinity (pH-4)	meq/L	5.3	22.8
VFA (Wageningen method)	meq/L	14.0	63.0
Total Organic Carbon (TOC)	mg/L	1428	22860
Chloride (Cl^-)	mg/L	1400	960
Nitrate (NO_3^-)	mg/L	5	0
Nitrite (NO_2^-)	mg/L	14	0
Sulphate (SO_4^{2-})	mg/L	47	84
Calcium (Ca^{2+})	mg/L	140	380
Potassium (K^+)	mg/L	110	1300
Magnesium (Mg^{2+})	mg/L	28	100
Sodium (Na^+)	mg/L	1200	490

Fat Oil and Grease (FOG)	mg/L	120	56

3.2 Reactor Set-up, Operating Conditions

The anaerobic membrane bioreactor incorporated several components mainly consisting of the ultrafiltration membrane, the influent tank, a buffer tank, the main sludge reactor, a conditioning tank and the permeate tank. For this study the buffer tank was removed and added at different stages of the experiment. Figure 3.1 shows the schematics of the reactor with and without the buffer tank. Peristaltic pumps (Watson Marlow 120U) were used for transporting the feed to the buffer tank and to the main reactor. The main reactor was operated as a continuous stirred tank reactor (CSTR).The main reactor had an approximate total volume of 13 L and the working volume was maintained between 9 to 10 L. A custom assembled motor 220V was used for the top stirrer of the main reactor, operating at 98 rpm.

A)

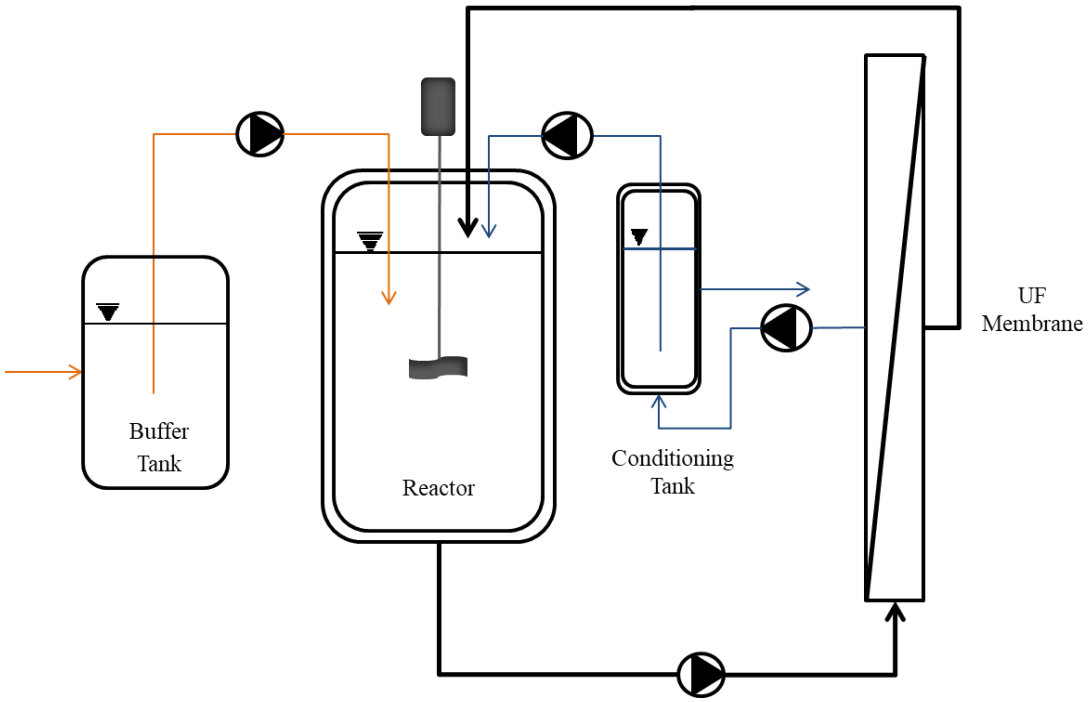

B)

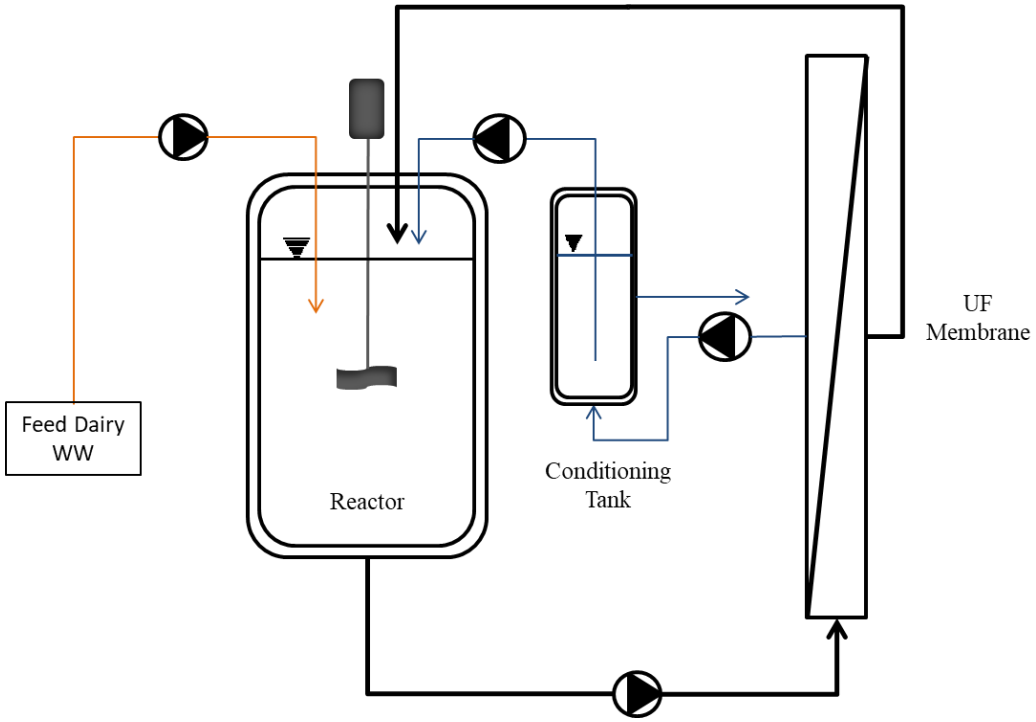

Figure 3.1 A) Reactor schematics full configuration. B) Reactor schematics excluding the buffer tank. For both Schematics the orange line shows the flow direction of the feed wastewater. The black line shows the flow direction of the mixed liquor. The blue line shows the flow direction of the permeate.

The recirculation pump used to feed the membrane was a Mono Compact C22A Pump (Axflow). Three membranes were used during the experimental procedure. The specifications of the membranes (Pentair plc, The Netherlands) can be found on Table 3.2. Three pressure sensors with a range of -1000 to 4000 mbar (AE sensors) were used to monitor the feed, retentate, and permeate pressure. The permeate flux was controlled with a Watson Marlow 520U pump. The conditioning tank with an approximate total volume of 3 L. Cole Parmer AMsterflex L/S economy drive pump was used to return permeate to control the water level in the main reactor.

Table 3.2 Specifications of membranes

Membrane model	Membrane Material	Hydraulic diameter	Membrane length	Membrane surface area	Nominal pore size
X-flow Compact 33 Helix	polyvinylidene fluoride	5.2 mm	3 m	0.049 m^2	0.30 µm
X-Flow Compact 27 Helix	polyvinylidene fluoride	8.0mm	1.5 m	0.038 m^2	0.30µm
X-Flow Compact 27	polyvinylidene fluoride	8.0 mm	1.5 m	0.038 m^2	0.30 µm

3.3 Objective of Experimental Phases

The objective of the experimental phases was to characterize the sludge under different operational conditions. The purpose of the first phase was to look at the behavior of the sludge at high SRT and how the characteristics changed after the removal of the buffer tank. The purpose of the second phase was to look at the characteristics of the sludge at a lower SRT and look at the changes of the sludge after reinstalling the buffer tank. The main reason of these operational changes was to obtain as much data of the sludge characteristics to relate it to the filtration and fouling characterization. There were some practical issues during the duration of the first experimental of the first phase which led to a second start-up of the reactor. The practical issues will be discussed further in the results section.

3.4 Characterization of Sludge & Filtration Methods

The sludge was sampled daily for capillary suction time (CST) measurements, all of the other measurements were done twice per week. CST of sludge was measured with Titron Capillary Suction Timer (304M) using standard CST filtration paper provided by Titron Electronics, Ltd.

Specific resistance to filtration (SRF) was measured with a dead end filtration cell Amicon cell unit (Micon Bioseparations, Millipore), determined by the method from Dereli et al. (2014a) and Pollice et al. (2008). GF/F glass microfilters (0.7 µm, 47 mm, Whatman, GE Healthcare Life Sciences, UK) were used. The Sludge was first diluted with permeate to have a TSS concentration of 10 g/L. The diluted sample was filtered under a pressure of 0.5 bar at non stirred conditions. The SRF was determined by plotting the ratio filtration time/filtrate volume (t/V) versus the filtrate volume (V). The filtration time was 30 minutes, and the data were recorded in intervals of 5 seconds. Using the slope of the line, the SRF was calculated according to the following formula (Dereli et al. 2014a, Pollice et al. 2008):

$$SRF = \frac{2 \cdot \Delta P \cdot A^2 \cdot b}{\mu \cdot C} \qquad \text{Equation (2.1)}$$

ΔP: Pressure, Pa

A: Effective filtration area, m^2

b: Slope, s/L^2

µ: Dynamic viscosity, Pa·s

C: TSS concentration, kg/m^3

Supernatant filterability (SF) method was adapted from Rosenberger et al. (2006) and Dereli et al. (2014a). The supernatant was prepared by centrifuging the sludge at 17,500 g for 10 min. The supernatant filterability was measured by filtering through 0.22 µm glass microfilter papers in a stirred dead-end filtration cell (Amicon filtration cell unit) under constant pressure of 0.5 bar. The permeate was collected for 10 mins and the weight of the

filtered permeate was collected in intervals of 5 seconds. The filterability was calculated by averaging the permeate flowrate after 5 min.

Particle size distribution (PSD) of sludge was measured between 0.01 to 2000 µm using (Blue wave light scattering Microtac, Reysch Technology GmbH) with Microtrac FLEX 11.1.0.2 software and a flow rate of 25%. For the PSD of the supernatant, first the supernatant was prepared by centrifuging the sludge at 17,500 g for 10 min and the conditions for the PSD were the same as the PSD for the sludge.

The viscosity of the sludge was measured was measured using HAAKE Viscotester 550 and RheoWin 4 job manager software at a constant temperature of 37° (water bath, HAAKE Viscotester DC10, Thermo Scientific).

The particle count method was adapted from Lousada-Ferreira et al. (2015). The sludge samples had to be pretreated by diluting the sample with permeate by a factor of 100, then sieved through a 90 µm sieve, and filtered filtrated though a paper filter with a pore size of 11 µm (Whatman Filter Paper Grade No 1). The PAMAS OLS4031 particle counter was used to measure the count of particles on a 5 ml sample. The average value of ten measurements is reported.

The Real flux measurement was adapted from Baudry et al. (2019) where the measured flux is recorded every 30 seconds for a period of 12 minutes. During the Real Flux Measurement the retentate and feed pressure are adjusted to induce the same pressure drop over the membrane as induced by the hydrostatic head in full scale. The real flux and its corresponding permeability are measured at 200 mbar TMP. It should be noted that cross-flow full-scale AnMBRs are usually operated at a TMP between 50-200 mbar (Baudry et al. 2019).

3.5 Analytical Methods

Solids and volatile fractions (TS, TSS, Vs, and VSS) of wastewater, buffer tank samples, sludge, and permeate were measured using standard methods (Association et al. 1915). Composition of volatile fatty acids (VFA) from C_2 to C_6 were determined by using gas chromatography (GC 7820A, Agilent Technologies) equipped with a silica column (25m and 0.53 mm internal diameter) and a flame ionization detector. Chemical Oxygen demand was determined with Hach-Lange kits. Soluble COD samples were prepared by centrifuging the sample at 6500 g followed by 0.45 µm filtration. The colloidal COD was calculated by subtracting soluble COD from the COD measured after 6500 g centrifugation followed by 1 µm filtration. Biogas composition (CO_2, CH_4 O_2 and others) was quantified using BIOGAS 500 (Biotechnical Instrument Ltd). Proteins were analyzed using Bicinchoninic acid kit (BCA protein assay, BCA1-1KT, Sigma Aldrich) following manufacturer protocol.

3.6 Membrane Maintenance

The clean water permeability (CWP) was done with water at 37 °C at a constant flux of 50 $Lm^{-2}h^{-1}$ and a cross flow velocity of 1 m/s. Permeate was collected for 2 minutes and the weight was recorded to calculate the actual flux and permeability. This was done in triplicates and the average flux and permeability were recorded.

Chemical cleaning in place (CIP) for the membranes were performed if the clean water permeability was below 250 $Lm^{-2}h^{-1}bar^{-1}$, or as needed for specific experimental purposes. A 1% chlorine solution was used to remove organics from the membranes. The chlorine solution was composed of 10ml/L of potassium hydroxide and 10ml/L of sodium hypochlorite. The chlorine solution was recirculated for 10 minutes and then left in the membrane for 20 minutes. This process was repeated until the concentration of the chlorine in the permeate was similar to the concentration of the solution. Citric acid solution was used to remove any inorganics in the membrane. The solution was composed of 10g/L of citric acid. Same cleaning procedure was followed as previously mentioned for the chlorine solution. The cleaning was stopped until the pH in the permeate was similar to the pH of the solution. Additionally, the clean water permeability was measured before any chemical cleaning, after cleaning with chlorine solution, and after cleaning with the citric acid solution to determine the flux recovery of the membrane.

3.7 Statistical Analysis

Multivariate principal component analysis (PCA) (Naessens et al. 2012, Wold et al. 1987)was performed to describe the correlation between the real flux and the sludge characterization data. A stepwise multiple linear regression was performed to determine the possible independent variables that can be used for estimation of the real flux. The model selection was based on the highest R-square value. The model then was simplified by taking collinearity into consideration. Statistical significance of the model was determined by using ANOVA with a confidence interval of 95% (p-value <0.05). All statistical analyses were performed using SPSS software (IBM SPSS Statistics, IBM,USA)

Chapter 4 Results

4.1 Summary of Reactor Biological Performance

Regardless of the fouling, the anMBR was able to treat the dairy wastewater successfully. Table 4.1 summarizes the COD removal and the biogas production for both experimental phases. Additional information on the biological performance can be found in Appendix A. The system was able to treat the dairy wastewater efficiently without any major complications.

Table 4.1 Summary of biological COD Removal and biogas production for both experimental phases.

Parameter	Phase 1	Phase 2
COD Removal (%)	99 (±1)	99 (±0.5)
Digestion Efficiency (%)	84.3% (±15.6)	86.3 (±7.6)
Biogas Production (L/d)	19.6 (±7.2)	23.5 (±6.2)
Methane Composition (%)	55.6 (±9.5)	60.74 (±10.3)

4.2 Characterization of Sludge Under Different Operating Conditions

The physiochemical characteristics of the anaerobic sludge were closely observed during the duration of the experiment. The changes over time of the different variables measured are reported in the following sections. Due to some limitations the results for the experimental phase 1 were restricted in comparison with the second experimental phase. Consequently, the results from the first phase did not add any additional weight to the final statistical analysis. Most of the results for the first experimental phase can be found under appendix A. However, some of the observations made during the first experimental phase remain relevant to this project. Those points are discussed in detail in the following section.

4.2.1 Operating Conditions of Experimental Phase One

The start-up phase for this experimental phase lasted 50 days. During the startup period the buffer tank was in place and the SRT was not fully controlled. On day 53 the buffer tank was removed, and the system was operated at a high SRT (74±14 days). The pH of the reactor was controlled at 6.86±0.17 with automated caustic (NaOH) dosing with a concentration of 2M. The changes of the sludge characteristics were closely observed after the removal of the buffer tank. From day 0 till 84 the helix membrane with a 5.2 mm diameter was on place. From day 84 till 90 the Helix membrane with 8mm diameter was in place. On day 109 a new Helix 8mm membrane was installed to look at the impacts of the sludge on a new membrane. The first experimental phase ended on day 110.

4.2.2 Sludge Characterization & Membrane Behavior for Experimental Phase One.

It was of interest to observe how the sludge behaved after the removal of a buffer tank at a high SRT. The average SRT after the removal of the buffer and until the end of the first experimental phase was 74± 14 days. Additionally, the feed pH was not controlled for this period. The average feed pH was 4.54±0.16. The reactor pH was controlled at 6.86±0.17, with automatized caustic dosing (molar concentration of 2). Over this period, some of the changes in the sludge seemed to have a clear impact on the filtration of the membrane.

Results

The concentration of solids had a cyclic behavior during this experimental phase ranging values in between of 10 and 20 g/L. This behavior was most likely caused by removal of sludge. This was true for the TS, VS, TSS, and VSS. However, the ratios of VS/TS and VSS/TSS stayed constant though the experimental phase. The results can be seen in Figure 4.1.

A)

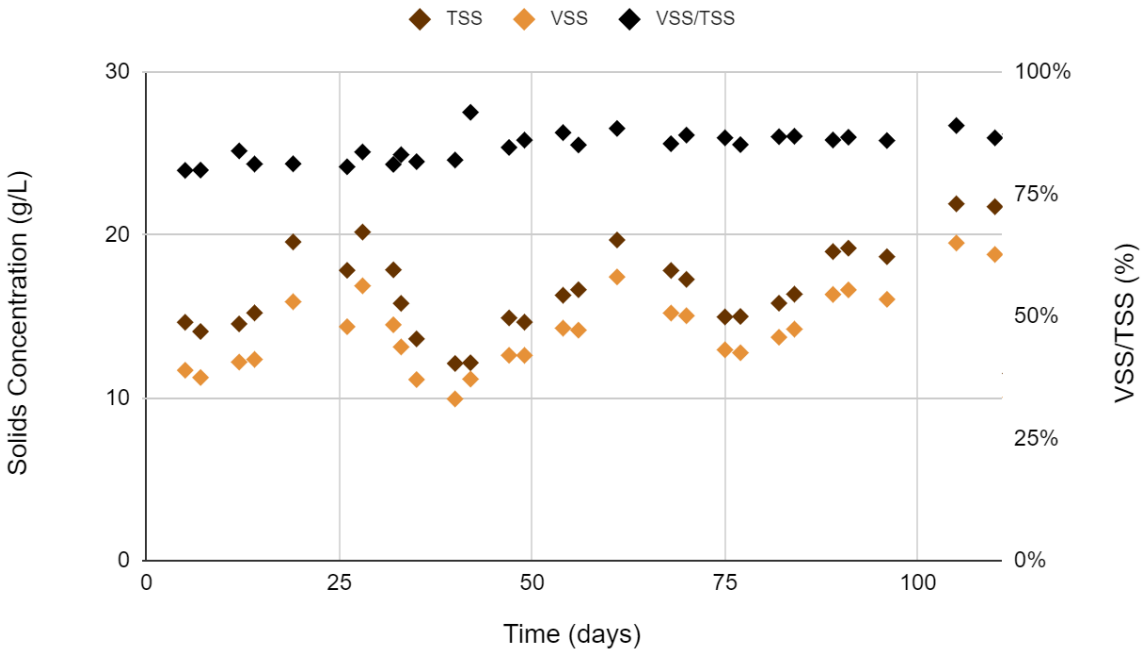

B)

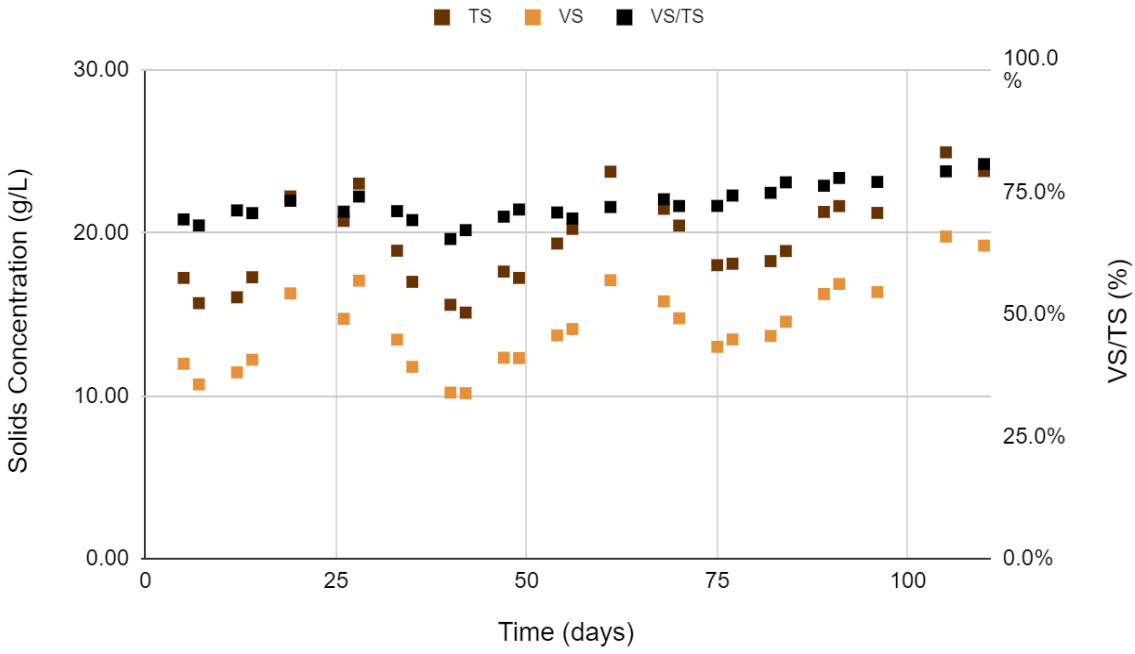

Figure 4.1 A) Total and volatile suspended solids and VSS/TSS ratio for experimental phase 1. B) Total and volatile solids and VS/TS ratio for experimental phase 1.

The values for the CST/TSS and the viscosity increased significantly after the removal of the buffer tank on day 53 (Figure 4.2.A). The high SRT could be the cause of this increase in CST and viscosity. The SRT has been reported to be the main parameter that affects the many of the biomass characteristics (Huang et al. 2011, Ng and Hermanowicz 2005). Additionally, the Colloidal and Soluble COD increased after the removal of the buffer tank, from day 53 until day 110 (Figure 4.2.B). This could also be explained because of the high SRT since it can lead to accumulation of non-biodegradable materials (Le-Clech et al. 2005).

A)

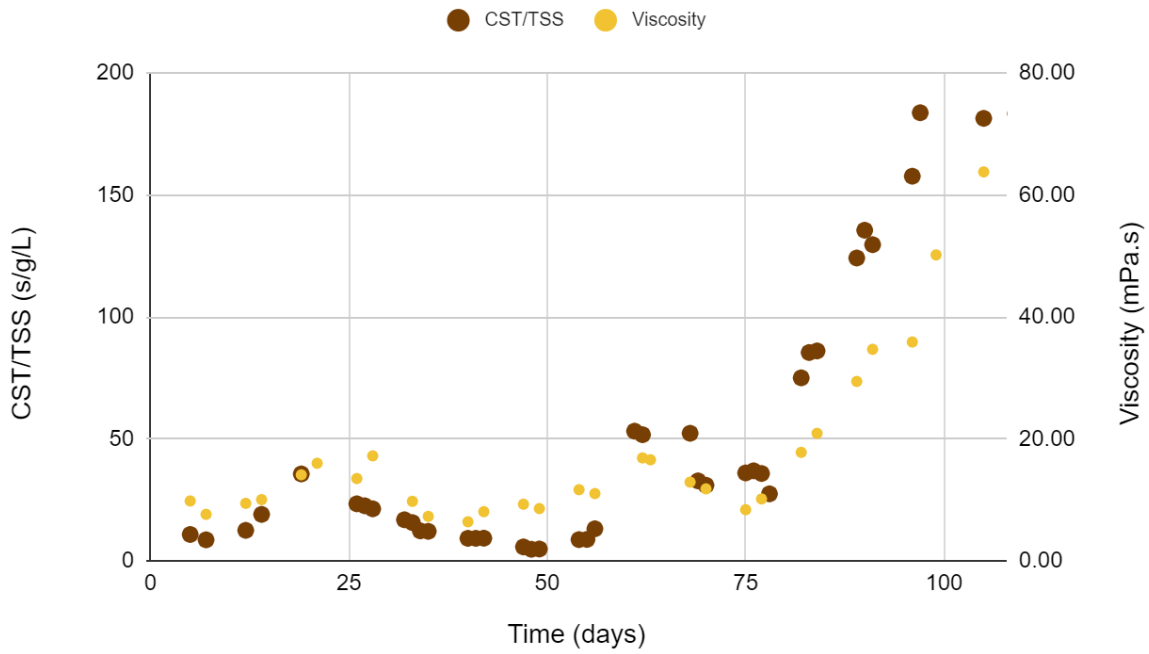

B)

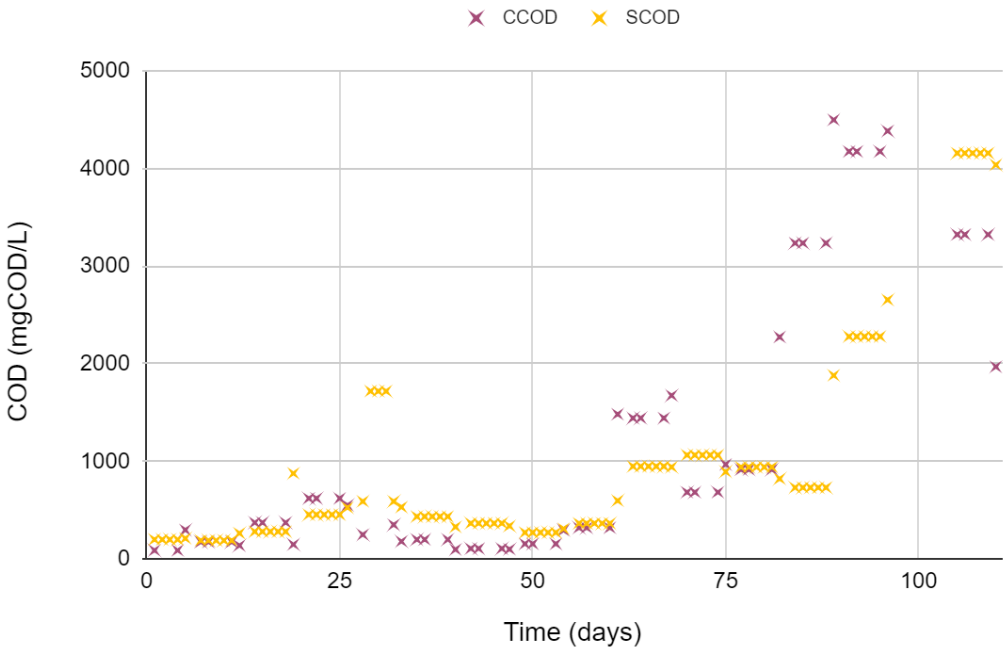

Figure 4.2 A) CST/TSS and Viscosity values during experimental phase 1. B) Concentration of soluble and colloidal COD during experimental phase 1.

There was an increase of particles smaller than 10 microns from the beginning till the end the experimental phase one. This can be seen from the particle count results (Figure 4.3). However, it is hard to determine the exact reason on why this increase in small particles happened in the first place. In terms of the filtration, the smaller particles could contribute to a more compact cake layer formation and/or pore blocking (Le-Clech et al. 2006, Petsev et al. 1993), additionally explaining why the flux decreased during this experimental period.

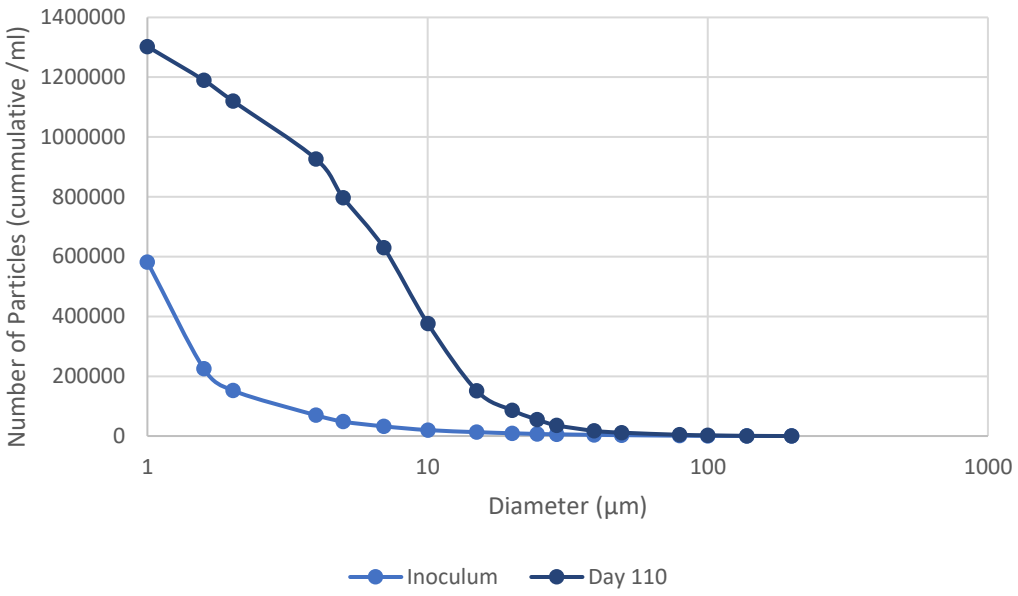

Figure 4.3 Results of particle count per volume for the inoculum sludge(day 0) and for day 100.

It was observed that the increase in CST and viscosity had an impact on the operation of the anMBR. As these variables increased the TMP pressure also increased consequently decreasing the permeability of the membrane. The reactor could not be operated at a crossflow velocity of 1m/s of higher, after the CST/TSS reached values higher than 100 s/g/kg and the viscosity higher than 50 mPa·s. The reactor had to be operated at lower cross flow velocities to avoid the TMP to increase over 1000 mbar. Figure 4.4 shows an increasing trend of operational TMP as the CST/TSS increases, and the changes of the TMP and CST/TSS over time. There is correlation between the operational TMP and the CST/TSS (Pearson coefficient =0.695 p-value <0.05). This suggest that the changes in the sludge characteristics have an impact on the TMP, which lead to a decrease in permeability. CST/TSS showed a correlation with the colloidal COD for this phase (Pearson correlation coefficient =0.802, p-value <0.05), this probably suggests that the increase in colloids cause pore blocking in the CST paper filter increasing the value of the CST. The increase of TMP in relation to the CST/TSS could be explained by either pore blocking due to an increase in colloidal particles or cake layer formation (Jiang et al. 2003).

A)

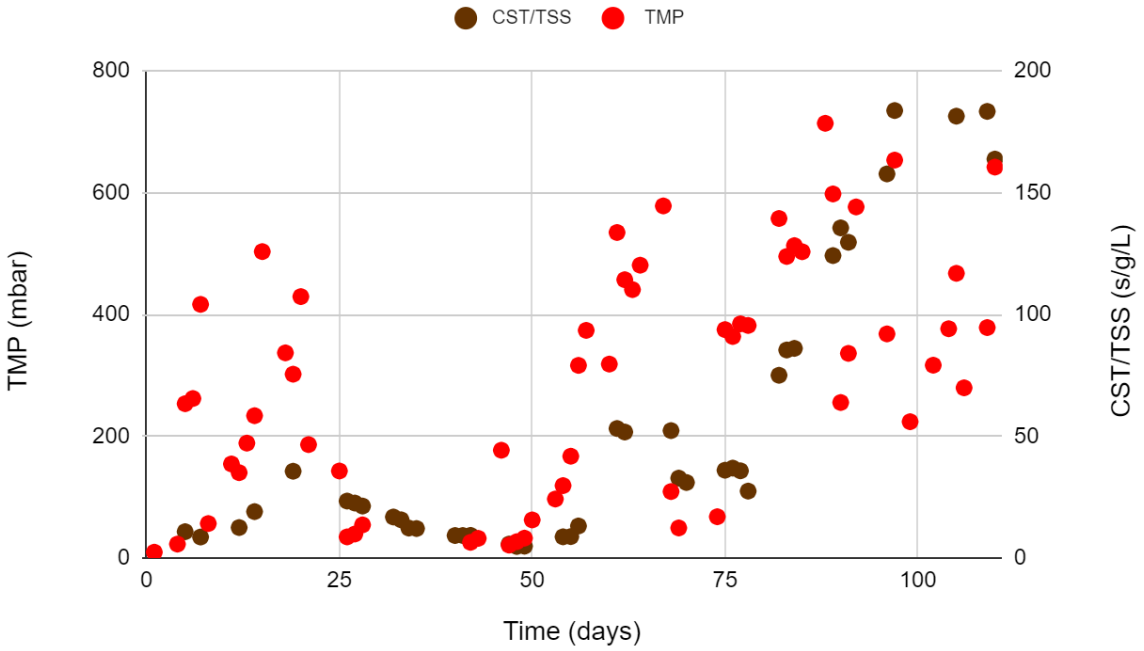

B)

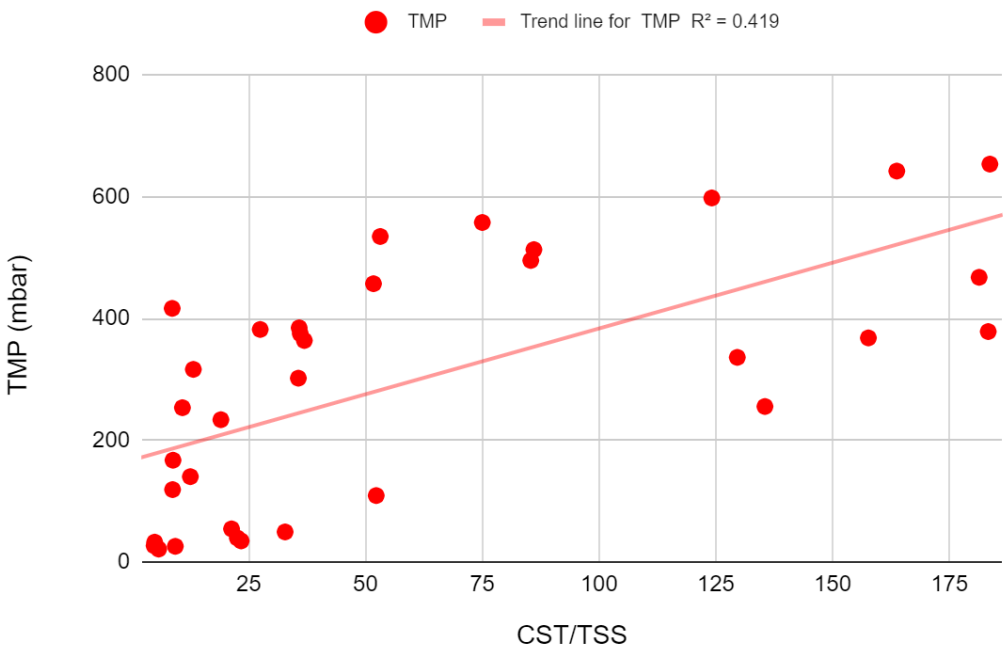

Figure 4.4 A) Operational transmembrane pressure and CST/TSS values for experimental phase 1. B) Operational transmembrane pressure plotted against CST/TSS for experimental phase 1.

Additionally, on Day 109 a new Helix 8mm membrane was installed to determine if system could be operated with a membrane with bigger hydraulic diameter (8mm) diameter when the values of CST/TSS (163.74 s/g/L) and the viscosity (70.68 mPa·s) were high. Changing the membrane did not help to mitigate the effects of the fouling caused by the sludge since the flux was 5.7 L/m^2·h, and the membrane still could not be operated at a crossflow velocity of 1 m/s. Since the decrease in flux was immediate, this could suggest that there was immediate fouling, most likely reversible fouling, was caused by blinding of the membrane

through pore blocking or compact cake layer formation. Additional mitigation techniques for reversible fouling like backwashing, membrane relaxation, or increasing the crossflow velocity were not effective due to the conditions of the sludge at this stage of the experiment.

4.2.3 Operating Conditions of Experimental Phase Two

A mixture of the inoculum sludge from the first phase (1.5 L) and waste anaerobic sludge from the first phase (7.5 L) was used for the start-up of the second experimental phase. The reactor was operated without a buffer tank from day 0 until day 43. The pH of the buffer tank was controlled at 5.3 ±0.12 with automated caustic dosing with a concentration of 2M. For this experimental phase, the Helix 8mm membrane and the Smooth 8mm membrane were interchanged as necessary for the filtration tests.

4.2.4 Sludge Characterization & Membrane Behavior for Experimental Phase Two

The total and particulate COD remained quite constant for the second experimental phase, while the Colloidal and Soluble COD had a more cyclic behavior. The results can be seen in Figure 4.5. The cyclic behavior of the CCOD and SCOD seemed to match the SRT (Approx. 30 days). These fractions of COD increased throughout and then decrease at the end of the SRT.

A)

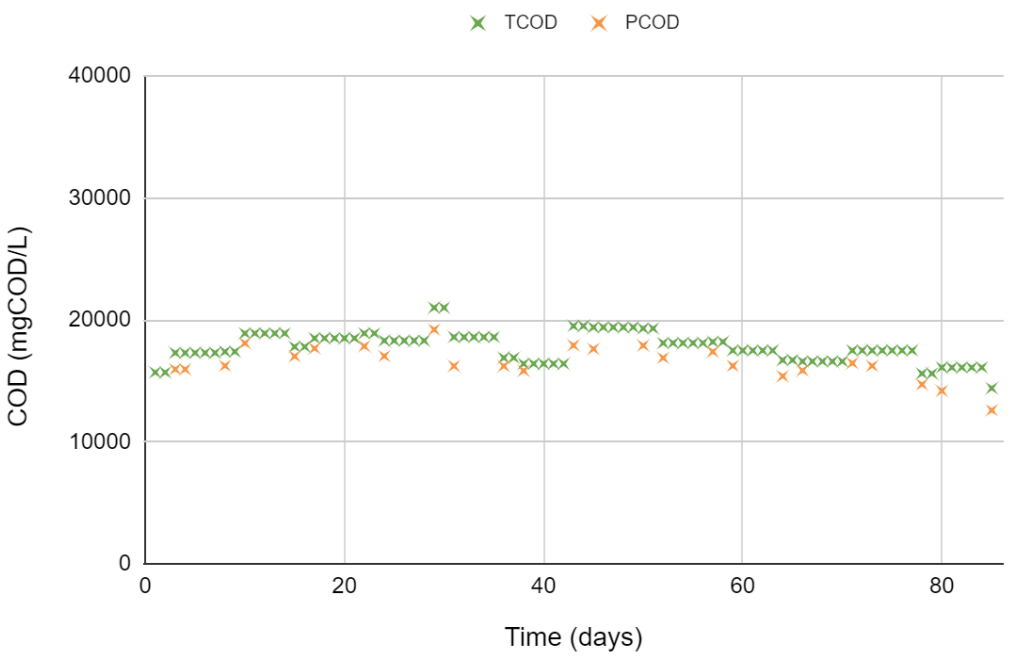

B)

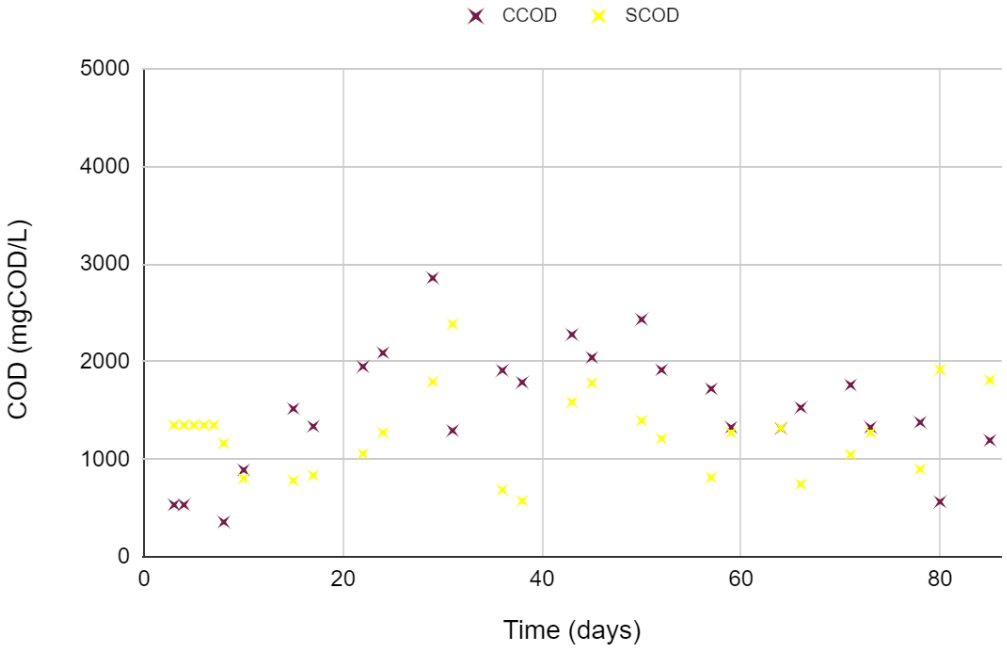

Figure 4.5 A) Total and particulate COD during experimental phase 2. B) Colloidal and soluble COD during experimental phase 2.

The solids contents (TS, VS, TSS, and VSS) did not fluctuate a lot as in the first phase and remained relatively stable through the entire second phase in terms of concentration with values ranging between 10 and 13 g/L (Figure 4.6). Having a lower SRT most likely helped with the prevention of solids accumulation. However, the VSS/TSS ratio increased after the addition of the buffer tank on day 43. The low SRT and the pre-acidified wastewater at a pH of 5.3 might have promoted the growth of acidifying bacteria (Henze 2008, Yu and Fang 2002). This could

A)

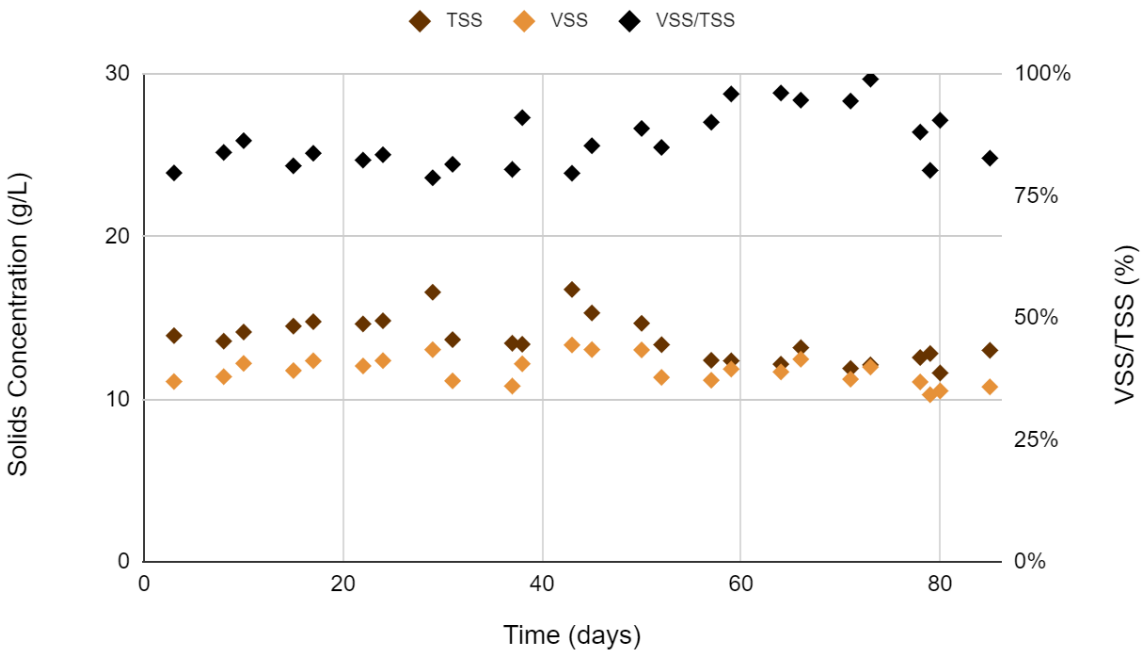

B)

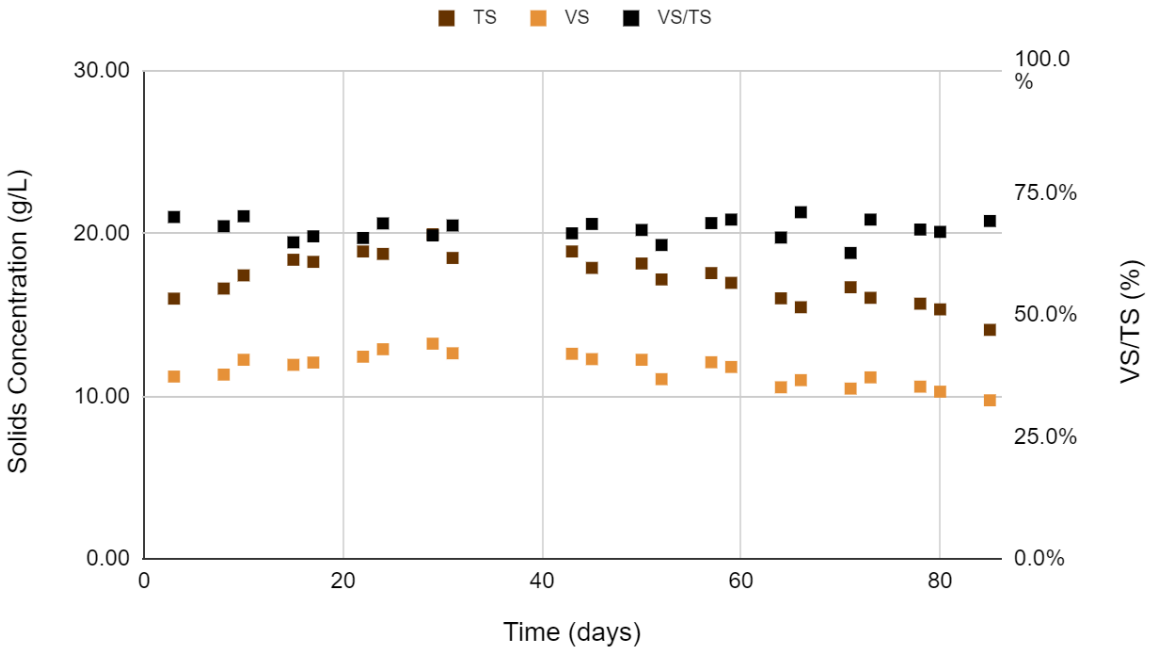

Figure 4.6 A) Total and volatile suspended solids concentration and VSS/TSS values for experimental phase 2. B) Total and volatile solids concentration and VS/TS values for experimental phase 2.

explain the increase of the VSS/TSS ratio. The VS/TS ratio remained constant throughout the phase.

The CST/TSS and the viscosity had a similar cyclic behavior as the Colloidal and Soluble COD (Figure 4.7). The washout of colloids and inert material due to the SRT could be the explanation of why the CST/TSS and viscosity did not increase as much, in comparison with the first phase (Dereli et al. 2014a). Note that in the first 40 days, when the system was operated without the buffer tank, the CST/TSS and the viscosity did not increase as much in comparison with the first phase. The increase of the CST and viscosity in the first phase is most likely attributed to the high SRT which caused an increased in colloidal particles, rather than the removal of the buffer tank. This additionally shows the importance of the impact of the operational parameters on the characteristics of the sludge. During the startup of the reactor, it is important to select the right operational parameters, for the sludge to acclimatize properly and to get a sludge that is good in terms of filtration and biological performance (Cho et al. 2005). The periods of this study were not long enough to determine the right conditions to determine the best operational parameters to get the best sludge in terms of filtration, but it does show the importance of the operational parameters.

A)

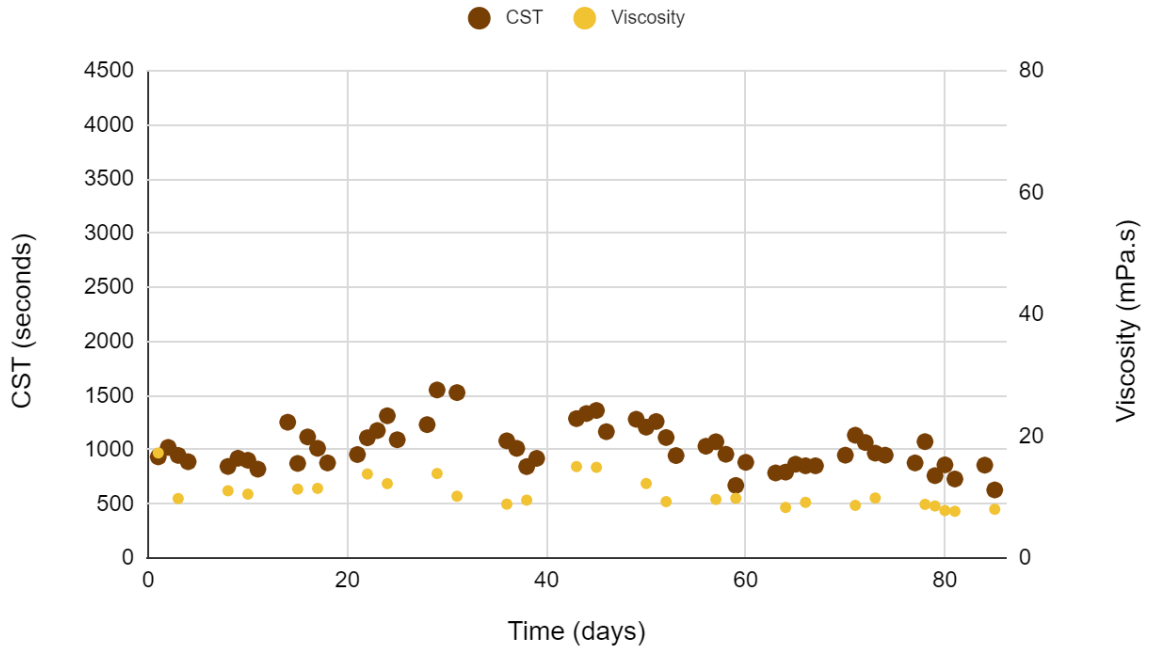

B)

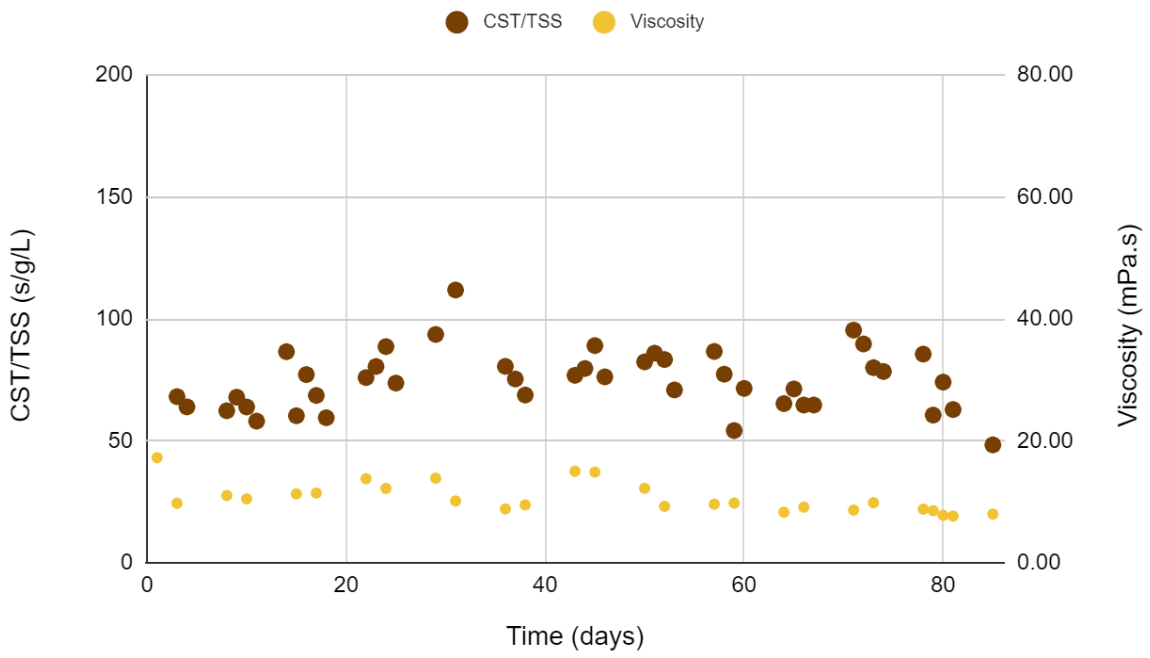

Figure 4.7 A) CST and viscosity values for experimental phase 2. B) CST/TSS and viscosity values for experimental phase 2.

The particle size distribution of the sludge seemed consistent until the addition of the buffer tank (Figure 4.7.A). After the addition of the buffer tank the particles smaller than 10 micrometers decreased, but then they started to slowly increase again. The supernatant particle size distribution clearly shows an increase in particles smaller than 10 micrometers after the addition of the buffer tank (Figure 4.7.B). The shift in the particle size distribution could also be explained if there was growth of single celled organisms, due to the changes in the substrate and pH in the buffer tank.

A)

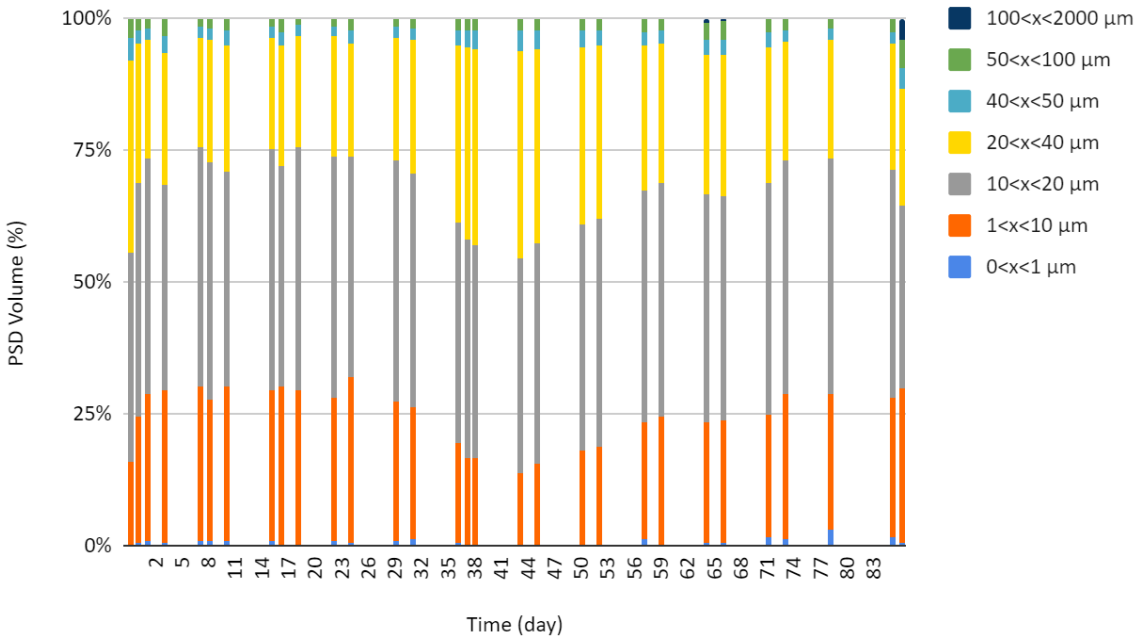

B)

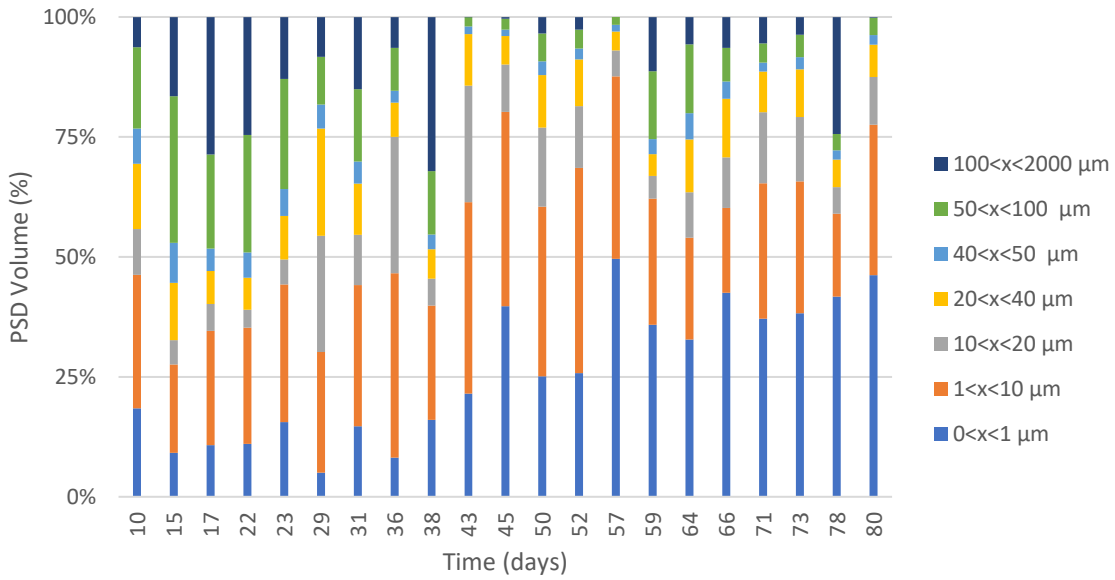

Figure 4.8 A) Particle size distribution for the sludge B) Particle size distribution for the supernatant.

No clear observations or conclusions were made from the results of the particle count per volume, because it showed barely any changes throughout the entire phase. Figure 4.9 shows the cumulative content of particles between 0 and 10 microns through the different days of the second phase. Note that the inoculum sludge was partly composed of waste anaerobic sludge from the first phase. This sludge already contained high amounts of smaller particles in comparison the inoculum sludge from the first phase.

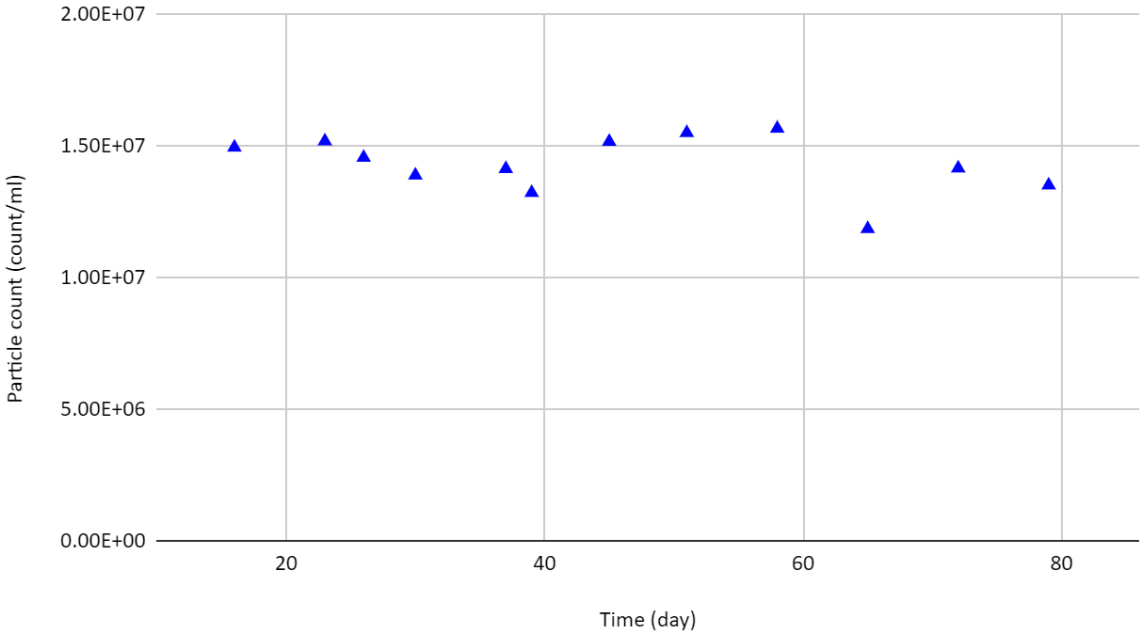

Figure 4.9 Cumulative particle count per volume of particles between 0 and 10 µm during experimental phase 2.

The specific resistance to filtration and the calculated total resistance results are shown in Figure 4.10. The SRF increased after the installation of the buffer tank (day 43). This could be explained by the increase in particles between 0 and 10 microns in the supernatant, as seen in Figure 4.11.A. Another possibility that could contribute to a more compact cake layer is the presence of filamentous bacteria and irregular flocs, these are more prone to accumulate in membrane surfaces (Meng et al. 2006b, Zhang et al. 2012).

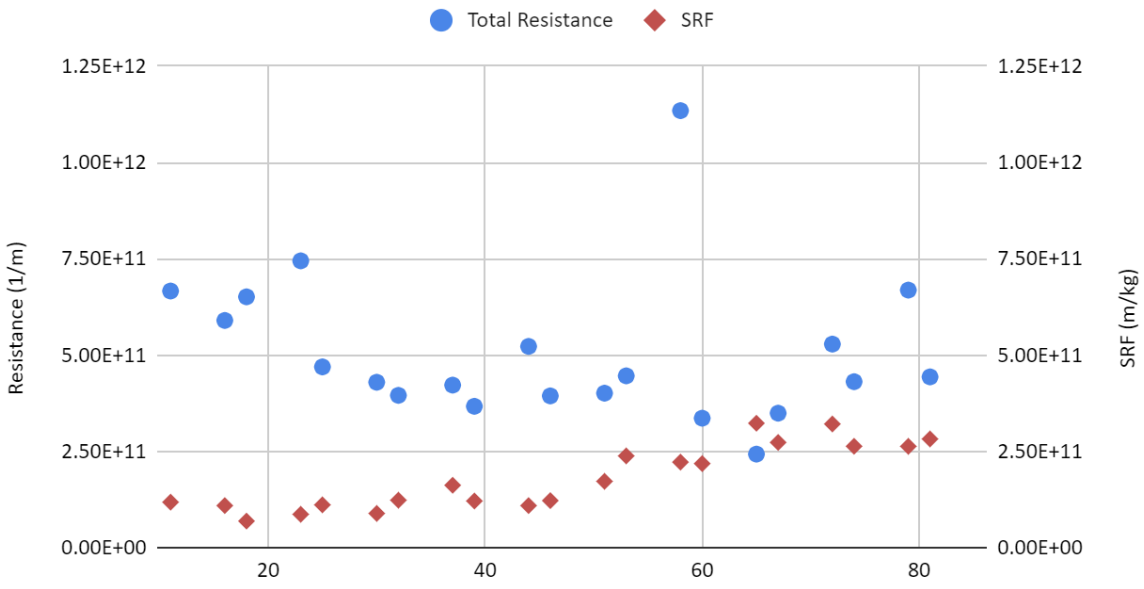

Figure 4.10 Total membrane resistance and specific resistance to filtration for experimental phase 2.

An increase of proteins in the supernatant was observed after the installation of the buffer tank (Figure 4.11.B). A study concluded that around 41% of protein was degraded at a pH of 5.5 and at a hydraulic retention time of 12 hours (Yu and Fang 2002). The buffer tank was operated at a pH of 5.3 and HRT was maintained around 6 hours. There might have resulted in less degradation of proteins once the buffer tank was installed, so this could indicate

A)

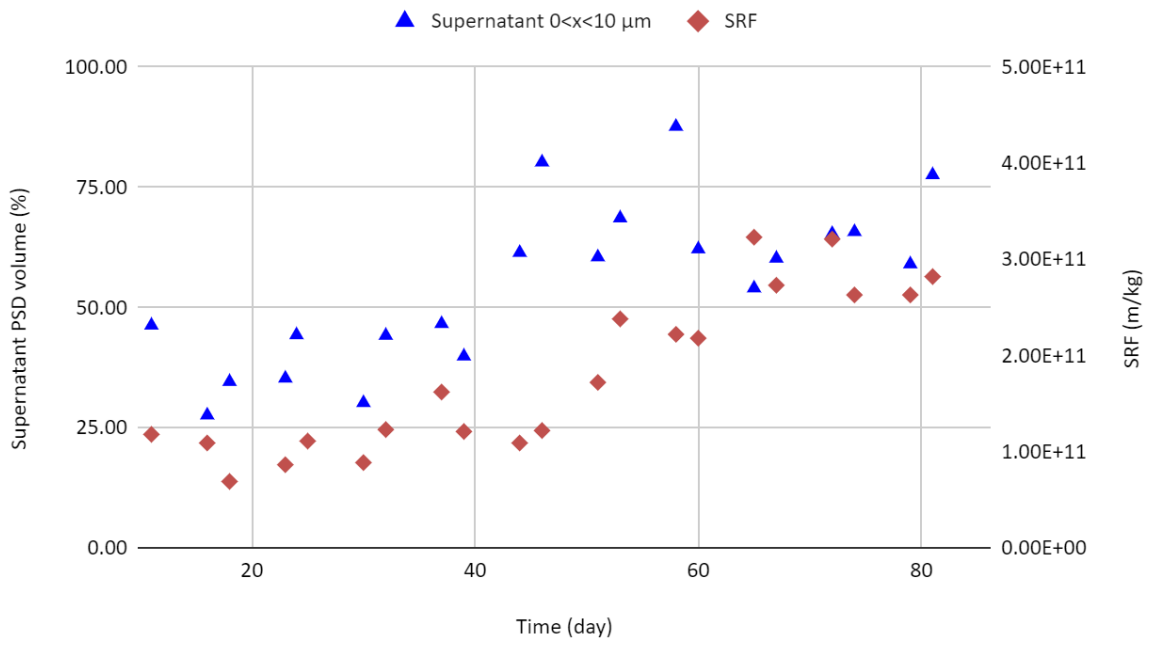

B)

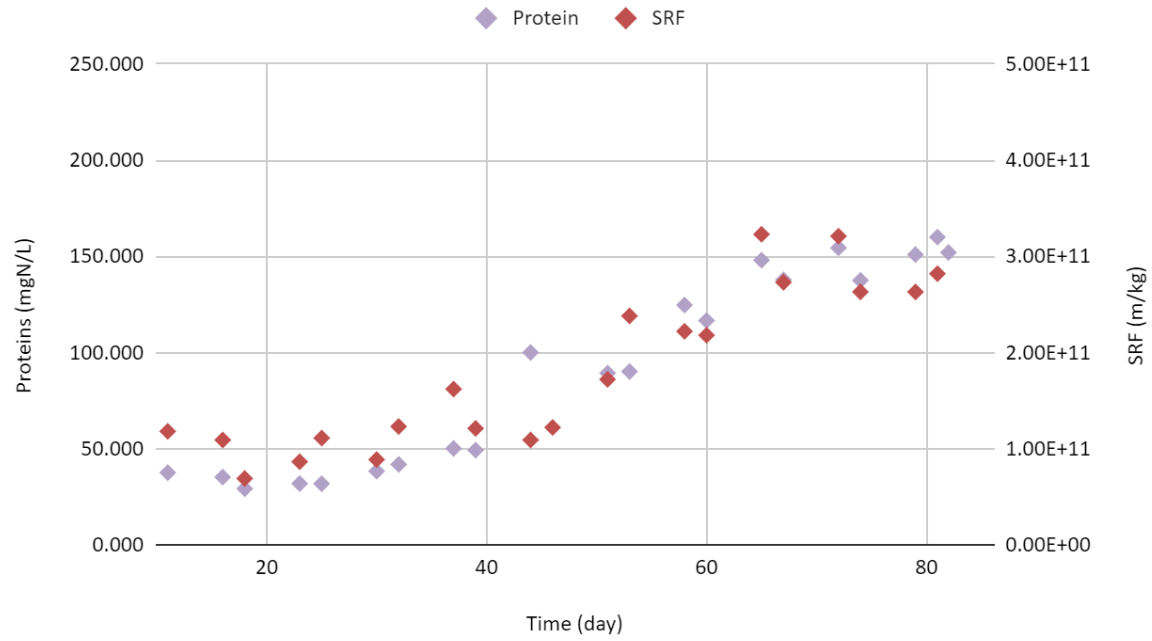

Figure 4.11 A)Specific resistance of filtration and increase of particles below 10 microns in the supernatant for experimental phase 2. B) Protein content and specific resistance to filtration for experimental phase 2

why there was an increase of proteins after the installation of the buffer tank. Additionally, as seen in the figure the trend of proteins and SRF was very similar. The proteins might have also

attributed to the resistance in the cell, proteins are complex compounds and their interaction with the membrane could be more complicated, so it's hard to conclude the exact degree of impact of the proteins on the membrane (Fane and Fell 1987, Marshall et al. 1993). Globular proteins with the same molecular weight of the membrane can be retained (Baker 2012). Whey protein, which is one of the most common proteins in dairy wastewater, can be found in globular form (Fox et al. 2004), so the protein content in this type of wastewater might be an attributing factor to the fouling of the membrane.

The supernatant filterability varied before the installation of the buffer tank, but once the buffer tank was installed, the supernatant filterability remained constant (Figure 4.12). There was no clear observation or correlation (correlation matrix in Appendix B) that could give a clear explanation on the changes in the supernatant filterability over time.

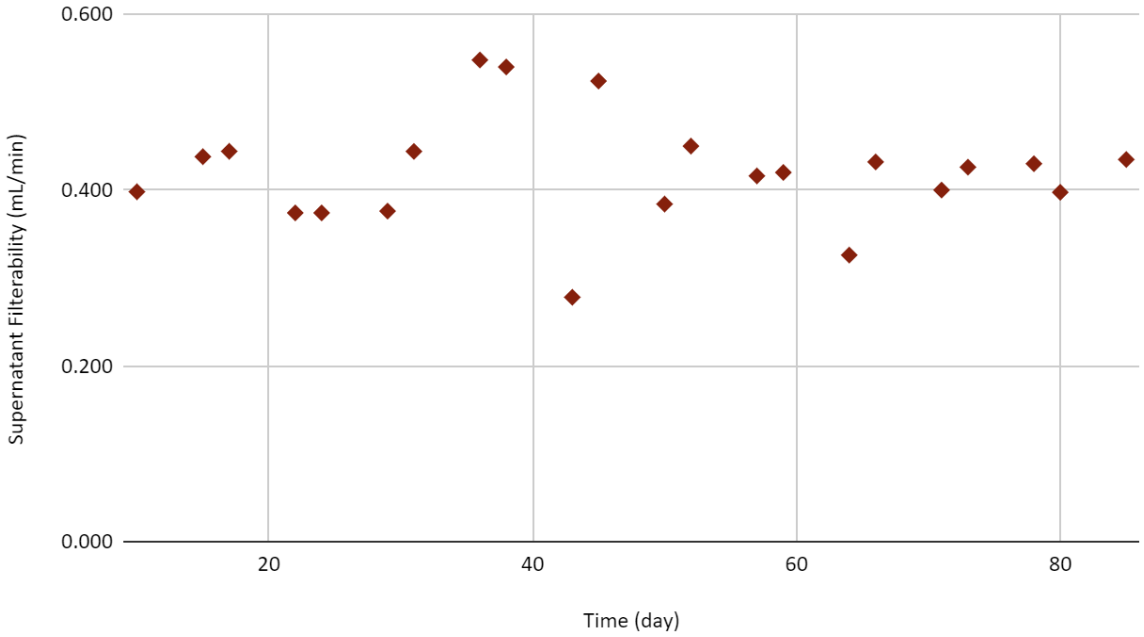

Figure 4.12 Supernatant filterability for experimental phase 2.

Overall, the operation of the membrane was more stable in comparison with the first experimental phase. Figure 4.13 shows the TMP and permeability of the membrane during the second experimental phase. The operation was done in reference to the real flux measurement

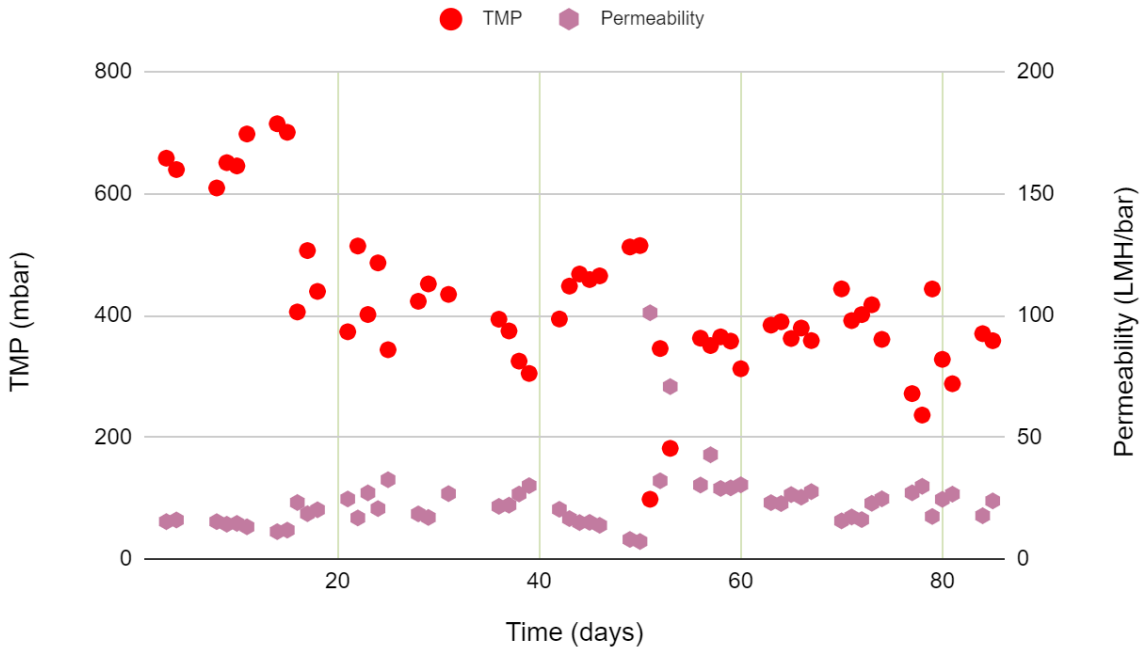

Figure 4.133 Operational TMP and operational permeability for experimental phase 2

rather than the critical flux. The reactor was operated at values under the measured real flux. This suggests that the real flux measurement might also be a good parameter to make decisions for the operation of the system since the purpose of this method is to replicate the operation conditions of full scale anMBRs. Additional studies should be done to compare the real flux and the critical flux to determine if one parameter can give you better insight for operation.

The SRT seemed to be one of the controlling parameters that affected most of the sludge variables, this has also been concluded in other studies (Dereli et al. 2014a, Le-Clech et al. 2006). As a result, there was less accumulation of colloidal material and a more constant concentration of solids. This might also suggest that the different types of solids play an important role on the filtration and fouling the membrane and that the SRT could be used to control them (Chew et al. 2020).

4.3 Cleaning in Place & Clean Water Permeability Observations

The cleaning in place provided some insight on the fouling of the membrane. From the original clean water flux of the new membrane about 59.61% was lost to fouling, most likely pore blocking. But after chemical cleaning with the chloride solution, 99.78% of the original flux was recovered, resulting in only 0.22% of irreversible flux. No extra significant improvements in the flux were observed after cleaning the membrane with citric solution. This suggest that most of the membrane fouling was attributed to biofouling.

4.4 Correlation Analysis for Real Flux measurements & Normalized CST variables

For these experiments it was of interest to determine if there was a relationship between the CST/TSS, CST/Viscosity, and CST/TSS/Viscosity with the Real Flux measurements. From the data collected all three parameters seemed to have a linear correlation, however the CST/TSS seemed to have more correlation among the three normalized variables. Table 4.2 shows the Pearson's correlation coefficient for the scenarios tested for both 8 mm Helix and 8 mm Smooth membrane. Most of the values had a confidence interval of 95% (p-value <0.05), apart from the values for the helix membrane at 1.5 and 1.8 m/s. For these cases, more data points are needed to determine if there is a strong correlation. Regardless of the lack of correlation, the same trend was observed, where there was a decrease in flux as the normalized CST variables increased.

Table 4.2 Pearson correlation coefficients for real flux and normalized CST values. (*) No statistical significance p value > 0.05.

Smooth 8 mm Membrane			
Crossflow velocity	CST/TSS	CST/Viscosity	CST/TSS/Viscosity
1.0 m/s	-0.776	-0.742	-0.791
1.2 m/s	-0.821	-0.726	-0.737
1.5 m/s	-0.856	-0.791	-0.691
1.8 m/s	-0.943	-0.809	-0.770
Helix 8 mm Membrane			
Crossflow velocity	CST/TSS	CST/Viscosity	CST/TSS/Viscosity
1.0 m/s	-0.776	-0.625	-0.555
1.2 m/s	-0.749	-0.657	-0.598
1.5 m/s	-0.902	-0.739	-0.506*
1.8 m/s	-0.656	-0.602	-0.527*

From these tests it was also determined that higher crossflow velocities would not yield much more flux when the values of the normalized CST variables are high. Figure 4.14 shows the results of the flux vs the CST/TSS at four different crossflow velocities for both membranes.

A)

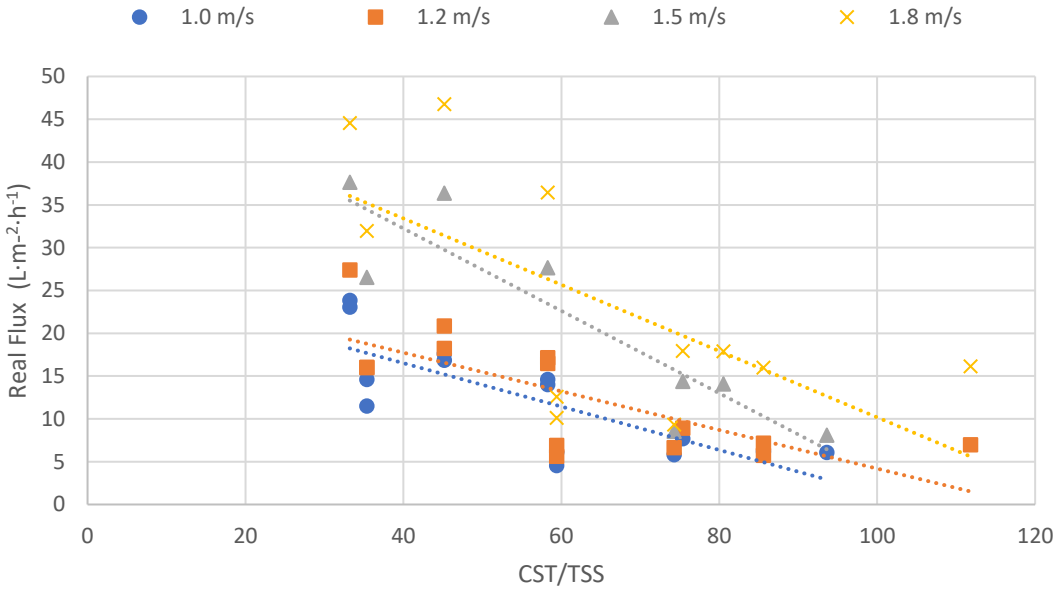

B)

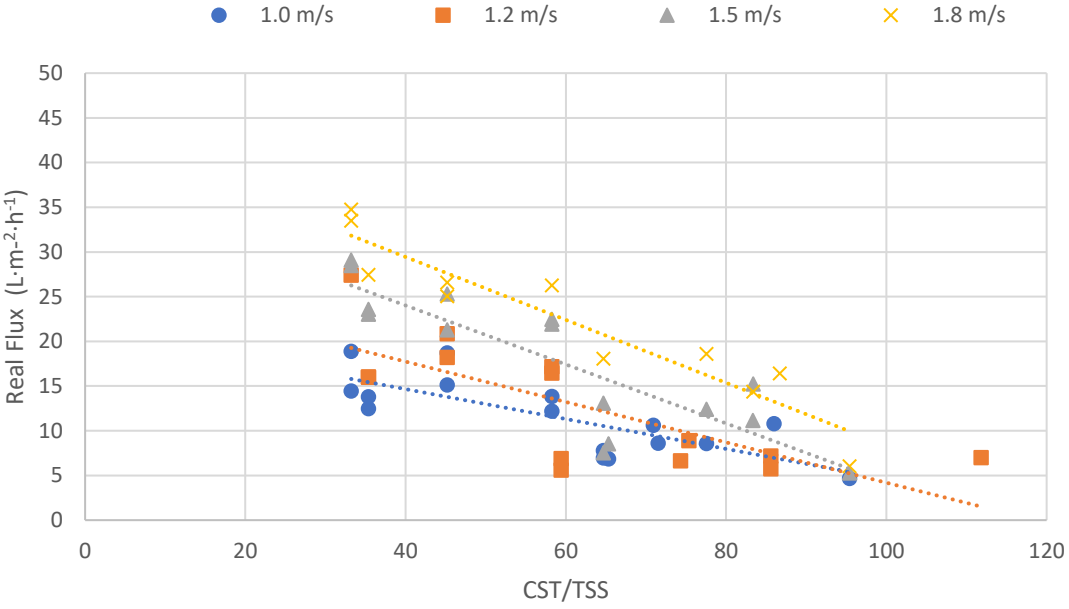

Figure 4.14 A) Real flux vs CST/TSS for helix 8mm membrane at different crossflow velocities. B) Real flux vs CST/TSS for smooth 8 mm membrane at different crossflow velocities.

4.5 Principal Component Analysis & Multiple Linear Regression for Sludge and Filterability

The principal component analysis was used to determine if there are any hidden relationships between the sludge variables and the real flux. The results obtained from the PCA were later used for a multiple linear regression to create an empirical linear model to predict

the real flux. Figure 4.15 shows the result of the PCA for all the variables in question. Five principal components were extracted based on an eigenvalue higher than 1, which attributed to 91% of the variance of the data. Table 4.3 shows the grouping of the variables in respect to each of the components. The variables are ranked from high to low correlation to their respective extracted component. The cutoff for the correlations selected was 0.5. The percentage in parenthesis is the variance from each component. The principal component (PC) 1 consisted of fraction of solids (total dissolved solids, VSS/TSS, and fixed suspended solids), the CST, and the normalized versions of the CST (CST/TSS, CST/Viscosity, CST/TSS/Viscosity). Five of the variables in PC1 are derived from the TSS concentration most likely indicating why they were grouped under this principal component. PC2 consisted of the particle size distribution of particles ranging from 0 to 10 micrometer. PC3 consisted mainly of a different fraction of solids (VSS, VS, TS, and TSS) and SRF. SRF is a function of TSS, this can explain why these variables were grouped together in PC3. PC4 consisted of the soluble and colloid particles. PC5 consisted of the hydrostatic conditions of the membrane.

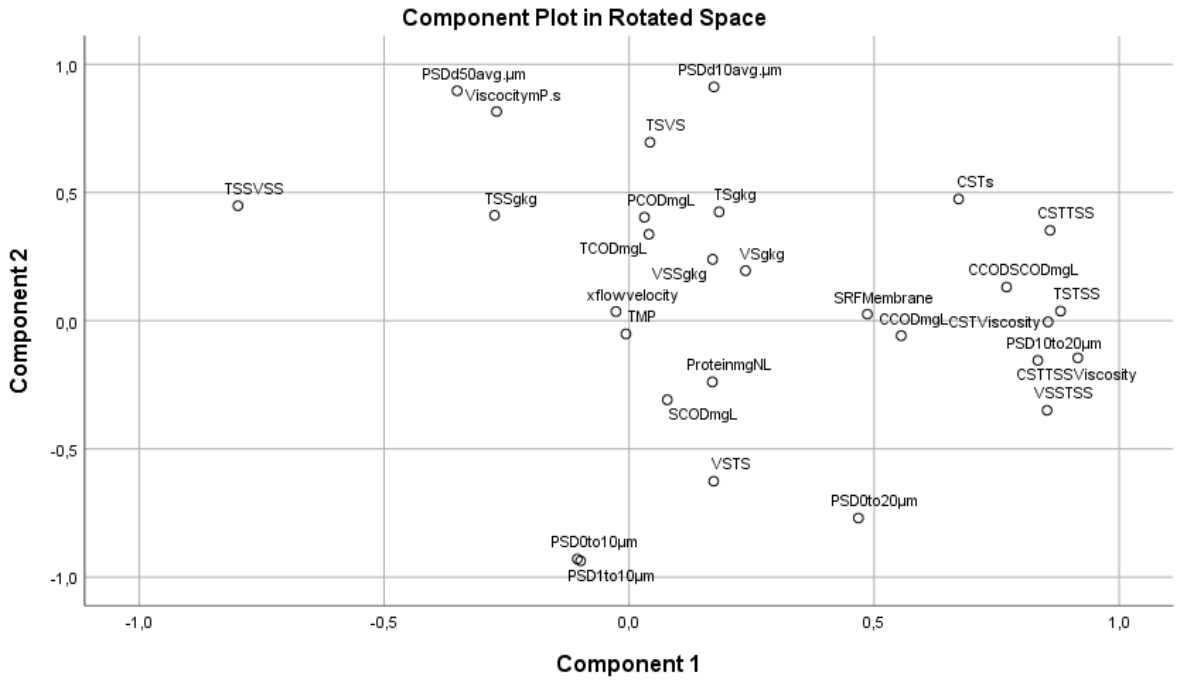

Figure 4.15 Component plot rotated in space for sludge characterization variables related to real flux tests.

Table 4.3 Extracted principal components and variables grouped to their respective component.

Component	**1 (25.7%)**	**2 (24.6%)**	**3 (23.7%)**	**4 (12.6%)**	**5 (3.7%)**
Group "Type"	Normalized CSTs and Solids	PSD, viscosity, and solids	Solids, SRF, and total and particulate COD	Protein, Soluble and Colloidal COD	Hydrostatic Conditions
Variables	CST/VSS/Viscosity Total dissolved solids CST/TSS CST/Viscosity VSS/TSS	PSD 1<x<10 µm PSD 0<x<10 µm PSD d10 µm PSD d50 µm Viscosity	VSS VS TS SRF PCOD	Protein SCOD CCOD (0-1µm) VS/TS	TMP Crossflow Velocity

	PSD 10 <x<20 µm Fixed suspended solids CCOD (0.45-1µm) CST CCOD (0-1µm)	Fixed solids VS/TS	TCOD CST TS-VS	CCOD (0.45- 1µm)

A multiple linear regression with the real flux as the dependent variable and the component scores as the fixed values was done to determine the statistical significance of doing an empirical linear model. The ANOVA results showed statistical significance with a confidence interval higher than 95% (p-value < 0.05).

A stepwise multiple linear regression analysis was done to identify the independent variables needed for the model to estimate the real flux. Equation 4.1 shows the output equation for the model prediction for the real flux. The model has an R square value 0.883, and the empirical coefficients for each variable had a confidence interval higher than 95%.

Equation (4.1)

$$\textbf{\textit{Real Flux}} = 120.867\text{-}0.176 \times \textbf{\textit{CST/TSS}} + 13.056 \times \textbf{\textit{Crossflow velocity}}\text{-}1.505E\text{-}11 \times \textbf{\textit{SRF}}\text{-}132.965 \times \textbf{\textit{VSS/TSS}} + 21.195 \times \textbf{\textit{VS/TS}} + 0.002 \times \textbf{\textit{CCOD (0.45-1 µm)}}\ \text{-}5{,}966 \times \textbf{\textit{TSS-VSS}} + 0.004 \times \textbf{\textit{TMP}}$$

This model was selected without taking into consideration the collinearity between each variable, in order to find the variables that would give the best flux prediction from the data obtained. Equation 4.1 was simplified to equation 4.2 once collinearity was taken into consideration. For this model, the R square value was 0.806 where the confidence interval for each coefficient was higher than 95%. For the CST/TSS, crossflow velocity, SRF and VS/TS the Variance Inflation Factors were 1.038, 1.008, 1.041, and 1.002, respectively.

Equation 4.2

$$\textbf{\textit{Real Flux}} = 6.710 - .227 \times \frac{\textbf{\textit{CST}}}{\textbf{\textit{TSS}}} + 14.067 \times \textbf{\textit{Crossflow velocity}} - 1.917 \times 10^{-11} \times \textbf{\textit{SRF}} + 12.085 \times \textbf{\textit{VS/TS}}$$

This model provides the independent variables that can be used to characterize the flux while also taking into consideration the impact of the fouling caused by the characteristics of the sludge. However, the R square value for this model is relatively low, the standard error of the estimate is 3.34624. This model partly answers the question of what variables could be the most important to characterize the membrane filtration and fouling. Based on the calculated standardized beta coefficients the CST/TSS and the crossflow velocity contribute to the most to the estimation of the real flux, followed by the SRF, and the VS/TS is the variable contributing the least.

Chapter 5 Discussion & Limitations

5.1 Real Flux Model

The statistical analysis showed that the CST/TSS, the crossflow velocity, the SRF and the VS/TS can be used as indicators to predict the flux and consider the impacts of fouling. It is important to understand the relationships and mechanisms of these variables to the flux to understand why they are good indicators for predicting the flux. The crossflow velocity is a well-studied variable where it is expected that a higher crossflow velocity will yield a higher flux. This increase of flux is caused by the an increase in shear forces that which enhances shear induced diffusion (Lee and Clark 1998). On the other hand, there are practical limitations to applying higher crossflows, such as higher energy cost. As well a higher crossflow can lead to higher TMP values which leads to lower permeability. Other studies also have shown that there can be other negative impacts on the sludge caused by the crossflow velocity, like continuous reduction of the particle size and disruption of flocs due to the shear forces (Choo and Lee 1998, Jeison et al. 2009, Le-Clech et al. 2006). Moreover, as presented earlier in Figure 4.14, the results showed that a high crossflow velocity might not necessarily yield a higher flux, depending on the characteristics of the sludge.

The CST is a well-studied parameter for the dewaterability of the sludge. As seen in this study the CST/TSS was correlated to the viscosity (Pearson coefficient=0.72, p-value<0.05) and the colloidal COD (Pearson coefficient=0.84, p-value< 0.05), and this has also been reported previously in literature (Vesilind 1988). A study showed that the content of colloidal and soluble matter had a significant impact on the fouling and filtration of the membrane (Rosenberger et al. 2006). For the characterization and prediction of the flux the CST/TSS might be better parameter than the CCOD or SCOD, since the CST/TSS is has shown good correlation to these parameters as well as with the viscosity. This suggests that the concentration of colloidal particles have an impact on the CST measurement. The colloidal particles might cause clogging on the paper filter increasing the final measurement of the CST. The solids concentration also impacts the results of the CST as well as the fouling of the membrane (Rosenberger et al. 2006, Vesilind 1988). This could explain why the CST/TSS was a better indicator for predicting the flux than just the CST. The CST/TSS/Viscosity also showed to be a good indicator for the prediction of the flux, however this variable also showed good linear correlation with the SRF. From a modeling aspect this can be an issue because of the collinearity between the SRF and the CST/TSS/Viscosity. The CST and the CST/TSS also showed some correlation with the SRF, but it was not a good linear correlation. Results of the correlation coefficients between all the studied variables can be found on Appendix B.

The specific resistance to filtration replicates the impacts of the cake layer formation on the membrane. However, the test is done in a dead-end filtration cell so, the behavior of the cake layer formation on the membrane in crossflow configuration might be different. On the other hand, it gave more insight on the behavior of the sludge, as it showed that an increase in particles smaller than 10 micrometers caused an increase in resistance. Additionally, it is also possible that the protein content can have an impact on the SRF. The changes in the particle size distribution of the sludge and supernatant clearly showed an impact on the SRF. The SRF could be a good indicator that an increase in particles smaller than 10 micrometers is

negatively impacting the filtration of the membrane. The smaller particles could either cause pore blocking or also create a more compact cake layer that has less porosity, therefore increasing the hydraulic resistance on the membrane. From an operation point of view, it could give us an insight that the sludge is changing, from this study it could indicate that there is an increment in smaller particles. Therefore, a more adequate mitigation technique can be selected for the operation of the membrane (e.g. increase backwash time or add polymer to increase the particle size)(Odriozola et al. 2020).

The VS/TS ratio was an interesting parameter obtained from the multiple linear regression. From the variables of the solid contents, it seemed to have the most impact on the estimation. From the model it can be concluded that as the ratio decreased the flux decreases, meaning that the higher content of inorganic solids causes more fouling. From this study it was hard to draw any conclusions about the fouling caused from the inorganic solids. In cheese wastewater the calcium and salt content has been reported to be detrimental to the membrane (Dereli et al. 2019, Zhang et al. 2018, Zhang et al. 2017), fouling caused by scaling from inorganic solids was not observed in this study. However, it is likely that inorganic foulants such as calcium to be present in the cake layer as seen in Dereli et al. (2019). The exact impact from this variable could be more complicated than expected, since we know from literature that the impact of solids concentration on the fouling can vary (Chew et al. 2020, Le-Clech et al. 2006).

The model helped narrowing down the variables that can be used as indicators to characterize the flux and the fouling, but there are some limitations that need to be taken into consideration. As mentioned, the model presented in this study can still be refined by looking at various variables that were not studied in this research. Extra study can be done to look at extra variables that were not investigated in this study (e.g. relative hydrophobicity, EPS, SMP, etc.), to determine if there are extra variables that can increase the accuracy of this empirical model. Van den Broeck et al. (2011) developed an empirical parameter between the hydrophobicity and the sludge morphology to determine an estimation of sludge filterability. This parameter alone was not able to provide a more accurate estimation of the actual sludge filterability, and concluded that more detailed measurements would be needed (Van den Broeck et al. 2011). This study did not take into consideration the relative hydrophobicity and the sludge morphology; therefore, the empirical parameter developed by Van den Broeck et al. (2011) could be a good complement to the model regression presented in this study.

There are other limitations for the model that need to be taken into consideration. The model was only done for one type of membrane and one type of wastewater. The impacts of different membranes and module configuration needs to be taken into consideration. Different types of wastewater can also have different impacts on the characteristics of the sludge. These limitations are discussed further in the following sections.

5.2 Membrane Comparisons

This statistical analysis was done only for the results of the smooth 8 mm membrane. A membrane comparison test between the helix 8mm membrane and the smooth 8 mm membrane showed to have different results for the flux when the membranes were compared with the same sludge, at the same crossflow velocities, and with less than 5% difference of

clean water flux (Appendix D). Even though both membranes had the same hydraulic diameter, surface area, and nominal pore size, the difference of flux between the membranes was most likely caused by the different flow conditions due to the different shape of the inside lining of the helix membrane. The results presented from the multiple linear regression are exclusive for the smooth 8 mm membrane. The model still needs to take into consideration different physical characteristics of membranes in crossflow configuration.

A possible approach to this problem would be to incorporate the flow conditions (i.e. Reynolds number) when comparing membranes with same nominal pore size but with different hydraulic diameters. Additionally, a proper mathematical approach needs to be developed to estimate the turbulent flow conditions for non-Newtonian fluids for the helix technology developed by Pentair plc. Comparing different membranes can also be a challenge due to irreversible fouling, the best approach to compare the membranes was to do all the flux test for both membranes on the same day to try to have the same sludge conditions for both membranes and when the tests are done, to ensure to remove the sludge with water and to perform a CIP immediately. For more practical recommendation it would be optimal to ensure to have one membrane for continuous operation of the system and use different membranes for the comparison test. This might provide good insight on how different membranes behave under the same characteristics of the sludge.

5.3 Different Wastewaters

This test was done specifically for dairy wastewater and as discussed in the project; the wastewater had specific impacts on the sludge characteristics. The multiple linear regression model needs to be validated with extra data from different anMBRs treating different wastewater. If the model is validated under different cases, and the results agree with this study then it probably means that the independent variables presented (SRF, CST/TSS, Crossflow velocity, and VS/TS) are good parameters that can quantify the impact of fouling on the membrane. As previously mentioned, an extra variable or more data is needed to improve the model since the model did not have an R square value above 0.9. it was recommended to incorporate the term presented by Van den Broeck et al. (2011) which takes into consideration the hydrophobicity and morphology of the sludge. Additionally, different type of modeling can be used to compare or expand on the model presented on this study. Modeling the complex interaction of foulants with the membrane and with the different the variables (SRF, CST/TSS, and crossflow velocity) could provide extra insight on the different mechanisms dominating fouling. Once the model is validated it can be used as a tool that can provide help into decision making for design and operation of anMBRs.

5.4 Filtration Methods

This study mainly focused on the real flux measurement developed by Baudry et al. (2019), since the goal of this method is to determine the flux under similar hydrostatic conditions found in full scale plants. Additional methods to characterize filtration have been developed, the most commonly used method is the critical flux method. Additionally, the DFCm has been studied and reported more in research literature since its development. To the author's knowledge, a comparison study between the real flux method with the critical flux method and the DFCm has not been done. The model presented in the results might not be

comparable to the data reported in the other studies since the filtration methods are different. It would be interesting to further validate the model with more data obtained from the different filtration methods and determine if they show the same relationships to the sludge characteristics that were presented in this study.

5.5 SRF and CST/TSS/Viscosity

Sludge data obtained from another project was used to try to validate the flux model. However, there was missing data for the flux so the data could not be used to validate the multiple linear regression model. On the other hand, a PCA and a multilinear regression revealed that there was a good linear relationship between the SRF and the CST/TSS/Viscosity (appendix C). A previous study by Sawalha and Scholz (2010) modeled the relationship between the CST and the SRF, however they did not consider the normalization of the CST/TSS/Viscosity. An external pressure source is required to perform the SRF, which is not always available on site, but CST, TSS and viscosity are tests that can easily be performed on site. If the relationship between normalized CST/TSS/viscosity and SRF is further studied and if the results are promising, then it would be easy to estimate the SRF in cases where the proper equipment for performing the SRF is not available (e.g. external pressure source).

Chapter 6 Recommendations & Conclusion

6.1 Recommendations

The previous chapter covered the limitations of the results. For prediction of the real flux the model can only be applied to anMBRs with a smooth 8 mm membrane from Pentair plc, treating dairy cheese wastewater with similar characteristics as the wastewater used in this research. The model needs to be improved to consider different scenarios, the most important being anMBRs treating different types of wastewater, and different membrane characteristics and module configurations. The model can be validated with data from anMBR treating different types of wastewater to ensure that the correlations and the relationships between the variables used in the model still remain the similar.

It was suggested to incorporate the flow conditions (i.e. Reynolds number) to consider membranes with different hydraulic diameters into the model. The Reynolds number is a function of the geometry of the water channel, in this case the membrane, and is also a function of the fluid characteristics. The biggest challenge will be to make the right assumptions to apply this parameter since sludge is not considered a Newtonian fluid.

Lastly the model can only be used to predict the real flux method. As mentioned in the previous section other filtration methods are also used in research (critical flux and DFCm). All three methods have shown promising results; however, a comparison study would be beneficial to understand the strengths and weaknesses of each method. Clearly outlining the benefits and the differences of each method could be helpful for determining future guidelines for the operation and implementation of anMBRs. Additionally, the indicators found in this study can only be applied for the prediction of the real flux. Another study would be beneficial to determine if the same indicators have a similar relationship to the critical flux method and the DFCm.

6.2 Conclusion

The PCA extracted 5 components causing the variance of the real flux test. It was found that these five components mainly contributed to a fraction of the solids content and CST, particle size distribution, the volatile solids and SRF, the soluble/colloidal particles, and the hydrostatic conditions, respectively. The first four components seemed to encompass different types of foulants, methods, and/or characteristics that have an impact on the filtration and fouling (e.g. the third component was mainly composed of the volatile solids and the SRF).

Already from the PCA it was clear which of the variables showed more collinearity and the multiple linear regression confirmed this as well. It was found that the best variables to model the prediction of the real flux were the CST/TSS, crossflow velocity, SRF, and VS/TS.

From the sludge characterization the SRT was the operational parameter that seemed to have the biggest impact on the biomass, agreeing with what has been previously reported in literature. From the observations of both experimental phases it seemed that the SRT was responsible for the increment in CST, TSS, Viscosity, and CCOD. This was not observed during the second experimental phase during the period where the reactor was operated without the buffer tank for 43 days. The addition of the buffer tank seemed to also have an impact on the sludge, since there was an increase in the SRF most likely caused by the increase of the number of particles between 0 and 10 micrometers in the supernatant.

The CST/TSS, the SRF, and the VS/TS showed to be the best indicators that can provide us with insight on the fouling caused by the sludge. The model created can give us an insight on how severe the fouling caused by the sludge can be by predicting the value of the flux. Hopefully, the results presented in this research can be used to further implement anaerobic membrane bioreactors for wastewater treatment.

References

Andrade, L.H., Motta, G.E. and Amaral, M.C.S. (2013) Treatment of dairy wastewater with a membrane bioreactor, pp. 759-770.
Association, A.P.H., Association, A.W.W., Federation, W.P.C. and Federation, W.E. (1915) Standard methods for the examination of water and wastewater, American Public Health Association.
Baker, R.W. (2012) Membrane technology and applications, John Wiley & Sons, Chichester, West Sussex ;.
Baudry, M., Zhou, T., Van Gaelen, P., Smets, I. and Pacheco-Ruiz, S. (2019) Protocol to evaluate and correlate membrane performance and mixed-liquor characteristics of full-scale and pilot-scale AnMBRs.
Bugge, T.V., Larsen, P., Saunders, A.M., Kragelund, C., Wybrandt, L., Keiding, K., Christensen, M.L. and Nielsen, P.H. (2013) Filtration properties of activated sludge in municipal MBR wastewater treatment plants are related to microbial community structure. Water Research 47(17), 6719-6730.
Carvalho, F., Prazeres, A.R. and Rivas, J. (2013) Cheese whey wastewater: characterization and treatment. Science of the total environment 445, 385-396.
Chew, J.W., Kilduff, J. and Belfort, G. (2020) The behavior of suspensions and macromolecular solutions in crossflow microfiltration: An update. Journal of Membrane Science 601, 117865.
Cho, J., Song, K.-G., Lee, S.H. and Ahn, K.-H. (2005) Sequencing anoxic/anaerobic membrane bioreactor (SAM) pilot plant for advanced wastewater treatment. Desalination 178(1-3), 219-225.
Choi, H., Zhang, K., Dionysiou, D.D., Oerther, D.B. and Sorial, G.A. (2005) Effect of permeate flux and tangential flow on membrane fouling for wastewater treatment. Separation and Purification Technology 45(1), 68-78.
Choi, H., Zhang, K., Dionysiou, D.D., Oerther, D.B. and Sorial, G.A. (2006) Effect of activated sludge properties and membrane operation conditions on fouling characteristics in membrane bioreactors. Chemosphere 63(10), 1699-1708.
Choo, K.-H. and Lee, C.-H. (1998) Hydrodynamic behavior of anaerobic biosolids during crossflow filtration in the membrane anaerobic bioreactor. Water Research 32(11), 3387-3397.
Cicek, N., Winnen, H., Suidan, M.T., Wrenn, B.E., Urbain, V. and Manem, J. (1998) Effectiveness of the membrane bioreactor in the biodegradation of high molecular weight compounds. Water Research 32(5), 1553-1563.
Demirel, B., Yenigun, O. and Onay, T.T. (2005) Anaerobic treatment of dairy wastewaters: a review. Process Biochemistry 40(8), 2583-2595.
Dereli, R.K., Grelot, A., Heffernan, B., van der Zee, F.P. and van Lier, J.B. (2014a) Implications of changes in solids retention time on long term evolution of sludge filterability in anaerobic membrane bioreactors treating high strength industrial wastewater. Water Research 59, 11-22.
Dereli, R.K., Heffernan, B., Grelot, A., van der Zee, F.P. and van Lier, J.B. (2015) Influence of high lipid containing wastewater on filtration performance and fouling in AnMBRs operated at different solids retention times. Separation and Purification Technology 139, 43-52.
Dereli, R.K., van der Zee, F.P., Heffernan, B., Grelot, A. and van Lier, J.B. (2014b) Effect of sludge retention time on the biological performance of anaerobic membrane bioreactors treating corn-to-ethanol thin stillage with high lipid content. Water Research 49, 453-464.
Dereli, R.K., van der Zee, F.P., Ozturk, I. and van Lier, J.B. (2019) Treatment of cheese whey by a cross-flow anaerobic membrane bioreactor: Biological and filtration performance. Environmental research 168, 109-117.
Espinasse, B., Bacchin, P. and Aimar, P. (2002) On an experimental method to measure critical flux in ultrafiltration. Desalination 146(1-3), 91-96.
Fane, A. and Fell, C. (1987) A review of fouling and fouling control in ultrafiltration. Desalination 62, 117-136.

References

Fox, P.F., McSweeney, P.L., Cogan, T.M. and Guinee, T.P. (2004) Cheese: Chemistry, Physics and Microbiology, Volume 1: General Aspects, Elsevier.

Fuchs, W., Theiss, M. and Braun, R. (2006) Influence of standard wastewater parameters and pre-flocculation on the fouling capacity during dead end membrane filtration of wastewater treatment effluents. Separation and Purification Technology 52(1), 46-52.

Geilvoet, S.P. (2010) The Delft Filtration Characterisation method: Assessing membrane bioreactor activated sludge filterability.

Goli, A., Shamiri, A., Khosroyar, S., Talaiekhozani, A., Sanaye, R. and Azizi, K. (2019) A review on different aerobic and anaerobic treatment methods in dairy industry wastewater. Journal of Environmental Treatment Techniques 6(1), 113-141.

Henze, M. (2008) Biological wastewater treatment : principles, modelling and design, IWA Pub., London.

Hong, S., Bae, T.-H., Tak, T., Hong, S. and Randall, A. (2002) Fouling control in activated sludge submerged hollow fiber membrane bioreactors. Desalination 143(3), 219-228.

Huang, Z., Ong, S.L. and Ng, H.Y. (2011) Submerged anaerobic membrane bioreactor for low-strength wastewater treatment: effect of HRT and SRT on treatment performance and membrane fouling. Water Research 45(2), 705-713.

Itonaga, T., Kimura, K. and Watanabe, Y. (2004) Influence of suspension viscosity and colloidal particles on permeability of membrane used in membrane bioreactor (MBR). Water Science and Technology 50(12), 301-309.

Jeison, D., Telkamp, P. and Van Lier, J. (2009) Thermophilic sidestream anaerobic membrane bioreactors: the shear rate dilemma. Water Environment Research 81(11), 2372-2380.

Jeong, T.-Y., Cha, G.-C., Yoo, I.-K. and Kim, D.-J. (2007) Characteristics of bio-fouling in a submerged MBR. Desalination 207(1-3), 107-113.

Jiang, T., Kennedy, M.D., Guinzbourg, B., Vanrolleghem, P.A. and Schippers, J. (2005) Optimising the operation of a MBR pilot plant by quantitative analysis of the membrane fouling mechanism. Water Science and Technology 51(6-7), 19-25.

Jiang, T., Kennedy, M.D., van der Meer, W.G.J., Vanrolleghem, P.A. and Schippers, J.C. (2003) The role of blocking and cake filtration in MBR fouling. Desalination 157(1), 335-343.

Judd, S. and Jefferson, B. (2003) Membranes for industrial wastewater recovery and re-use, Elsevier.

Kalyuzhnyi, S.V. (1997) Anaerobic treatment of high-strength cheese-whey wastewaters in laboratory and pilot UASB-reactors. Bioresource Technology 60(1), 59.

Knoell, T., Safarik, J., Cormack, T., Riley, R., Lin, S. and Ridgway, H. (1999) Biofouling potentials of microporous polysulfone membranes containing a sulfonated polyether-ethersulfone/polyethersulfone block copolymer: correlation of membrane surface properties with bacterial attachment. Journal of Membrane Science 157(1), 117-138.

Le-Clech, P., Chen, V. and Fane, T.A. (2006) Fouling in membrane bioreactors used in wastewater treatment. Journal of Membrane Science 284(1-2), 17-53.

Le-Clech, P., Fane, A., Leslie, G. and Childress, A. (2005) MBR focus: the operators' perspective. Filtration & separation 42(5), 20-23.

Le Clech, P., Jefferson, B., Chang, I.S. and Judd, S.J. (2003) Critical flux determination by the flux-step method in a submerged membrane bioreactor. Journal of Membrane Science 227(1-2), 81-93.

Lee, J., Ahn, W.-Y. and Lee, C.-H. (2001) Comparison of the filtration characteristics between attached and suspended growth microorganisms in submerged membrane bioreactor. Water Research 35(10), 2435-2445.

Lee, K. and Yeom, I. (2007) Evaluation of a membrane bioreactor system coupled with sludge pretreatment for aerobic sludge digestion. Environmental technology 28(7), 723-730.

Lee, W., Kang, S. and Shin, H. (2003) Sludge characteristics and their contribution to microfiltration in submerged membrane bioreactors. Journal of Membrane Science 216(1-2), 217-227.

Lee, Y. and Clark, M.M. (1998) Modeling of flux decline during crossflow ultrafiltration of colloidal suspensions. Journal of Membrane Science 149(2), 181-202.

References

Leslie, G., Fane, A., Fell, C., Schneider, R. and Marshall, K. (1993) Colloids in the Aquatic Environment, pp. 165-178, Elsevier.
Li, J., Li, Y., Ohandja, D.-G., Yang, F., Wong, F.-S. and Chua, H.-C. (2008) Impact of filamentous bacteria on properties of activated sludge and membrane-fouling rate in a submerged MBR. Separation and Purification Technology 59(3), 238-243.
Lousada-Ferreira, M., Krzeminski, P., Geilvoet, S., Moreau, A., Gil, J.A., Evenblij, H., Van Lier, J.B. and Van der Graaf, J.H. (2014) Filtration characterization method as tool to assess membrane bioreactor sludge filterability—the Delft experience. Membranes 4(2), 227-242.
Lousada-Ferreira, M., Moreau, A., van Lier, J.B. and van der Graaf, J.H. (2011) Particle counting as a tool to predict filterability in membrane bioreactors activated sludge? Water science and technology : a journal of the International Association on Water Pollution Research 64(1), 139-146.
Lousada-Ferreira, M., van Lier, J.B. and van der Graaf, J.H. Filterability and Floc size in Membrane Bioreactors: European Scale Assessment.
Lousada-Ferreira, M., van Lier, J.B. and van der Graaf, J.H. (2015) Impact of suspended solids concentration on sludge filterability in full-scale membrane bioreactors. Journal of Membrane Science 476, 68-75.
Ma, B.-C., Lee, Y.-N., Park, J.-S., Lee, C.-H., Lee, S.-H., Chang, I.-S. and Ahn, T.-S. (2006) Correlation between dissolved oxygen concentration, microbial community and membrane permeability in a membrane bioreactor. Process Biochemistry 41(5), 1165-1172.
Ma, L., Li, X., Du, G., Chen, J. and Shen, Z. (2005) Influence of the filtration modes on colloid adsorption on the membrane in submerged membrane bioreactor. Colloids and Surfaces A: Physicochemical and Engineering Aspects 264(1-3), 120-125.
Madaeni, S.S., Fane, A.G. and Wiley, D.E. (1999) Factors influencing critical flux in membrane filtration of activated sludge. Journal of Chemical Technology & Biotechnology: International Research in Process, Environmental & Clean Technology 74(6), 539-543.
Marshall, A., Munro, P. and Trägårdh, G. (1993) The effect of protein fouling in microfiltration and ultrafiltration on permeate flux, protein retention and selectivity: a literature review. Desalination 91(1), 65-108.
Matthiasson, E. (1983) The role of macromolecular adsorption in fouling of ultrafiltration membranes. Journal of Membrane Science 16, 23-36.
Meng, F., Yang, F., Xiao, J., Zhang, H. and Gong, Z. (2006a) A new insight into membrane fouling mechanism during membrane filtration of bulking and normal sludge suspension. Journal of Membrane Science 285(1-2), 159-165.
Meng, F., Zhang, H., Yang, F., Li, Y., Xiao, J. and Zhang, X. (2006b) Effect of filamentous bacteria on membrane fouling in submerged membrane bioreactor. Journal of Membrane Science 272(1-2), 161-168.
Metsämuuronen, S., Howell, J. and Nyström, M. (2002) Critical flux in ultrafiltration of myoglobin and baker's yeast. Journal of Membrane Science 196(1), 13-25.
Naessens, W., Maere, T. and Nopens, I. (2012) Critical review of membrane bioreactor models - Part 1: Biokinetic and filtration models. Bioresource Technology 122, 95-106.
Ng, H.Y. and Hermanowicz, S.W. (2005) Membrane bioreactor operation at short solids retention times: performance and biomass characteristics. Water Research 39(6), 981-992.
Nilsson, J.L. (1990) Protein fouling of UF membranes: causes and consequences. Journal of Membrane Science 52(2), 121-142.
Odriozola, M., Lousada-Ferreira, M., Spanjers, H. and van Lier, J.B. (2020) Effect of sludge characteristics on optimal required dosage of flux enhancer in anaerobic membrane bioreactors. Journal of Membrane Science 619, 118776.
Ognier, S., Wisniewski, C. and Grasmick, A. (2002a) Influence of macromolecule adsorption during filtration of a membrane bioreactor mixed liquor suspension. Journal of Membrane Science 209(1), 27-37.

References

Ognier, S., Wisniewski, C. and Grasmick, A. (2002b) Membrane fouling during constant flux filtration in membrane bioreactors. Membrane Technology 2002(7), 6-10.
Pasmore, M., Todd, P., Smith, S., Baker, D., Silverstein, J., Coons, D. and Bowman, C.N. (2001) Effects of ultrafiltration membrane surface properties on Pseudomonas aeruginosa biofilm initiation for the purpose of reducing biofouling. Journal of Membrane Science 194(1), 15-32.
Petsev, D., Starov, V. and Ivanov, I. (1993) Concentrated dispersions of charged colloidal particles: sedimentation, ultrafiltration and diffusion. Colloids and Surfaces A: Physicochemical and Engineering Aspects 81(13), 65-81.
Pollice, A., Laera, G., Saturno, D. and Giordano, C. (2008) Effects of sludge retention time on the performance of a membrane bioreactor treating municipal sewage. Journal of Membrane Science 317(1-2), 65-70.
Prazeres, A.R., Carvalho, F. and Rivas, J. (2012) Cheese whey management: A review. Journal of Environmental Management 110, 48-68.
Rosenberger, S., Laabs, C., Lesjean, B., Gnirss, R., Amy, G., Jekel, M. and Schrotter, J.-C. (2006) Impact of colloidal and soluble organic material on membrane performance in membrane bioreactors for municipal wastewater treatment. Water Research 40(4), 710-720.
Sato, T. and Ishii, Y. (1991) Effects of Activated Sludge Properties on Water Flux of Ultrafiltration Membrane Used for Human Excrement Treatment. Water Science and Technology 23(7-9), 1601-1608.
Sawalha, O. and Scholz, M. (2010) Modeling the relationship between capillary suction time and specific resistance to filtration. Journal of Environmental Engineering 136(9), 983-991.
Schrader, G., Zwijnenburg, A. and Wessling, M. (2005) The effect of WWTP effluent zeta-potential on direct nanofiltration performance. Journal of Membrane Science 266(1-2), 80-93.
Shin, H.-S. (2002) Contribution of solids and soluble materials of sludge to UF behavior under starvation.
Tchobanoglous, G., Burton, F.L., Stensel, H.D., Metcalf and Eddy (2003) Wastewater engineering : treatment and reuse, McGraw-Hill, Boston.
Van den Broeck, R., Krzeminski, P., Van Dierdonck, J., Gins, G., Lousada-Ferreira, M., Van Impe, J., Van der Graaf, J., Smets, I. and Van Lier, J. (2011) Activated sludge characteristics affecting sludge filterability in municipal and industrial MBRs: Unraveling correlations using multi-component regression analysis. Journal of Membrane Science 378(1-2), 330-338.
Vesilind, P.A. (1988) Capillary suction time as a fundamental measure of sludge dewaterability. Journal (Water Pollution Control Federation), 215-220.
Vourch, M., Balannec, B., Chaufer, B. and Dorange, G. (2008) Treatment of dairy industry wastewater by reverse osmosis for water reuse. Desalination 219(1-3), 190-202.
Wold, S., Esbensen, K. and Geladi, P. (1987) Principal component analysis. Chemometrics and intelligent laboratory systems 2(1-3), 37-52.
Yu, H.-Q. and Fang, H. (2002) Acidogenesis of dairy wastewater at various pH levels. Water Science and Technology 45(10), 201-206.
Zhang, J., Chua, H.C., Zhou, J. and Fane, A. (2006) Factors affecting the membrane performance in submerged membrane bioreactors. Journal of Membrane Science 284(1-2), 54-66.
Zhang, M., Hong, H., Lin, H., Shen, L., Yu, H., Ma, G., Chen, J. and Liao, B.-Q. (2018) Mechanistic insights into alginate fouling caused by calcium ions based on terahertz time-domain spectra analyses and DFT calculations. Water Research 129, 337-346.
Zhang, M., Lin, H., Shen, L., Liao, B.-Q., Wu, X. and Li, R. (2017) Effect of calcium ions on fouling properties of alginate solution and its mechanisms. Journal of Membrane Science 525, 320-329.
Zhang, T.C., Environmental, Water Resources Institute. Membrane Technology Task, C. and American Society of Civil, E. (2012) Membrane technology and environmental applications, American Society of Civil Engineers, Reston.

Appendix

A. Additional Operational and Biological Performance Data

A)

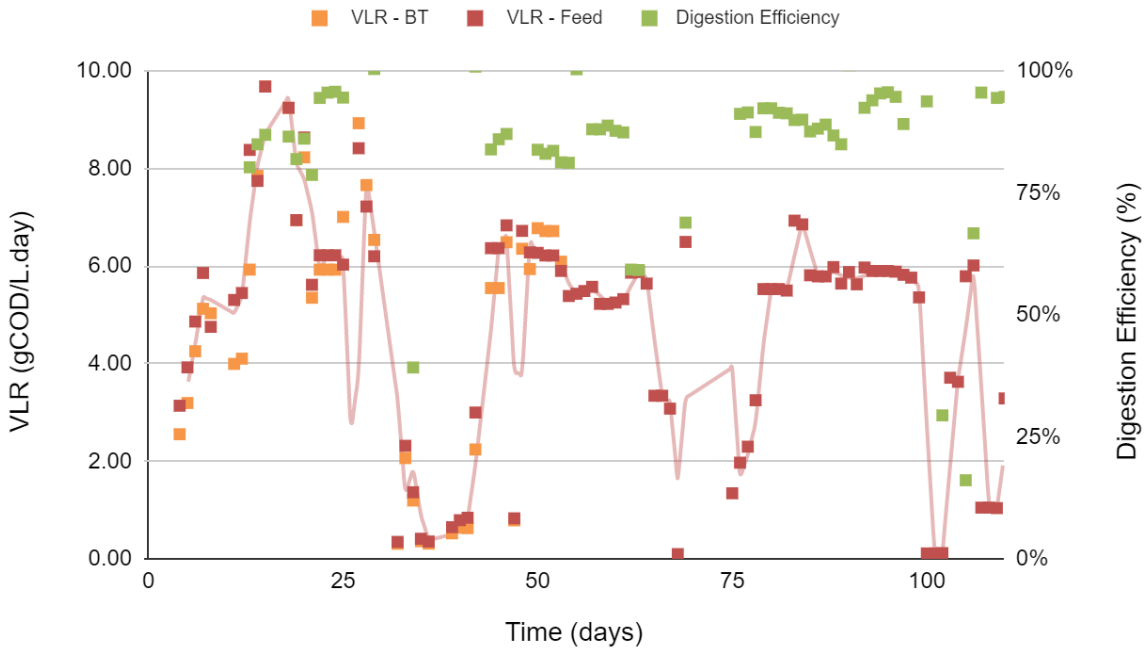

B)

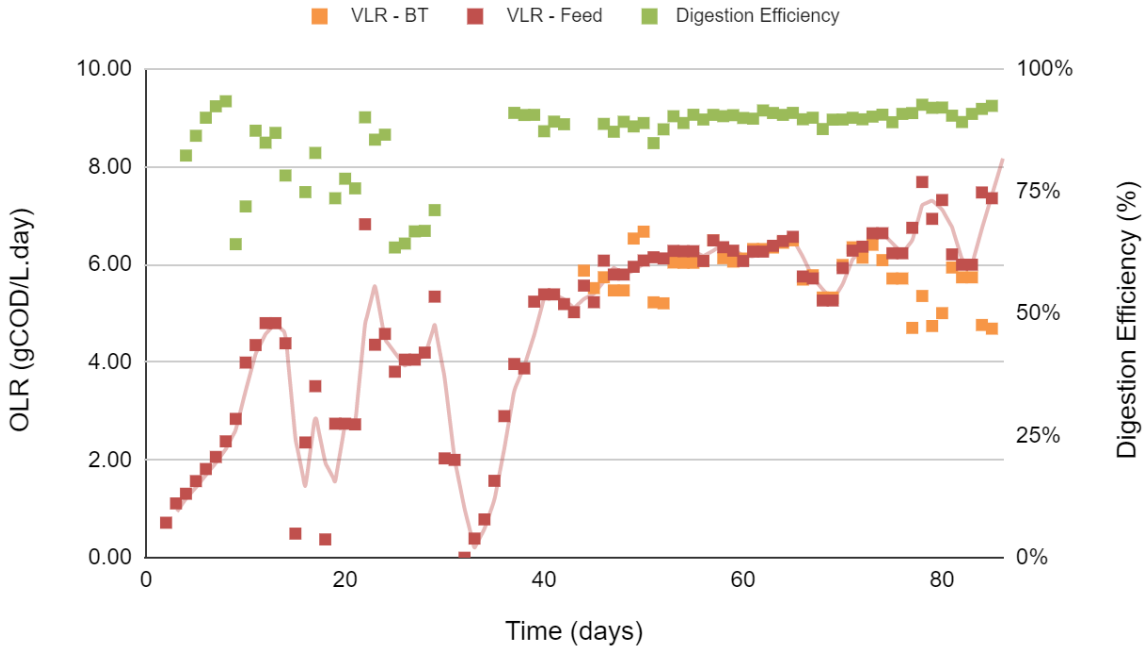

Fig. 1 Digestion Efficeincy and operational VLR. A) Experimental Phase 1. B)Experimental Phase 2

A)

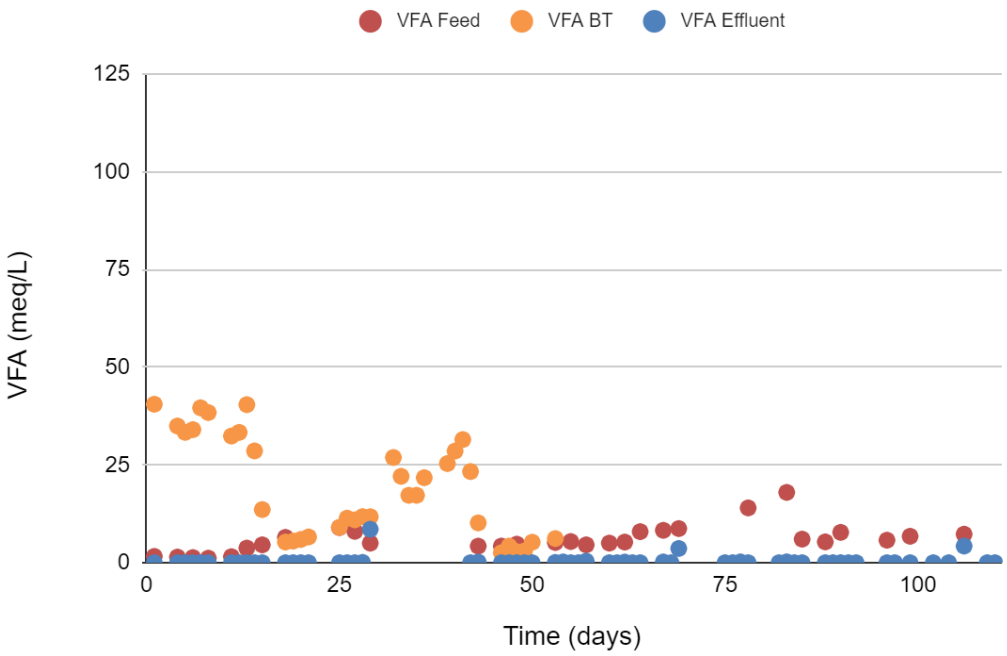

B)

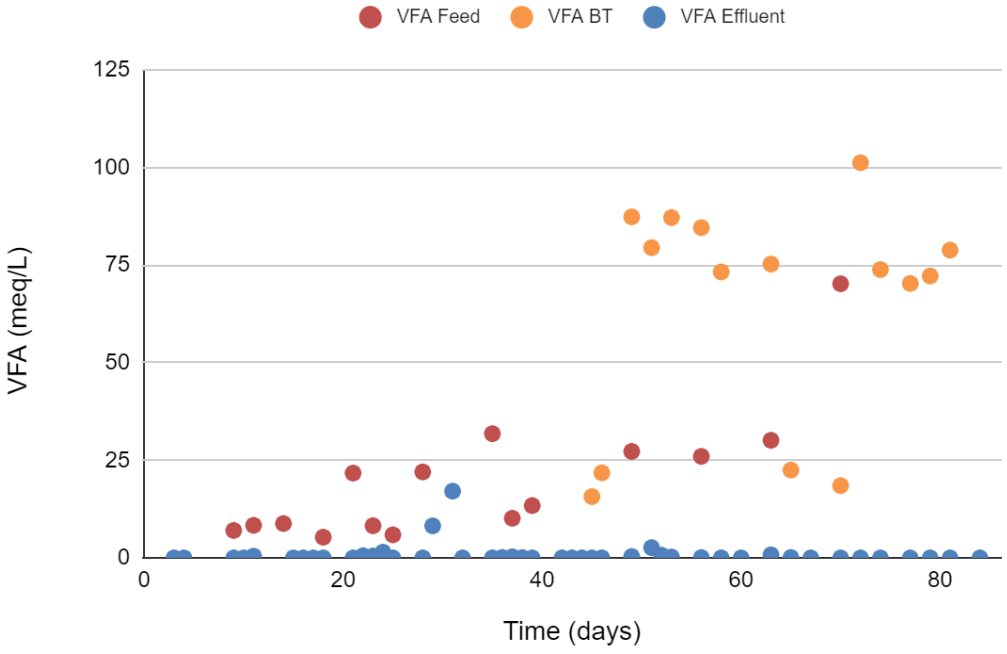

Fig. 2 VFA concentration in feed, buffer tank, and effluent. A) Experimental Phase 1. B)Experimental Phase 2

A)

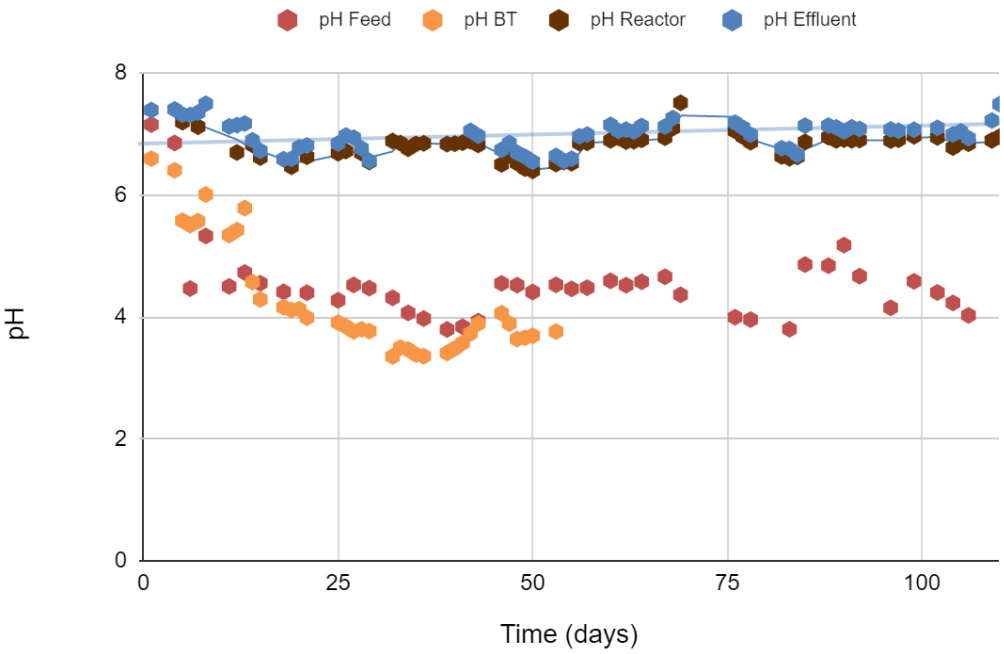

B)

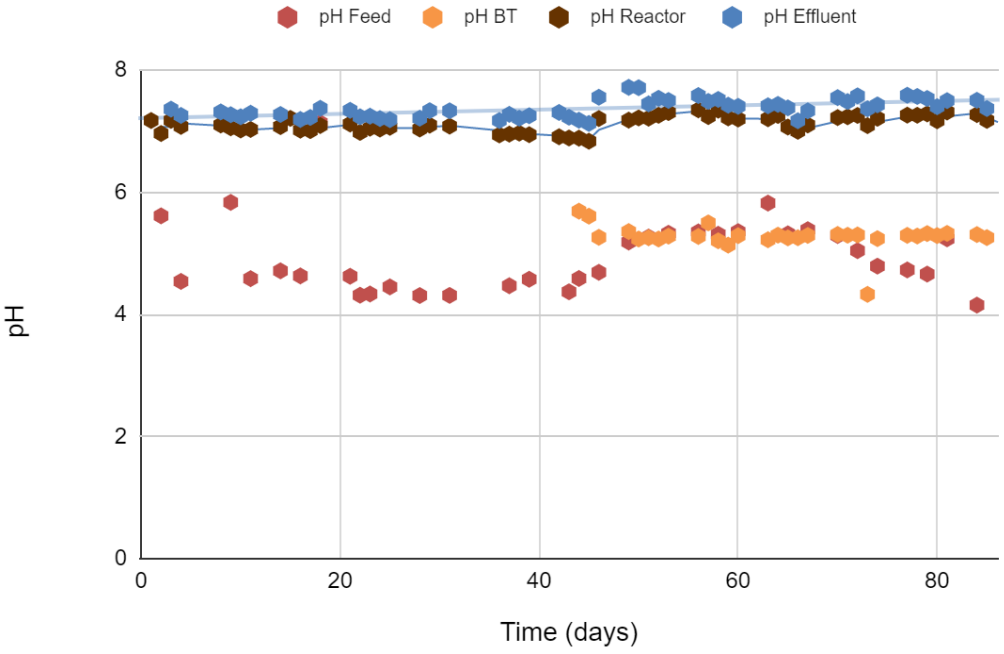

Fig. 3 pH in the feed, buffer tank, reactor, and effluent. A) Experimental Phase 1. B) Experimental Phase 2.

A)

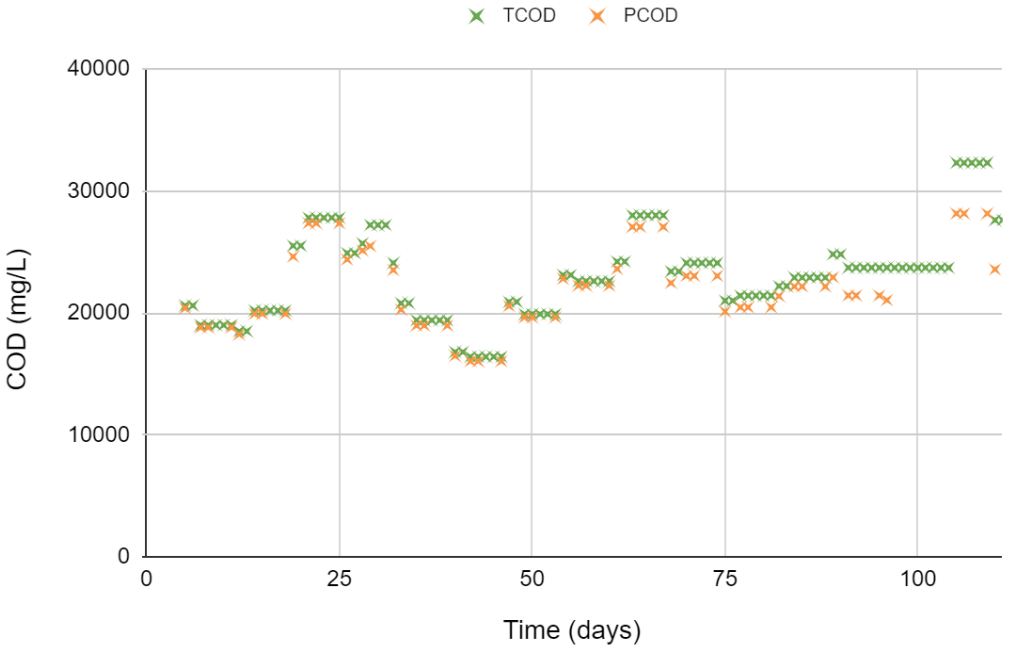

B)

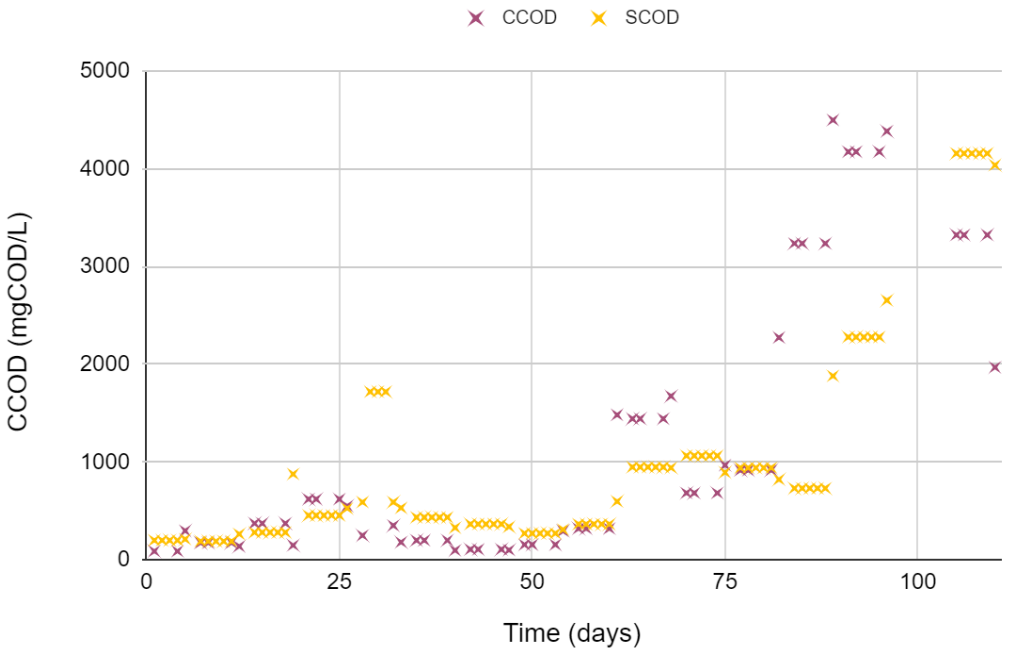

Fig. 4 A) Total and Particulate COD for experimental phase 1. B) Colloidal and soluble COD for experimental phase 2

B. Supplementary Statistical Results from SPSS for Flux and Sludge Data

The following tables correspond to the principal component analysis and the multilinear regression of the real flux and the sludge characterization data.

Descriptive Statistics

	Mean	Std. Deviation	Analysis N
x-flow velocity	1,336	,2900	1392
TMP	223,2668	41,96086	1392
TCOD (mg/L)	17043,41379	3376,457220	1392
PCOD (mg/L)	15889,23	3182,292	1392
CCOD (mg/L)	2360,51724	997,413926	1392
CCOD-SCOD (mg/L)	1206,33	671,024	1392
SCOD (mg/L)	1154,19	474,367	1392
TS (g/kg)	15,727615365953419	2,336075546715582	1392
VS (g/kg)	10,56355	1,632298	1392
VS/TS	,671878391325421	,032902466186106	1392
TS-TSS	3,296623986642967	1,205841689273320	1392
TS-VS	5,164066515378548	,968185045253219	1392
TSS (g/kg)	12,43099	2,303405	1392
VSS (g/kg)	10,77390	1,765246	1392

VSS/TSS	,872829365444708	,070742886993947	1392
TSS-VSS	1,657090517241384	1,169246999294564	1392
CST (s)	746,685	284,8907	1392
Viscocity (mP.s)	8,9076	2,81174	1392
CST/TSS	59,433476378953880	20,677783301407693	1392
CST/Viscosity	84,901273544866260	28,344869237266483	1392
CST/TSS/Viscosity	6,998045167340112	2,249455320552122	1392
PSD d50 avg. (µm)	15,6272	1,82556	1392
PSD d10 avg. (µm)	5,6242	1,25315	1392
SRF Membrane	234463340317,3829300	108687523781,26237000	1392
Protein (mgN/L)	133,50022	39,493478	1392
PSD 0 to 20 µm	62,223268678161794	7,442608694205598	1392
PSD 0 to 10 µm	22,7843	5,35455	1392
PSD 10 to 20 µm	39,438979885057556	4,855521848016051	1392
PSD 1 to 10 µm	22,2172	4,93626	1392

Correlation Matrix[a,b]

		x-flow velocity	TMP	TCOD (mg/L)	PCOD (mg/L)	CCOD (mg/L)
Correlation	x-flow velocity	1,000	,075	,029	,046	-,072
	TMP	,075	1,000	-,044	-,046	,010
	TCOD (mg/L)	,029	-,044	1,000	,991	,596
	PCOD (mg/L)	,046	-,046	,991	1,000	,511

	CCOD (mg/L)	-,072	,010	,596	,511	1,000
	CCOD-SCOD (mg/L)	-,032	,016	,555	,514	,911
	SCOD (mg/L)	-,106	-,001	,468	,347	,813
	TS (g/kg)	,027	-,049	,894	,927	,398
	VS (g/kg)	,012	-,031	,912	,918	,566
	VS/TS	-,040	,053	,175	,099	,548
	TS-TSS	-,026	-,080	,187	,160	,623
	TS-VS	,045	-,068	,619	,688	,007
	TSS (g/kg)	,041	-,008	,809	,856	,078
	VSS (g/kg)	-,012	,014	,830	,860	,372
	VSS/TSS	-,109	,034	-,147	-,187	,493
	TSS-VSS	,099	-,038	,341	,389	-,408
	CST (s)	,036	-,038	,650	,681	,564
	Viscocity (mP.s)	,036	-,028	,615	,691	-,109
	CST/TSS	,030	-,051	,438	,456	,594
	CST/Viscosity	,021	-,044	,435	,412	,748
	CST/TSS/Viscosity	,006	-,049	,017	-,024	,641
	PSD d50 avg. (µm)	,041	-,050	,443	,520	-,240
	PSD d10 avg. (µm)	,012	-,031	,519	,589	,105
	SRF Membrane	-,065	,002	-,487	-,520	,165
	Protein (mgN/L)	-,035	-,067	,490	,399	,745
	PSD 0 to 20 µm	-,054	,047	-,588	-,646	,143
	PSD 0 to 10 µm	-,021	,030	-,398	-,483	,061
	PSD 10 to 20 µm	-,060	,040	-,461	-,457	,152
	PSD 1 to 10 µm	-,016	,031	-,343	-,428	,101

Correlation Matrix[a,b]

		CCOD-SCOD (mg/L)	SCOD (mg/L)	TS (g/kg)	VS (g/kg)	VS/TS
Correlation	x-flow velocity	-,032	-,106	,027	,012	-,040
	TMP	,016	-,001	-,049	-,031	,053
	TCOD (mg/L)	,555	,468	,894	,912	,175
	PCOD (mg/L)	,514	,347	,927	,918	,099
	CCOD (mg/L)	,911	,813	,398	,566	,548
	CCOD-SCOD (mg/L)	1,000	,502	,487	,603	,407
	SCOD (mg/L)	,502	1,000	,148	,336	,577
	TS (g/kg)	,487	,148	1,000	,942	-,046
	VS (g/kg)	,603	,336	,942	1,000	,292
	VS/TS	,407	,577	-,046	,292	1,000
	TS-TSS	,744	,257	,285	,363	,249
	TS-VS	,158	-,208	,825	,587	-,602
	TSS (g/kg)	,104	,016	,865	,765	-,177
	VSS (g/kg)	,452	,142	,924	,899	,047
	VSS/TSS	,587	,207	-,097	,044	,397
	TSS-VSS	-,477	-,184	,309	,151	-,419
	CST (s)	,796	,059	,789	,732	-,070
	Viscocity (mP.s)	,019	-,257	,671	,487	-,450
	CST/TSS	,840	,061	,578	,551	-,015
	CST/Viscosity	,877	,333	,504	,562	,228
	CST/TSS/Viscosity	,754	,281	,047	,131	,244
	PSD d50 avg. (µm)	-,124	-,330	,529	,304	-,596
	PSD d10 avg. (µm)	,336	-,255	,678	,506	-,425
	SRF Membrane	,230	,022	-,582	-,555	,004
	Protein (mgN/L)	,531	,816	,137	,322	,571
	PSD 0 to 20 µm	,108	,148	-,610	-,432	,446

	PSD 0 to 10 µm	-,194	,402	-,595	-,392	,527
	PSD 10 to 20 µm	,379	-,216	-,279	-,230	,102
	PSD 1 to 10 µm	-,155	,431	-,549	-,334	,570

Correlation Matrix[a,b]

		TS-TSS	TS-VS	TSS (g/kg)	VSS (g/kg)	VSS/TSS	TSS-VSS
Correlation	x-flow velocity	-,026	,045	,041	-,012	-,109	,099
	TMP	-,080	-,068	-,008	,014	,034	-,038
	TCOD (mg/L)	,187	,619	,809	,830	-,147	,341
	PCOD (mg/L)	,160	,688	,856	,860	-,187	,389
	CCOD (mg/L)	,623	,007	,078	,372	,493	-,408
	CCOD-SCOD (mg/L)	,744	,158	,104	,452	,587	-,477
	SCOD (mg/L)	,257	-,208	,016	,142	,207	-,184
	TS (g/kg)	,285	,825	,865	,924	-,097	,309
	VS (g/kg)	,363	,587	,765	,899	,044	,151
	VS/TS	,249	-,602	-,177	,047	,397	-,419
	TS-TSS	1,000	,076	-,234	,133	,706	-,663
	TS-VS	,076	1,000	,797	,715	-,308	,490
	TSS (g/kg)	-,234	,797	1,000	,867	-,468	,660
	VSS (g/kg)	,133	,715	,867	1,000	,031	,199
	VSS/TSS	,706	-,308	-,468	,031	1,000	-,969
	TSS-VSS	-,663	,490	,660	,199	-,969	1,000
	CST (s)	,626	,668	,472	,700	,300	-,127
	Viscocity (mP.s)	-,230	,796	,801	,598	-,504	,674
	CST/TSS	,803	,466	,166	,478	,522	-,396
	CST/Viscosity	,806	,270	,089	,454	,608	-,510
	CST/TSS/Viscosity	,857	-,107	-,401	-,016	,766	-,766
	PSD d50 avg. (µm)	-,262	,764	,674	,377	-,645	,757

	PSD d10 avg. (µm)	,200	,783	,583	,525	-,209	,356
	SRF Membrane	,345	-,468	-,771	-,555	,605	-,680
	Protein (mgN/L)	,300	-,211	-,018	,154	,326	-,268
	PSD 0 to 20 µm	,314	-,744	-,783	-,450	,753	-,864
	PSD 0 to 10 µm	-,114	-,775	-,544	-,447	,265	-,397
	PSD 10 to 20 µm	,607	-,287	-,601	-,197	,861	-,887
	PSD 1 to 10 µm	-,102	-,762	-,504	-,400	,266	-,388

Correlation Matrix[a,b]

		CST (s)	Viscocity (mP.s)	CST/TSS	CST/Viscosity	CST/TSS/Viscosity
Correlation	x-flow velocity	,036	,036	,030	,021	,006
	TMP	-,038	-,028	-,051	-,044	-,049
	TCOD (mg/L)	,650	,615	,438	,435	,017
	PCOD (mg/L)	,681	,691	,456	,412	-,024
	CCOD (mg/L)	,564	-,109	,594	,748	,641
	CCOD-SCOD (mg/L)	,796	,019	,840	,877	,754
	SCOD (mg/L)	,059	-,257	,061	,333	,281
	TS (g/kg)	,789	,671	,578	,504	,047
	VS (g/kg)	,732	,487	,551	,562	,131
	VS/TS	-,070	-,450	-,015	,228	,244
	TS-TSS	,626	-,230	,803	,806	,857
	TS-VS	,668	,796	,466	,270	-,107
	TSS (g/kg)	,472	,801	,166	,089	-,401
	VSS (g/kg)	,700	,598	,478	,454	-,016
	VSS/TSS	,300	-,504	,522	,608	,766
	TSS-VSS	-,127	,674	-,396	-,510	-,766
	CST (s)	1,000	,430	,945	,831	,552

	Viscocity (mP.s)	,430	1,000	,176	-,121	-,457
	CST/TSS	,945	,176	1,000	,910	,775
	CST/Viscosity	,831	-,121	,910	1,000	,872
	CST/TSS/Viscosity	,552	-,457	,775	,872	1,000
	PSD d50 avg. (µm)	,309	,938	,077	-,238	-,501
	PSD d10 avg. (µm)	,693	,825	,535	,220	-,049
	SRF Membrane	-,076	-,396	,186	,121	,517
	Protein (mgN/L)	,142	-,132	,184	,360	,357
	PSD 0 to 20 µm	-,278	-,911	-,006	,225	,553
	PSD 0 to 10 µm	-,603	-,833	-,450	-,103	,135
	PSD 10 to 20 µm	,239	-,478	,486	,458	,698
	PSD 1 to 10 µm	-,570	-,815	-,426	-,072	,143

Correlation Matrix[a,b]

		PSD d50 avg. (µm)	PSD d10 avg. (µm)	SRF Membrane	Protein (mgN/L)
Correlation	x-flow velocity	,041	,012	-,065	-,035
	TMP	-,050	-,031	,002	-,067
	TCOD (mg/L)	,443	,519	-,487	,490
	PCOD (mg/L)	,520	,589	-,520	,399
	CCOD (mg/L)	-,240	,105	,165	,745
	CCOD-SCOD (mg/L)	-,124	,336	,230	,531
	SCOD (mg/L)	-,330	-,255	,022	,816
	TS (g/kg)	,529	,678	-,582	,137
	VS (g/kg)	,304	,506	-,555	,322
	VS/TS	-,596	-,425	,004	,571
	TS-TSS	-,262	,200	,345	,300
	TS-VS	,764	,783	-,468	-,211

	TSS (g/kg)	,674	,583	-,771	-,018
	VSS (g/kg)	,377	,525	-,555	,154
	VSS/TSS	-,645	-,209	,605	,326
	TSS-VSS	,757	,356	-,680	-,268
	CST (s)	,309	,693	-,076	,142
	Viscocity (mP.s)	,938	,825	-,396	-,132
	CST/TSS	,077	,535	,186	,184
	CST/Viscosity	-,238	,220	,121	,360
	CST/TSS/Viscosity	-,501	-,049	,517	,357
	PSD d50 avg. (µm)	1,000	,846	-,365	-,315
	PSD d10 avg. (µm)	,846	1,000	-,170	-,251
	SRF Membrane	-,365	-,170	1,000	,230
	Protein (mgN/L)	-,315	-,251	,230	1,000
	PSD 0 to 20 µm	-,955	-,754	,562	,194
	PSD 0 to 10 µm	-,877	-,985	,162	,382
	PSD 10 to 20 µm	-,497	-,068	,682	-,123
	PSD 1 to 10 µm	-,876	-,974	,128	,416

Correlation Matrix[a,b]

		PSD 0 to 20 µm	PSD 0 to 10 µm	PSD 10 to 20 µm	PSD 1 to 10 µm
Correlation	x-flow velocity	-,054	-,021	-,060	-,016
	TMP	,047	,030	,040	,031
	TCOD (mg/L)	-,588	-,398	-,461	-,343
	PCOD (mg/L)	-,646	-,483	-,457	-,428
	CCOD (mg/L)	,143	,061	,152	,101
	CCOD-SCOD (mg/L)	,108	-,194	,379	-,155
	SCOD (mg/L)	,148	,402	-,216	,431

	TS (g/kg)	-,610	-,595	-,279	-,549
	VS (g/kg)	-,432	-,392	-,230	-,334
	VS/TS	,446	,527	,102	,570
	TS-TSS	,314	-,114	,607	-,102
	TS-VS	-,744	-,775	-,287	-,762
	TSS (g/kg)	-,783	-,544	-,601	-,504
	VSS (g/kg)	-,450	-,447	-,197	-,400
	VSS/TSS	,753	,265	,861	,266
	TSS-VSS	-,864	-,397	-,887	-,388
	CST (s)	-,278	-,603	,239	-,570
	Viscocity (mP.s)	-,911	-,833	-,478	-,815
	CST/TSS	-,006	-,450	,486	-,426
	CST/Viscosity	,225	-,103	,458	-,072
	CST/TSS/Viscosity	,553	,135	,698	,143
	PSD d50 avg. (µm)	-,955	-,877	-,497	-,876
	PSD d10 avg. (µm)	-,754	-,985	-,068	-,974
	SRF Membrane	,562	,162	,682	,128
	Protein (mgN/L)	,194	,382	-,123	,416
	PSD 0 to 20 µm	1,000	,759	,696	,743
	PSD 0 to 10 µm	,759	1,000	,060	,997
	PSD 10 to 20 µm	,696	,060	1,000	,039
	PSD 1 to 10 µm	,743	,997	,039	1,000

a. Determinant = ,000

b. This matrix is not positive definite.

Communalities

	Initial	Extraction

x-flow velocity	1,000	,525
TMP	1,000	,551
TCOD (mg/L)	1,000	,993
PCOD (mg/L)	1,000	,985
CCOD (mg/L)	1,000	,958
CCOD-SCOD (mg/L)	1,000	,953
SCOD (mg/L)	1,000	,888
TS (g/kg)	1,000	,989
VS (g/kg)	1,000	,962
VS/TS	1,000	,698
TS-TSS	1,000	,819
TS-VS	1,000	,887
TSS (g/kg)	1,000	,975
VSS (g/kg)	1,000	,905
VSS/TSS	1,000	,877
TSS-VSS	1,000	,943
CST (s)	1,000	,972
Viscocity (mP.s)	1,000	,925
CST/TSS	1,000	,963
CST/Viscosity	1,000	,921
CST/TSS/Viscosity	1,000	,907
PSD d50 avg. (µm)	1,000	,996
PSD d10 avg. (µm)	1,000	,959
SRF Membrane	1,000	,921
Protein (mgN/L)	1,000	,882
PSD 0 to 20 µm	1,000	,986
PSD 0 to 10 µm	1,000	,964

PSD 10 to 20 µm	1,000	,947
PSD 1 to 10 µm	1,000	,968

Extraction Method: Principal Component Analysis.

Total Variance Explained

	Initial Eigenvalues			Extraction Sums of Squared Loadings		
Component	Total	% of Variance	Cumulative %	Total	% of Variance	Cumulative %
1	11,255	38,812	38,812	11,255	38,812	38,812
2	8,528	29,409	68,221	8,528	29,409	68,221
3	4,014	13,841	82,062	4,014	13,841	82,062
4	1,357	4,680	86,742	1,357	4,680	86,742
5	1,064	3,669	90,411	1,064	3,669	90,411
6	1,008	3,476	93,886			
7	,675	2,326	96,212			
8	,549	1,894	98,106			
9	,269	,928	99,034			
10	,247	,852	99,885			
11	,022	,077	99,963			
12	,007	,025	99,988			
13	,002	,008	99,997			
14	,001	,003	100,000			
15	9,360E-5	,000	100,000			
16	1,725E-5	5,950E-5	100,000			
17	2,189E-7	7,547E-7	100,000			
18	4,370E-8	1,507E-7	100,000			
19	2,220E-8	7,655E-8	100,000			
20	2,030E-14	6,999E-14	100,000			

21	1,423E-14	4,909E-14	100,000			
22	7,944E-15	2,739E-14	100,000			
23	5,134E-15	1,770E-14	100,000			
24	-1,404E-15	-4,841E-15	100,000			
25	-4,560E-15	-1,573E-14	100,000			
26	-6,021E-15	-2,076E-14	100,000			
27	-1,038E-14	-3,580E-14	100,000			
28	-1,148E-14	-3,959E-14	100,000			
29	-1,571E-14	-5,416E-14	100,000			

Total Variance Explained

	Rotation Sums of Squared Loadings		
Component	Total	% of Variance	Cumulative %
1	7,464	25,739	25,739
2	7,127	24,576	50,315
3	6,880	23,722	74,037
4	3,662	12,627	86,665
5	1,086	3,746	90,411
6			
7			
8			
9			
10			
11			
12			
13			
14			
15			

16			
17			
18			
19			
20			
21			
22			
23			
24			
25			
26			
27			
28			
29			

Extraction Method: Principal Component Analysis.

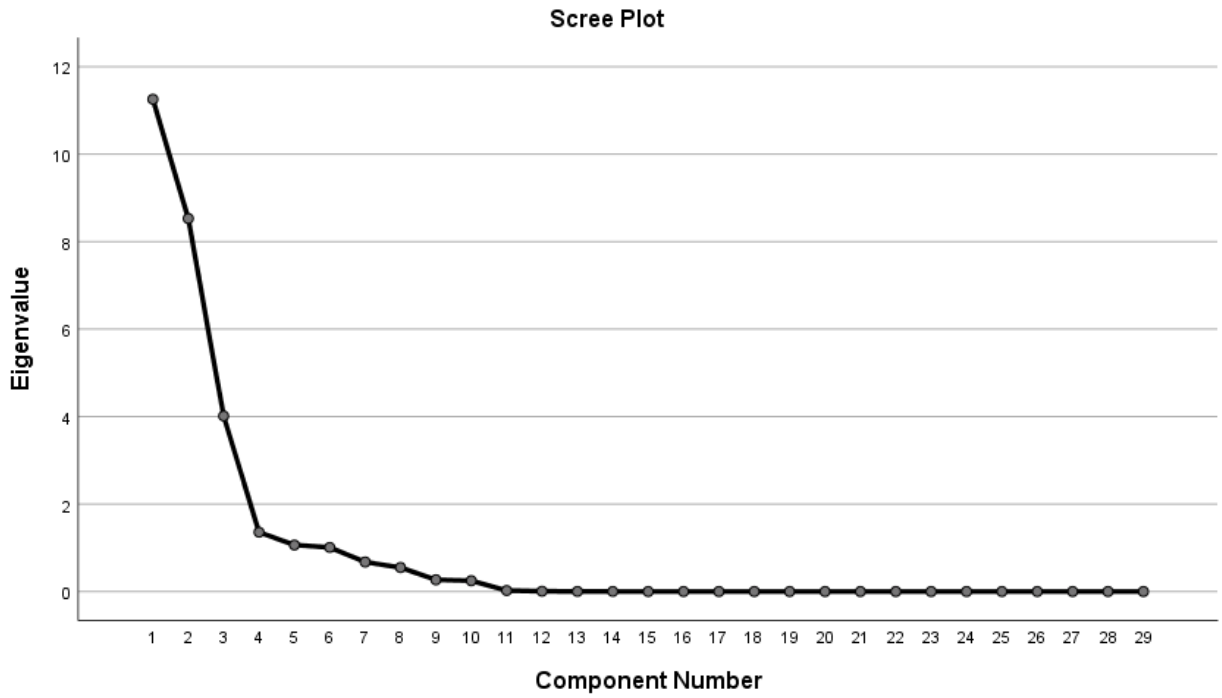

Rotated Component Matrix[a]

	Component				
	1	2	3	4	5
CST/TSS/Viscosity	,916				
TS-TSS	,881				
CST/TSS	,859				
CST/Viscosity	,855				
VSS/TSS	,853				
PSD 10 to 20 µm	,834				
TSS-VSS	-,798				
CCOD-SCOD (mg/L)	,770			,518	
CST (s)	,672		,531		
PSD 1 to 10 µm		-,937			
PSD 0 to 10 µm		-,929			
PSD d10 avg. (µm)		,912			
PSD d50 avg. (µm)		,897			

Viscocity (mP.s)		,816			
PSD 0 to 20 µm		-,770			
TS-VS		,695	,611		
VS/TS		-,626		,503	
VSS (g/kg)			,901		
VS (g/kg)			,879		
TS (g/kg)			,868		
TSS (g/kg)			,853		
SRF Membrane			-,811		
PCOD (mg/L)			,788		
TCOD (mg/L)			,763	,544	
Protein (mgN/L)				,887	
SCOD (mg/L)				,873	
CCOD (mg/L)	,555			,764	
TMP					,740
x-flow velocity					,721

Extraction Method: Principal Component Analysis.

Rotation Method: Varimax with Kaiser Normalization.[a]

a. Rotation converged in 7 iterations.

Component Transformation Matrix

Component	1	2	3	4	5
1	-,052	,703	,703	,094	,006
2	,876	-,169	,179	,415	-,015
3	-,467	-,506	,389	,612	,002
4	,109	-,456	,547	-,643	,262

5	-,015	,117	-,151	,180	,965

Extraction Method: Principal Component Analysis.

Rotation Method: Varimax with Kaiser Normalization.

Multilinear regression Simplified model

Model	R	R Square	Adjusted R Square	Std. Error of the Estimate
1	,652[a]	,425	,425	5,76436
2	,856[b]	,732	,732	3,93800
3	,897[c]	,804	,804	3,36859
4	,898[d]	,807	,806	3,34624

a. Predictors: (Constant), CST/TSS

b. Predictors: (Constant), CST/TSS, x-flow velocity

c. Predictors: (Constant), CST/TSS, x-flow velocity , SRF Membrane

d. Predictors: (Constant), CST/TSS, x-flow velocity , SRF Membrane , VS/TS

ANOVA[a]

Model		Sum of Squares	df	Mean Square	F	Sig.
1	Regression	34170,681	1	34170,681	1028,375	,000[b]
	Residual	46186,694	1390	33,228		
	Total	80357,375	1391			
2	Regression	58816,992	2	29408,496	1896,364	,000[c]
	Residual	21540,382	1389	15,508		
	Total	80357,375	1391			
3	Regression	64607,148	3	21535,716	1897,850	,000[d]

	Residual	15750,227	1388	11,347		
	Total	80357,375	1391			
4	Regression	64826,694	4	16206,673	1447,371	,000[e]
	Residual	15530,681	1387	11,197		
	Total	80357,375	1391			

a. Dependent Variable: Flux

b. Predictors: (Constant), CST/TSS

c. Predictors: (Constant), CST/TSS, x-flow velocity

d. Predictors: (Constant), CST/TSS, x-flow velocity , SRF Membrane

e. Predictors: (Constant), CST/TSS, x-flow velocity , SRF Membrane , VS/TS

Coefficients[a]

Model		Unstandardized Coefficients		Standardized Coefficients		
		B	Std. Error	Beta	t	Sig.
1	(Constant)	29,904	,470		63,581	,000
	CST/TSS	-,240	,007	-,652	-32,068	,000
2	(Constant)	10,867	,576		18,880	,000
	CST/TSS	-,246	,005	-,669	-48,129	,000
	x-flow velocity	14,522	,364	,554	39,866	,000
3	(Constant)	14,915	,524		28,466	,000
	CST/TSS	-,227	,004	-,617	-51,012	,000
	x-flow velocity	14,013	,312	,535	44,854	,000
	SRF Membrane	-1,915E-11	,000	-,274	-22,589	,000
4	(Constant)	6,710	1,925		3,486	,001
	CST/TSS	-,227	,004	-,617	-51,286	,000
	x-flow velocity	14,067	,311	,537	45,293	,000

	SRF Membrane	-1,917E-11	,000	-,274	-22,759	,000
	VS/TS	12,085	2,729	,052	4,428	,000

Coefficients[a]

Model		95,0% Confidence Interval for B		Collinearity Statistics	
		Lower Bound	Upper Bound	Tolerance	VIF
1	(Constant)	28,982	30,827		
	CST/TSS	-,254	-,225	1,000	1,000
2	(Constant)	9,738	11,996		
	CST/TSS	-,256	-,236	,999	1,001
	x-flow velocity	13,807	15,237	,999	1,001
3	(Constant)	13,887	15,942		
	CST/TSS	-,236	-,218	,964	1,038
	x-flow velocity	13,400	14,626	,994	1,006
	SRF Membrane	,000	,000	,961	1,041
4	(Constant)	2,934	10,485		
	CST/TSS	-,235	-,218	,964	1,038
	x-flow velocity	13,458	14,676	,992	1,008
	SRF Membrane	,000	,000	,961	1,041
	VS/TS	6,731	17,440	,998	1,002

a. Dependent Variable: Flux

Collinearity Diagnostics[a]

Model	Dimension	Eigenvalue	Condition Index	Variance Proportions		
				(Constant)	CST/TSS	x-flow velocity
1	1	1,945	1,000	,03	,03	
	2	,055	5,920	,97	,97	

2	1	2,898	1,000	,00	,01	,01
	2	,081	5,969	,03	,86	,16
	3	,021	11,873	,97	,13	,84
3	1	3,760	1,000	,00	,01	,00
	2	,140	5,185	,01	,04	,05
	3	,081	6,809	,02	,87	,14
	4	,019	13,958	,96	,08	,81
4	1	4,739	1,000	,00	,00	,00
	2	,146	5,696	,00	,01	,03
	3	,086	7,439	,00	,94	,07
	4	,029	12,866	,01	,03	,87
	5	,001	63,978	,98	,01	,02

Collinearity Diagnostics[a]

		Variance Proportions	
Model	Dimension	SRF Membrane	VS/TS
1	1		
	2		
2	1		
	2		
	3		
3	1	,01	
	2	,91	
	3	,01	
	4	,07	
4	1	,01	,00
	2	,93	,00
	3	,02	,00

4	,05	,02
5	,00	,98

a. Dependent Variable: Flux

Multilinear regression long formular

Model Summary

Model	R	R Square	Adjusted R Square	Std. Error of the Estimate
1	.652[a]	0.425	0.425	5.76436
2	.856[b]	0.732	0.732	3.93800
3	.902[c]	0.813	0.812	3.29157
4	.926[d]	0.858	0.857	2.87292
5	.935[e]	0.874	0.874	2.70117
6	.937[f]	0.877	0.877	2.67067
7	.938[g]	0.880	0.879	2.63990
8	.938[h]	0.880	0.879	2.63974
9	.939[i]	0.882	0.882	2.61297
10	.940[j]	0.883	0.882	2.60950

a. Predictors: (Constant), CST/TSS

b. Predictors: (Constant), CST/TSS, x-flow velocity

c. Predictors: (Constant), CST/TSS, x-flow velocity , VSS/TSS

d. Predictors: (Constant), CST/TSS, x-flow velocity , VSS/TSS, VS/TS

e. Predictors: (Constant), CST/TSS, x-flow velocity , VSS/TSS, VS/TS, Viscocity (mP.s)

f. Predictors: (Constant), CST/TSS, x-flow velocity , VSS/TSS, VS/TS, Viscocity (mP.s), SRF Membrane

g. Predictors: (Constant), CST/TSS, x-flow velocity , VSS/TSS, VS/TS, Viscocity (mP.s), SRF Membrane , TSS-VSS

h. Predictors: (Constant), CST/TSS, x-flow velocity , VSS/TSS, VS/TS, SRF Membrane , TSS-VSS

i. Predictors: (Constant), CST/TSS, x-flow velocity , VSS/TSS, VS/TS, SRF Membrane , TSS-VSS, CCOD-SCOD (mg/L)

j. Predictors: (Constant), CST/TSS, x-flow velocity , VSS/TSS, VS/TS, SRF Membrane , TSS-VSS, CCOD-SCOD (mg/L), TMP

ANOVAa

Model		Sum of Squares	df	Mean Square	F	Sig.
1	Regression	34170,681	1	34170,681	1028,375	,000[b]
	Residual	46186,694	1390	33,228		
	Total	80357,375	1391			
2	Regression	58816,992	2	29408,496	1896,364	,000[c]
	Residual	21540,382	1389	15,508		
	Total	80357,375	1391			
3	Regression	65319,173	3	21773,058	2009,616	,000[d]
	Residual	15038,202	1388	10,834		
	Total	80357,375	1391			
4	Regression	68909,509	4	17227,377	2087,234	,000[e]
	Residual	11447,865	1387	8,254		
	Total	80357,375	1391			
5	Regression	70244,671	5	14048,934	1925,481	,000[f]
	Residual	10112,703	1386	7,296		
	Total	80357,375	1391			
6	Regression	70571,921	6	11761,987	1664,752	,000[g]
	Residual	9785,454	1385	7,065		
	Total	80357,375	1391			
7	Regression	70571,533	5	14114,307	1999,054	,000[h]
	Residual	9785,842	1386	7,060		
	Total	80357,375	1391			
8	Regression	70649,768	6	11774,961	1679,953	,000[i]
	Residual	9707,606	1385	7,009		
	Total	80357,375	1391			
9	Regression	70713,734	7	10101,962	1449,776	,000[j]

	Residual	9643,641	1384	6,968		
	Total	80357,375	1391			
10	Regression	70859,823	8	8857,478	1289,795	,000[k]
	Residual	9497,551	1383	6,867		
	Total	80357,375	1391			

a. Dependent Variable: Flux

b. Predictors: (Constant), CST/TSS

c. Predictors: (Constant), CST/TSS, x-flow velocity

d. Predictors: (Constant), CST/TSS, x-flow velocity , VSS/TSS

e. Predictors: (Constant), CST/TSS, x-flow velocity , VSS/TSS, VS/TS

f. Predictors: (Constant), CST/TSS, x-flow velocity , VSS/TSS, VS/TS, Viscocity (mP.s)

g. Predictors: (Constant), CST/TSS, x-flow velocity , VSS/TSS, VS/TS, Viscocity (mP.s), CST/TSS/Viscosity

h. Predictors: (Constant), x-flow velocity , VSS/TSS, VS/TS, Viscocity (mP.s), CST/TSS/Viscosity

i. Predictors: (Constant), x-flow velocity , VSS/TSS, VS/TS, Viscocity (mP.s), CST/TSS/Viscosity , CCOD (mg/L)

j. Predictors: (Constant), x-flow velocity , VSS/TSS, VS/TS, Viscocity (mP.s), CST/TSS/Viscosity , CCOD (mg/L), TSS-VSS

Coefficientsa

		Unstandardized Coefficients		Standardized Coefficients			95,0% Confidence Interval for B	
Model		B	Std. Error	Beta	t	Sig.	Lower Bound	Upper Bound
1	(Constant)	29,904	,470		63,581	,000	28,982	30,827
	CST/TSS	-,240	,007	-,652	-32,068	,000	-,254	-,225
2	(Constant)	10,867	,576		18,880	,000	9,738	11,996
	CST/TSS	-,246	,005	-,669	-48,129	,000	-,256	-,236
	x-flow velocity	14,522	,364	,554	39,866	,000	13,807	15,237
3	(Constant)	40,074	1,286		31,171	,000	37,552	42,596
	CST/TSS	-,181	,005	-,492	-35,940	,000	-,191	-,171

	x-flow velocity	13,422	,308	,512	43,612	,000	12,819	14,026
	VSS/TSS	-36,212	1,478	-,337	-24,498	,000	-39,112	-33,313
4	(Constant)	14,065	1,678		8,384	,000	10,774	17,356
	CST/TSS	-,153	,005	-,418	-33,510	,000	-,162	-,145
	x-flow velocity	13,232	,269	,505	49,230	,000	12,705	13,759
	VSS/TSS	-50,718	1,466	-,472	-34,603	,000	-53,593	-47,843
	VS/TS	55,521	2,662	,240	20,857	,000	50,299	60,743
5	(Constant)	34,434	2,181		15,791	,000	30,156	38,712
	CST/TSS	-,114	,005	-,310	-21,860	,000	-,124	-,104
	x-flow velocity	12,890	,254	,492	50,752	,000	12,392	13,388
	VSS/TSS	-66,022	1,783	-,614	-37,029	,000	-69,519	-62,524
	VS/TS	49,077	2,548	,212	19,262	,000	44,079	54,075
	Viscocity (mP.s)	-,514	,038	-,190	-13,527	,000	-,589	-,440
6	(Constant)	42,227	2,432		17,361	,000	37,456	46,999
	CST/TSS	-,004	,017	-,011	-,234	,815	-,037	,029
	x-flow velocity	12,896	,250	,492	51,598	,000	12,405	13,386
	VSS/TSS	-66,022	1,755	-,615	-37,630	,000	-69,464	-62,581
	VS/TS	47,204	2,522	,204	18,715	,000	42,256	52,152
	Viscocity (mP.s)	-1,084	,092	-,401	-11,819	,000	-1,264	-,904
	CST/TSS/Viscosity	-1,142	,168	-,338	-6,806	,000	-1,472	-,813
7	(Constant)	42,542	2,027		20,989	,000	38,566	46,518
	x-flow velocity	12,893	,250	,492	51,649	,000	12,403	13,383
	VSS/TSS	-66,113	1,711	-,615	-38,645	,000	-69,469	-62,757
	VS/TS	47,165	2,516	,204	18,747	,000	42,230	52,100
	Viscocity (mP.s)	-1,104	,031	-,409	-35,214	,000	-1,166	-1,043
	CST/TSS/Viscosity	-1,180	,051	-,349	-23,240	,000	-1,279	-1,080
8	(Constant)	48,155	2,627		18,331	,000	43,002	53,308

	x-flow velocity	13,032	,252	,497	51,677	,000	12,538	13,527
	VSS/TSS	-65,066	1,733	-,606	-37,542	,000	-68,465	-61,666
	VS/TS	38,358	3,638	,166	10,545	,000	31,222	45,494
	Viscocity (mP.s)	-1,183	,039	-,438	-30,258	,000	-1,260	-1,106
	CST/TSS/Viscosity	-1,353	,072	-,400	-18,705	,000	-1,494	-1,211
	CCOD (mg/L)	,000	,000	,062	3,341	,001	,000	,001
9	(Constant)	71,319	8,081		8,825	,000	55,465	87,172
	x-flow velocity	13,079	,252	,499	51,918	,000	12,585	13,573
	VSS/TSS	-89,039	8,099	-,829	-10,994	,000	-104,926	-73,151
	VS/TS	37,232	3,646	,161	10,212	,000	30,080	44,384
	Viscocity (mP.s)	-1,025	,065	-,379	-15,713	,000	-1,153	-,897
	CST/TSS/Viscosity	-1,424	,076	-,421	-18,772	,000	-1,573	-1,275
	CCOD (mg/L)	,001	,000	,085	4,267	,000	,000	,001
	TSS-VSS	-1,739	,574	-,268	-3,030	,002	-2,865	-,613
10	(Constant)	121,075	13,444		9,006	,000	94,702	147,447
	x-flow velocity	13,167	,251	,502	52,496	,000	12,675	13,659
	VSS/TSS	-131,782	12,269	-1,227	-10,741	,000	-155,849	-107,714
	VS/TS	26,424	4,312	,114	6,128	,000	17,966	34,883
	Viscocity (mP.s)	-,768	,085	-,284	-9,002	,000	-,936	-,601
	CST/TSS/Viscosity	-1,568	,082	-,464	-19,231	,000	-1,728	-1,408
	CCOD (mg/L)	,001	,000	,138	6,023	,000	,001	,001
	TSS-VSS	-5,301	,960	-,816	-5,523	,000	-7,184	-3,418
	SRF Membrane	-6,912E-12	,000	-,099	-4,612	,000	,000	,000

Correlation Matrix[a]

		x-flow velocity	TMP	Flux	Permeability	TCOD (mg/L)	PCOD (mg/L)
Correlation	x-flow velocity	1,000	,051	,824	,553	-,357	-,175
	TMP	,051	1,000	,047	-,619	,386	,118
	Flux	,824	,047	1,000	,706	-,174	-,169
	Permeability	,553	-,619	,706	1,000	-,288	-,142
	TCOD (mg/L)	-,357	,386	-,174	-,288	1,000	,748
	PCOD (mg/L)	-,175	,118	-,169	-,142	,748	1,000
	CCOD (mg/L)	-,332	,444	-,064	-,268	,632	-,042
	CCOD-SCOD (mg/L)	-,371	,464	-,108	-,299	,818	,229
	SCOD (mg/L)	-,276	,397	-,020	-,222	,423	-,285
	TS (g/kg)	-,223	,181	-,178	-,180	,836	,990
	VS (g/kg)	-,028	-,069	-,128	-,023	,427	,919
	VS/TS	,074	-,187	-,089	,059	,174	,784
	TS-TSS	,250	-,373	,003	,202	-,337	,373
	TS-VS	-,152	,273	,052	-,122	,040	-,633
	TSS (g/kg)	-,341	,450	-,072	-,275	,669	,007
	VSS (g/kg)	-,382	,445	-,149	-,308	,955	,516
	VSS/TSS	,061	-,172	-,094	,048	,208	,805
	TSS-VSS	-,122	,240	,067	-,098	-,045	-,697
	CST (s)	-,368	,464	-,104	-,297	,801	,202
	Viscocity (mP.s)	-,346	,365	-,178	-,279	,997	,796
	CST/TSS	,254	-,378	,006	,205	-,356	,354
	CST/Viscosity	,220	-,177	,178	,178	-,831	-,991
	CST/TSS/Viscosity	,374	-,419	,164	,302	-,989	-,644
	PSD d50 avg. (µm)	-,313	,429	-,047	-,252	,555	-,138
	PSD d10 avg. (µm)	-,310	,427	-,045	-,250	,545	-,149
	SRF Membrane	,322	,024	,140	,023	-,613	-,371

	Supernatant Filterability (mL/min)	,163	-,101	,167	,132	-,724	-,999
	Protein (mgN/L)	,216	-,340	-,018	,174	-,229	,475
	PSD 0 to 20 µm	,312	-,428	,047	,251	-,551	,141
	PSD 0 to 10 µm	,308	-,425	,044	,248	-,538	,158
	PSD 10 to 20 µm	,319	-,434	,052	,257	-,578	,109
	PSD 1 to 10 µm	,308	-,425	,044	,248	-,538	,158
	Supernatant x<10 µm (%)	,272	-,393	,017	,219	-,409	,300

Correlation Matrix[a]

		CCOD (mg/L)	CCOD-SCOD (mg/L)	SCOD (mg/L)	TS (g/kg)	VS (g/kg)	VS/TS
Correlation	x-flow velocity	-,332	-,371	-,276	-,223	-,028	,074
	TMP	,444	,464	,397	,181	-,069	-,187
	Flux	-,064	-,108	-,020	-,178	-,128	-,089
	Permeability	-,268	-,299	-,222	-,180	-,023	,059
	TCOD (mg/L)	,632	,818	,423	,836	,427	,174
	PCOD (mg/L)	-,042	,229	-,285	,990	,919	,784
	CCOD (mg/L)	1,000	,963	,970	,102	-,432	-,654
	CCOD-SCOD (mg/L)	,963	1,000	,868	,368	-,172	-,424
	SCOD (mg/L)	,970	,868	1,000	-,143	-,639	-,818
	TS (g/kg)	,102	,368	-,143	1,000	,853	,686
	VS (g/kg)	-,432	-,172	-,639	,853	1,000	,965
	VS/TS	-,654	-,424	-,818	,686	,965	1,000
	TS-TSS	-,943	-,818	-,996	,235	,708	,868
	TS-VS	,800	,608	,922	-,515	-,886	-,977
	TSS (g/kg)	,999	,975	,957	,151	-,387	-,615
	VSS (g/kg)	,834	,952	,674	,635	,138	-,127

	VSS/TSS	-,627	-,393	-,798	,711	,973	,999
	TSS-VSS	,746	,538	,886	-,586	-,923	-,992
	CST (s)	,970	1,000	,881	,341	-,199	-,450
	Viscocity (mP.s)	,572	,772	,354	,875	,493	,248
	CST/TSS	-,949	-,829	-,997	,215	,693	,858
	CST/Viscosity	-,094	-,359	,152	-1,000	-,858	-,692
	CST/TSS/Viscosity	-,737	-,892	-,550	-,748	-,291	-,030
	PSD d50 avg. (µm)	,995	,932	,989	,007	-,516	-,723
	PSD d10 avg. (µm)	,994	,928	,990	-,005	-,526	-,731
	SRF Membrane	-,489	-,577	-,379	-,441	-,143	,022
	Supernatant Filterability (mL/min)	,078	-,195	,319	-,984	-,933	-,805
	Protein (mgN/L)	-,899	-,748	-,979	,343	,783	,919
	PSD 0 to 20 µm	-,995	-,931	-,989	-,003	,519	,726
	PSD 0 to 10 µm	-,993	-,925	-,992	,014	,533	,737
	PSD 10 to 20 µm	-,998	-,942	-,984	-,035	,491	,703
	PSD 1 to 10 µm	-,993	-,925	-,992	,014	,533	,737
	Supernatant x<10 µm (%)	-,966	-,860	-1,000	,159	,651	,827

Correlation Matrix[a]

		TS-TSS	TS-VS	TSS (g/kg)	VSS (g/kg)	VSS/TSS	TSS-VSS	CST (s)
Correlation	x-flow velocity	,250	-,152	-,341	-,382	,061	-,122	-,368
	TMP	-,373	,273	,450	,445	-,172	,240	,464
	Flux	,003	,052	-,072	-,149	-,094	,067	-,104
	Permeability	,202	-,122	-,275	-,308	,048	-,098	-,297
	TCOD (mg/L)	-,337	,040	,669	,955	,208	-,045	,801
	PCOD (mg/L)	,373	-,633	,007	,516	,805	-,697	,202

	CCOD (mg/L)	-,943	,800	,999	,834	-,627	,746	,970
	CCOD-SCOD (mg/L)	-,818	,608	,975	,952	-,393	,538	1,000
	SCOD (mg/L)	-,996	,922	,957	,674	-,798	,886	,881
	TS (g/kg)	,235	-,515	,151	,635	,711	-,586	,341
	VS (g/kg)	,708	-,886	-,387	,138	,973	-,923	-,199
	VS/TS	,868	-,977	-,615	-,127	,999	-,992	-,450
	TS-TSS	1,000	-,954	-,925	-,602	,851	-,925	-,834
	TS-VS	-,954	1,000	,770	,336	-,969	,996	,630
	TSS (g/kg)	-,925	,770	1,000	,860	-,588	,713	,981
	VSS (g/kg)	-,602	,336	,860	1,000	-,093	,255	,943
	VSS/TSS	,851	-,969	-,588	-,093	1,000	-,986	-,418
	TSS-VSS	-,925	,996	,713	,255	-,986	1,000	,562
	CST (s)	-,834	,630	,981	,943	-,418	,562	1,000
	Viscocity (mP.s)	-,266	-,035	,611	,930	,281	-,120	,754
	CST/TSS	1,000	-,948	-,933	-,618	,840	-,917	-,845
	CST/Viscosity	-,243	,522	-,142	-,628	-,717	,593	-,333
	CST/TSS/Viscosity	,470	-,185	-,769	-,988	-,065	-,100	-,879
	PSD d50 avg. (µm)	-,970	,854	,990	,777	-,698	,806	,942
	PSD d10 avg. (µm)	-,973	,860	,988	,770	-,707	,813	,938
	SRF Membrane	,331	-,156	-,508	-,625	,001	-,104	-,570
	Supernatant Filterability (mL/min)	-,405	,660	,029	-,486	-,826	,722	-,167
	Protein (mgN/L)	,994	-,982	-,877	-,509	,904	-,962	-,766
	PSD 0 to 20 µm	,971	-,856	-,989	-,775	,701	-,809	-,941
	PSD 0 to 10 µm	,975	-,864	-,986	-,764	,713	-,818	-,935
	PSD 10 to 20 µm	,963	-,839	-,993	-,795	,678	-,789	-,951
	PSD 1 to 10 µm	,975	-,864	-,986	-,764	,713	-,818	-,935

	Supernatant x<10 µm (%)	,997	-,928	-,952	-,662	,807	-,893	-,874

Correlation Matrix[a]

		Viscocity (mP.s)	CST/TSS	CST/Viscosity	CST/TSS/Viscosity	PSD d50 avg. (µm)
Correlation	x-flow velocity	-,346	,254	,220	,374	-,313
	TMP	,365	-,378	-,177	-,419	,429
	Flux	-,178	,006	,178	,164	-,047
	Permeability	-,279	,205	,178	,302	-,252
	TCOD (mg/L)	,997	-,356	-,831	-,989	,555
	PCOD (mg/L)	,796	,354	-,991	-,644	-,138
	CCOD (mg/L)	,572	-,949	-,094	-,737	,995
	CCOD-SCOD (mg/L)	,772	-,829	-,359	-,892	,932
	SCOD (mg/L)	,354	-,997	,152	-,550	,989
	TS (g/kg)	,875	,215	-1,000	-,748	,007
	VS (g/kg)	,493	,693	-,858	-,291	-,516
	VS/TS	,248	,858	-,692	-,030	-,723
	TS-TSS	-,266	1,000	-,243	,470	-,970
	TS-VS	-,035	-,948	,522	-,185	,854
	TSS (g/kg)	,611	-,933	-,142	-,769	,990
	VSS (g/kg)	,930	-,618	-,628	-,988	,777
	VSS/TSS	,281	,840	-,717	-,065	-,698
	TSS-VSS	-,120	-,917	,593	-,100	,806
	CST (s)	,754	-,845	-,333	-,879	,942
	Viscocity (mP.s)	1,000	-,285	-,870	-,976	,491
	CST/TSS	-,285	1,000	-,224	,488	-,975
	CST/Viscosity	-,870	-,224	1,000	,742	,002

	CST/TSS/Viscosity	-,976	,488	,742	1,000	-,669
	PSD d50 avg. (µm)	,491	-,975	,002	-,669	1,000
	PSD d10 avg. (µm)	,480	-,978	,014	-,660	1,000
	SRF Membrane	-,602	,342	,437	,626	-,450
	Supernatant Filterability (mL/min)	-,774	-,387	,985	,616	,173
	Protein (mgN/L)	-,155	,991	-,351	,368	-,937
	PSD 0 to 20 µm	-,487	,976	-,006	,666	-1,000
	PSD 0 to 10 µm	-,473	,979	-,022	,654	-1,000
	PSD 10 to 20 µm	-,515	,968	,027	,690	-1,000
	PSD 1 to 10 µm	-,473	,979	-,022	,654	-1,000
	Supernatant x<10 µm (%)	-,339	,998	-,168	,537	-,986

Correlation Matrix[a]

		PSD d10 avg. (µm)	SRF Membrane	Supernatant Filterability (mL/min)	Protein (mgN/L)	PSD 0 to 20 µm
Correlation	x-flow velocity	-,310	,322	,163	,216	,312
	TMP	,427	,024	-,101	-,340	-,428
	Flux	-,045	,140	,167	-,018	,047
	Permeability	-,250	,023	,132	,174	,251
	TCOD (mg/L)	,545	-,613	-,724	-,229	-,551
	PCOD (mg/L)	-,149	-,371	-,999	,475	,141
	CCOD (mg/L)	,994	-,489	,078	-,899	-,995
	CCOD-SCOD (mg/L)	,928	-,577	-,195	-,748	-,931
	SCOD (mg/L)	,990	-,379	,319	-,979	-,989
	TS (g/kg)	-,005	-,441	-,984	,343	-,003
	VS (g/kg)	-,526	-,143	-,933	,783	,519

	VS/TS	-,731	,022	-,805	,919	,726
	TS-TSS	-,973	,331	-,405	,994	,971
	TS-VS	,860	-,156	,660	-,982	-,856
	TSS (g/kg)	,988	-,508	,029	-,877	-,989
	VSS (g/kg)	,770	-,625	-,486	-,509	-,775
	VSS/TSS	-,707	,001	-,826	,904	,701
	TSS-VSS	,813	-,104	,722	-,962	-,809
	CST (s)	,938	-,570	-,167	-,766	-,941
	Viscocity (mP.s)	,480	-,602	-,774	-,155	-,487
	CST/TSS	-,978	,342	-,387	,991	,976
	CST/Viscosity	,014	,437	,985	-,351	-,006
	CST/TSS/Viscosity	-,660	,626	,616	,368	,666
	PSD d50 avg. (µm)	1,000	-,450	,173	-,937	-1,000
	PSD d10 avg. (µm)	1,000	-,444	,184	-,941	-1,000
	SRF Membrane	-,444	1,000	,354	,268	,448
	Supernatant Filterability (mL/min)	,184	,354	1,000	-,506	-,177
	Protein (mgN/L)	-,941	,268	-,506	1,000	,938
	PSD 0 to 20 µm	-1,000	,448	-,177	,938	1,000
	PSD 0 to 10 µm	-1,000	,441	-,193	,944	1,000
	PSD 10 to 20 µm	-,999	,462	-,144	,927	,999
	PSD 1 to 10 µm	-1,000	,441	-,193	,944	1,000
	Supernatant x<10 µm (%)	-,988	,371	-,334	,982	,987

Correlation Matrix[a]

		PSD 0 to 10 µm	PSD 10 to 20 µm	PSD 1 to 10 µm	Supernatant x<10 µm (%)
Correlation	x-flow velocity	,308	,319	,308	,272

	TMP	-,425	-,434	-,425	-,393
	Flux	,044	,052	,044	,017
	Permeability	,248	,257	,248	,219
	TCOD (mg/L)	-,538	-,578	-,538	-,409
	PCOD (mg/L)	,158	,109	,158	,300
	CCOD (mg/L)	-,993	-,998	-,993	-,966
	CCOD-SCOD (mg/L)	-,925	-,942	-,925	-,860
	SCOD (mg/L)	-,992	-,984	-,992	-1,000
	TS (g/kg)	,014	-,035	,014	,159
	VS (g/kg)	,533	,491	,533	,651
	VS/TS	,737	,703	,737	,827
	TS-TSS	,975	,963	,975	,997
	TS-VS	-,864	-,839	-,864	-,928
	TSS (g/kg)	-,986	-,993	-,986	-,952
	VSS (g/kg)	-,764	-,795	-,764	-,662
	VSS/TSS	,713	,678	,713	,807
	TSS-VSS	-,818	-,789	-,818	-,893
	CST (s)	-,935	-,951	-,935	-,874
	Viscocity (mP.s)	-,473	-,515	-,473	-,339
	CST/TSS	,979	,968	,979	,998
	CST/Viscosity	-,022	,027	-,022	-,168
	CST/TSS/Viscosity	,654	,690	,654	,537
	PSD d50 avg. (µm)	-1,000	-1,000	-1,000	-,986
	PSD d10 avg. (µm)	-1,000	-,999	-1,000	-,988
	SRF Membrane	,441	,462	,441	,371
	Supernatant Filterability (mL/min)	-,193	-,144	-,193	-,334
	Protein (mgN/L)	,944	,927	,944	,982

	PSD 0 to 20 µm	1,000	,999	1,000	,987
	PSD 0 to 10 µm	1,000	,999	1,000	,989
	PSD 10 to 20 µm	,999	1,000	,999	,981
	PSD 1 to 10 µm	1,000	,999	1,000	,989
	Supernatant x<10 µm (%)	,989	,981	,989	1,000

C. Supplementary Statistical Results from SPSS for Sludge and SRF Data

PCA and Multilinear Regression for the Sludge data

The individual sludge data was not beneficial for the formation of the previous model presented, however another PCA was performed to understand the relationship between the sludge variables and also to see if we could use this information to form another empirical model to predict the SRF. Additional data from a different project was also included in the statistical analysis. A principal component analysis was performed to the two data sets individually and combined. Three multilinear regression models were obtained from each scenario. Equation 1, 2, and 3 correspond to the data obtained from this project, the additional data obtained from a different project, and both projects combined, respectively. Equation 1 and 2 showed good linear relationship with the normalized CST/TSS/Viscosity for predicting the SRF, with respective R squared values of 0.884 and 0.760. On the other hand, equation 3 didn't show any relationship with the CST/TSS/Viscosity in order to estimate the values for the SRF.

$$SRF = 7873110168.501 + 30530728393.1347 \times CST/TSS/Viscosity$$

Equation (1)

$$SRF = 26056137586.8044 \times CST/TSS/Viscosity$$

Equation (2)

$$SRF = 118303150.3 \times Protein\ (mgCOD/L) - 2.3474E+10 \times Viscosity + 34814925.85 \times CCOD\ (0.45\text{-}1\ \mu m)$$

Equation (3)

Model Summary

Model	R	R Square	Adjusted R Square	Std. Error of the Estimate
1	,940[a]	,884	,882	28379073,139664270000000

a. Predictors: (Constant), CST/TSS/Viscosity

ANOVA[a]

Model		Sum of Squares	df	Mean Square	F	Sig.
1	Regression	3065245172342 91710,000	1	3065245172342 91710,000	380,600	,000[b]
	Residual	4026858961332 0704,000	50	8053717922664 14,100		
	Total	3467931068476 12420,000	51			

a. Dependent Variable: SRF

b. Predictors: (Constant), CST/TSS/Viscosity

Coefficients[a]

Model		Unstandardized Coefficients		Standardized Coefficients		
		B	Std. Error	Beta	t	Sig.
1	(Constant)	-22907904,971	7756145,362		-2,954	,005
	CST/TSS/Viscosity	53539750,575	2744365,445	,940	19,509	,000

Coefficients[a]

Model		95,0% Confidence Interval for B	
		Lower Bound	Upper Bound
1	(Constant)	-38486581,413	-7329228,529
	CST/TSS/Viscosity	48027530,354	59051970,796

a. Dependent Variable: SRF

Model Summary

Model	R	R Square	Adjusted R Square	Std. Error of the Estimate

1	,872[a]	,760	,757	41150681861,212630000

a. Predictors: (Constant), CST/TSS/viscosity

ANOVA[a]

Model		Sum of Squares	df	Mean Square	F	Sig.
1	Regression	381455814863970200000000,000	1	381455814863970200000000,000	225,263	,000[b]
	Residual	120229881852634130000000,000	71	1693378617642734300000,000		
	Total	501685696716604300000000,000	72			

a. Dependent Variable: SRF Membrane

b. Predictors: (Constant), CST/TSS/viscosity

Coefficients[a]

Model		Unstandardized Coefficients		Standardized Coefficients		
		B	Std. Error	Beta	t	Sig.
1	(Constant)	-7873110168,501	8302508446,006		-,948	,346
	CST/TSS/viscosity	26056137586,804	1736060895,642	,872	15,009	,000

Coefficients[a]

Model		95,0% Confidence Interval for B	
		Lower Bound	Upper Bound
1	(Constant)	-24427841820,894	8681621483,892
	CST/TSS/viscosity	22594530477,763	29517744695,845

a. Dependent Variable: SRF Membrane

Model Summary

Model	R	R Square	Adjusted R Square	Std. Error of the Estimate
1	,932[a]	,868	,860	32844242911,401980000
2	,972[b]	,944	,937	21976994820,313652000
3	,983[c]	,966	,960	17615246088,562378000

a. Predictors: (Constant), Protein (mgCOD/L)

b. Predictors: (Constant), Protein (mgCOD/L), Viscosity

c. Predictors: (Constant), Protein (mgCOD/L), Viscosity, CCOD-SCOD

ANOVA[a]

Model		Sum of Squares	df	Mean Square	F	Sig.
1	Regression	120501614814809470000000,000	1	120501614814809470000000,000	111,705	,000[b]
	Residual	183386529711940490000000,000	17	107874429242317930000000,000		

	Total	1388402677860 03520000000,00 0	18			
2	Regression	1311124549646 90030000000,00 0	2	6555622748234 5010000000,00 0	135,730	,000[c]
	Residual	7727812821313 489000000,000	16	4829883013320 93100000,000		
	Total	1388402677860 03520000000,00 0	18			
3	Regression	1341858143645 94330000000,00 0	3	4472860478819 8110000000,00 0	144,148	,000[d]
	Residual	4654453421409 182400000,000	15	3102968947606 12130000,000		
	Total	1388402677860 03520000000,00 0	18			

a. Dependent Variable: SRF Membrane

b. Predictors: (Constant), Protein (mgCOD/L)

c. Predictors: (Constant), Protein (mgCOD/L), Viscosity

d. Predictors: (Constant), Protein (mgCOD/L), Viscosity, CCOD-SCOD

Coefficients[a]

Model		Unstandardized Coefficients		Standardized Coefficients		
		B	Std. Error	Beta	t	Sig.
1	(Constant)	40045262273,66 6	16351115572,5 48		2,449	,025
	Protein (mgCOD/L)	177639820,575	16807501,082	,932	10,569	,000

2	(Constant)	247219681338,850	45534719295,360		5,429	,000
	Protein (mgCOD/L)	128859934,959	15322881,565	,676	8,410	,000
	Viscosity	-15693084647,448	3348125565,873	-,377	-4,687	,000
3	(Constant)	290808642228,448	39037129641,652		7,450	,000
	Protein (mgCOD/L)	116230020,467	12920795,452	,610	8,996	,000
	Viscosity	-24345280575,236	3841877880,584	-,584	-6,337	,000
	CCOD-SCOD	36109351,742	11473653,537	,226	3,147	,007

Coefficients[a]

Model		95,0% Confidence Interval for B	
		Lower Bound	Upper Bound
1	(Constant)	5547423923,751	74543100623,580
	Protein (mgCOD/L)	142179092,968	213100548,181
2	(Constant)	150690388606,066	343748974071,634
	Protein (mgCOD/L)	96376877,130	161342992,787
	Viscosity	-22790793777,000	-8595375517,896
3	(Constant)	207602969993,793	374014314463,104
	Protein (mgCOD/L)	88689996,873	143770044,060
	Viscosity	-32534049437,904	-16156511712,568
	CCOD-SCOD	11653838,125	60564865,358

a. Dependent Variable: SRF Membrane

Appendix

D. Membrane Comparison Results

Table 1. Sludge characterization done for membrane comparison tests.

Parameter	units	Sludge sample 1	Sludge sample 2	Sludge Sample 3	Sludge Sample 4
Date	-	Aug 19, 2020	Aug 21, 2020	Aug 25, 2020	Aug 27, 2020
Protein	mg/L N	88.4	125.6	120.525	225.115
Viscosity	mPa·s	7.0	14.8	4.98	7.08
CST	s	435.0	709.5	248	740
CST/TSS	s/g/kg	33.3	45.2	35.4	58.3
CST/Viscosity	s/mPa·s	61.7	48.1	49.8	104.5
CST/TSS/Viscosity	s/g/kg/mPa·s	4.7	3.1	7.1	8.2
pH		7.5	7.4	7.44	6.97
TS	g/kg	15.1	17.3	9.83	16.49
VS	g/kg	10.1	10.9	6.58	12.11
VS/TS	%	81%	63%	66.94%	73.44%
TSS	g/kg	13.1	15.7	7.01	12.7
VSS	g/kg	10.6	11.6	6.2	11.26
VSS/TSS	%	81%	74%	88.45%	88.66%
TCOD	mg/L COD	14800.0	20000.0	9590	21500
PCOD	mg/L COD	13908.0	19496.0	8632	19158
CCOD	mg/L COD	163.0	964.0	549	1971
SCOD	mg/L COD	892.0	504.0	958	2342
SRF	m/kg	5.74E+10	1.54E+11	4.37E+11	2.11E+11

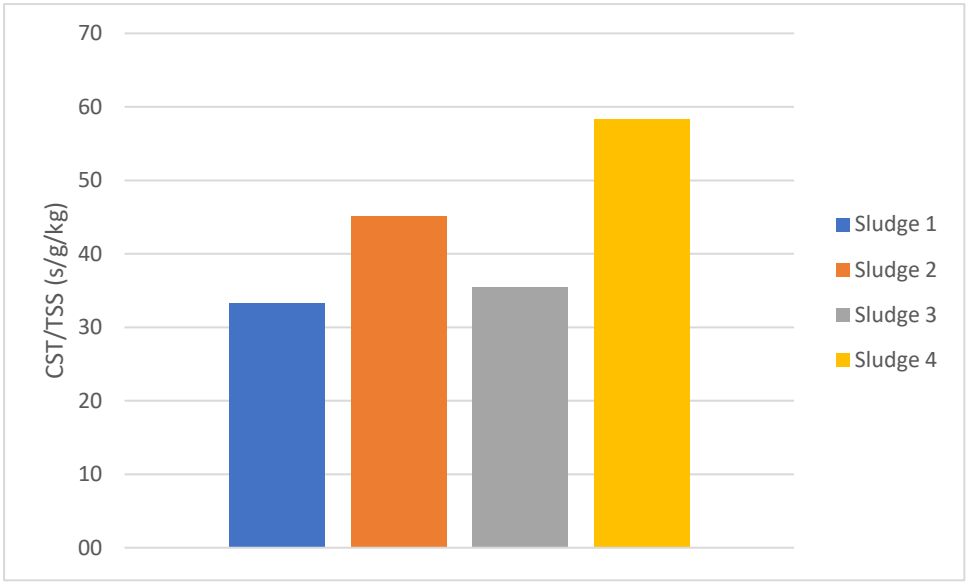

Fig. 5 Normalized CST/TSS for the four different sludge conditions.

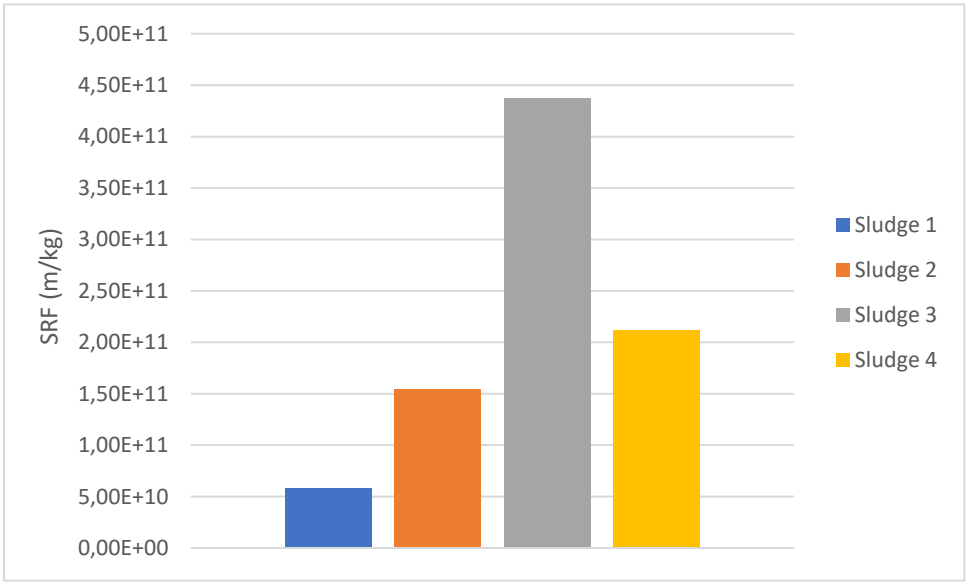

Fig. 6 SRF for the four different sludge conditions tested.

Appendix

A)

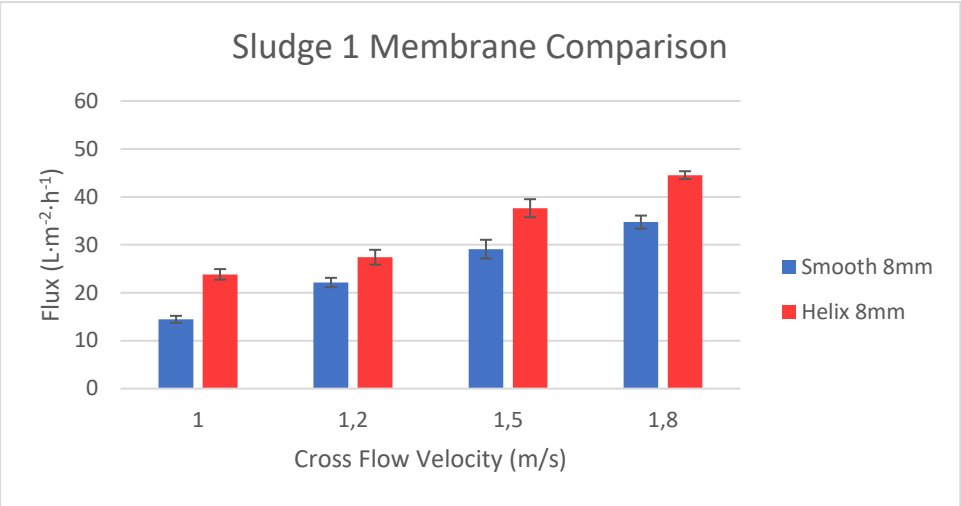

B)

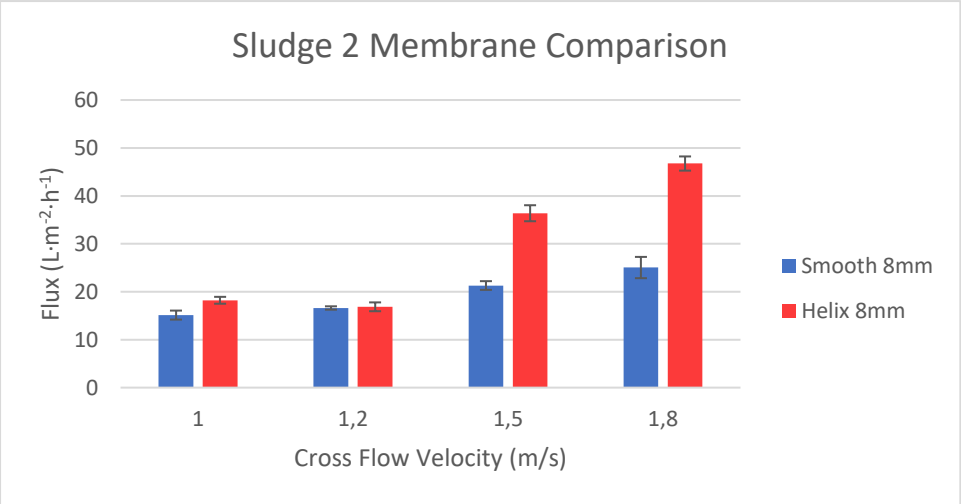

C)

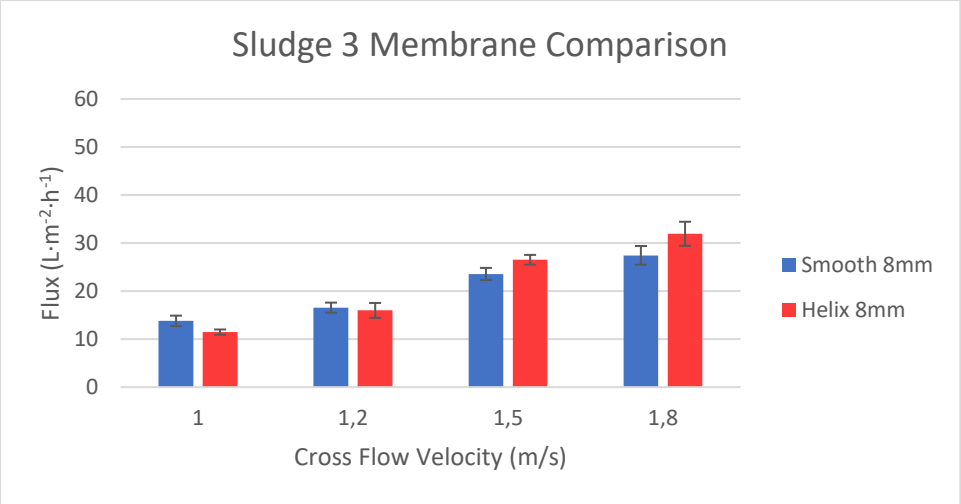

D)

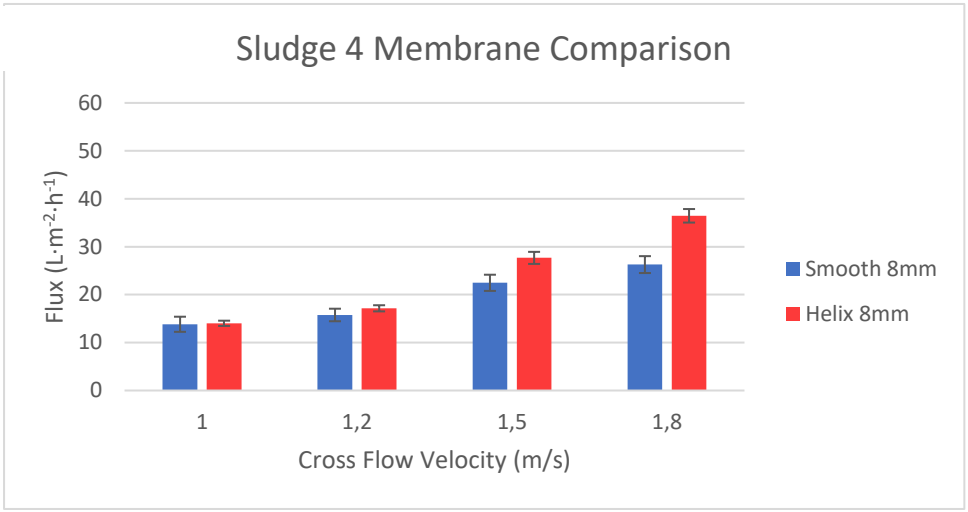

Fig. 7 Smooth and Helix 8 mm membranes comparison under four different crossflow velocities. A) Sludge condition 1. B) Sludge condition 2. C) Sludge condition 3. D) Sludge condition 4.